This is to certify that the

dissertation entitled

The Preresonance Raman Interference Effect in Linear Polyenes

presented by

Isaac W. Sztainbuch

has been accepted towards fulfillment
of the requirements for

Ph.D. degree in Chemical Physics

George A. Levin
Major professor

Date September 26, 1990

The Preresonance Raman Interference Effect in Linear Polyenes

By

Isaac W. Sztainbuch

A DISSERTATION

Submitted to

Michigan State University
in partial fulfillment of the requirements
for the degree of

DOCTOR OF PHILOSOPHY

Chemical Physics Program

1990

The Pr

The
electron
princip
profile
through
betwee
electr
ground
Kramer
to-one
2^1A_g
exper
decap
REP o
fluor
repre
exper
excit
hidde

ABSTRACT

The Preresonance Raman Interference Effect in Linear Polyenes

By

Isaac W. Sztainbuch

The presence of dipole-forbidden ("hidden") excited electronic states in centrosymmetric chromophores can in principle be inferred from preresonance Raman excitation profiles (REPs). As the excitation radiation is tuned through the appropriate energy range, vibronic coupling between the state of interest and nearby "allowed" electronic states will produce interference effects in the ground state scattering intensity. We have used the Kramers-Heisenberg dispersion relation to establish a one-to-one correspondence between the vibrational modes of the 2^1A_g excited state and the interference features in the experimental preresonance REP of all-trans diphenyl-decapentaene (DPDP). The parameters utilized to predict the REP of DPDP were obtained *without adjustment* from absorption and fluorescence excitation spectra. The satisfactory representation and interpretation of the structure in the experimental spectrum establishes preresonance Raman excitation as a viable technique for characterizing such hidden states in non-fluorescing molecules.

Sara-Rafka

Wolf and B

Hinda, Po

Michael,

A

(Poland

Nazis.*

* Yitzh

1987),

DEDICATED TO THE MEMORY OF

Sara-Rafka Sztainbuch.....*(great-grandmother)*

Wolf and Baila Sztainbuch.....*(grandparents)*

Hinda, Pola, Elka, and Esther Sztainbuch.....*(aunts)*

Michael, Rafael, and Phillip Sztainbuch.....*(uncles)*

Along with thousands of innocent men, women, and children from Deblin (Poland) on **6 May 1942** they were deported to Sobibor, and then murdered by the Nazis.*

* Yitzhak Arad, Belzec, Sobibor, Treblinka (Indiana University Press, Bloomington, 1987), P. 390.

ACKNOWLEDGMENTS

I would like to thank Professor George Leroi for his guidance as my research advisor. I would also like to thank Professors R. Schwendeman, J. Kovacs, and P. Parker for serving on my guidance committee. Dr. Tom Atkinson assistance with various computer programs is much appreciated.

My deepest gratitude is extended to my parents Mordechai and Elka Sztainbuch who were always available when needed. Their love and support has greatly facilitated the completion of this work.

Special thanks goes to Hinda and Barry Feinstein for their encouragement, in spite of their bewilderment as to why I am pursuing all this. Mike Gaisner deserve my appreciation for his friendship which goes back to our undergraduate years in physics at Hunter College. Surprisingly, his pessimistic view on life has always had the opposite effect on me.

I am most grateful to have had the privilege of knowing Professor Joachim Weyl at Hunter College. Even during his last days he was cheerful, full of life, and totally devoted to his students and to the teaching of mathematics. His faith in me as a potential scientist has been an inspiration. Dean Weyl died on 22 July 1977 after a long struggle with cancer. This dissertation would have been dedicated to his memory had it not been for members of our family who were victims of the holocaust in Poland during the war, for whom it is dedicated instead.

TABLE OF CONTENTS

TABLE

TABLE

TABL

TA

Ta

T

LIST OF TABLES

Figure

Figur

Figu

Fi

LIST OF FIGURES

Page

Figure 5

Figure 6

Figure 7

Figure

Figur

Page

Figure

Figure

Fig

Fig

F

Page

Page

Figure 1

Figure

Figure

Figu

Fig

Fi

CHAPTER I

INTRODUCTION

For centrosymmetric molecules, such as all-trans linear polyenes, $R\{CH=CH\}_nR$, in the absence of vibronic coupling approximately half of the electronic excited state manifold would be inaccessible from the ground state via conventional absorption spectroscopy because of the alternate parity dipole selection rule. As illustrated in Figure 1, group theory predicts selection rules for one photon absorption which require g→u transitions, while forbidding g→g or u→u transitions.[1] Since the ground state of a centrosymmetric linear molecule is generally of g parity,[2] then those excited electronic states which are also g states are "forbidden", although the associated vibrational levels of u symmetry are allowed. Thus a transition may be electronically forbidden but vibronically allowed. For two-photon absorption spectroscopy the opposite is true: g→g and u→u transitions are allowed,[3] as shown by the dotted arrow in Figure 1. Such "hidden" states have been studied by two-photon induced fluorescence spectroscopy[4,5] in which, for example, the polyene $1^1A_g \rightarrow 2^1A_g$ transition is allowed.

High resolution fluorescence excitation also has been utilized extensively in the characterization of the 2^1A_g

Figure 1. Electronic energy level ordering for a typical linear polyene. A one-photon (——) and two-photon (- -) dipole allowed transition are shown by their respective arrows. The transition $1^1A_g \rightarrow 2^1A_g$ indicated by (-X-) represents a one-photon forbidden transition.

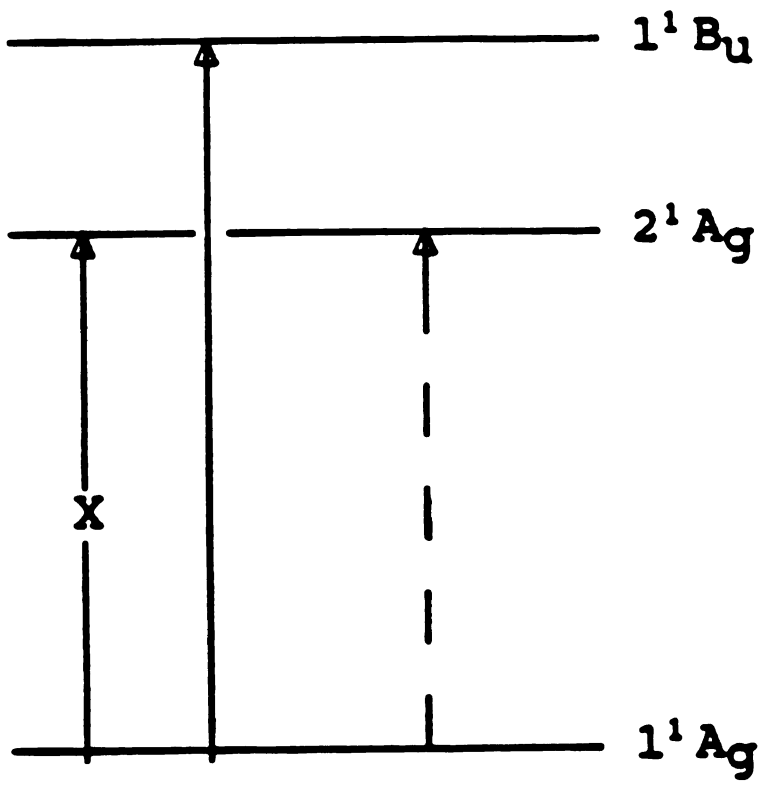

Figure 1.

state,
investig
A polye
either
equilib
parity
contin
molecu
E
diphe
state
reso
beer
incl
oct
the
inc
de
as
th
ex
Dp
ut
al
fo

state, via experiments where the molecule under investigation is placed in an n-alkane Shpolskii matrix.[6-10] A polyene placed in such a mixed crystal environment may either statically or dynamically deform from its C_{2h} equilibrium symmetry, which leads to relaxation of the parity selection rule.[11] Both techniques, however, are contingent upon an adequate fluorescence yield from the molecule of interest.

Evidence that the 2^1A_g parity-forbidden state in diphenyloctatetraene (DPO) is the lowest singlet excited state was first provided by Hudson and Kohler[12] via high resolution fluorescence excitation. This level ordering has been confirmed for several other all-trans polyenes, including the longest unsubstituted member studied to date, octadecaoctaene.[6] This approach is, however, hampered by the precipitous drop in fluorescence quantum yield with increasing chain length.[7,13] (Highly efficient radiationless decay pathways also exist for shorter chain polyenes, such as butadiene and hexatriene.[5,11,14])

Thus many linear polyenes of importance, particularly the longer chain members such as the carotenoids, have extremely low fluorescence quantum yields[15] (compared to the DPO paradigm, for example), so that other methods must be utilized to locate the gerade excited states.

Preresonance Raman excitation may provide a good alternative for the characterization of such parity forbidden excited states in many molecules. Although this

technique is laborious, determining the location of the 2^1A_g state in carotenoids can be of great importance in understanding energy transfer between these antenna pigments and chlorophyll in the photosynthetic system.[16,18]

In previous studies the preresonance Raman excitation profiles of β-carotene, lycopene and other long chain polyenes have been obtained.[20,22] However, the spectra were of uncertain reliability, and the assignment of the excitation profile features was not clearly established. Thus, the impetus for this project was the need to interpret the preresonanace Raman excitation profile of β-carotene, for which reproducible spectroscopic features have been recently obtained.[24]

In the preresonance Raman process, as with conventional Raman scattering, an incident photon is destroyed, a scattered photon is created, and the molecular system undergoes a transition from an initial vibronic state $|G\rangle$ to a final vibronic state $|F\rangle$. If $\omega_0 << \omega_\ell$, that is the excitation frequency, ω_0, is far from an "allowed" electronic excited state (e.g. 1^1B_u), the process is known as ordinary Raman scattering. In this case the denominators in equation (2) of Chapter III can be taken as roughly a constant and $(\omega_0 - \omega_{GF})^4$ is the primary contributor to the Raman cross-section. For resonance Raman scattering the excitation frequency is nearly coincident with an electronic excited state ℓ (i.e., $\omega_0 \simeq \omega_\ell$), and the cross-section for certain modes is significantly enhanced[26] (This scattering

process
inciden
level o
the gro
between
Raman s
in reso
process
hidden
plot o
functi
plot i
A
featur
and
under
benze
showe
of di
sourc
other
and
liter
prer
symm
C_6H_5

process differs from resonance fluorescence where the incident photon is absorbed, followed by a decay to a lower level of that electronic excited state and then emission to the ground state.) Scattering from excitation in a range between normal and resonance is defined as preresonance Raman scattering. The excitation frequency may, however, be in resonance with a dipole-forbidden state. These three processes are depicted in Figure 2. The presence of such hidden states is manifested as an interference pattern in a plot of the intensity of a Raman vibrational band as a function of the energy of the incident radiation. Such a plot is known as an excitation profile

As early as 1971 Rimai et al.[17] reported interference features in the Raman excitation profiles (REPs) of retinal and retinol, which were interpreted as arising from underlying triplet states. With the $^1B_{2u}$ excited state of benzene used as an example, Korenowski et al.[19] subsequently showed that the scattering of totally symmetric fundamentals of dipole-forbidden electronic transitions can be a possible source of measurable Raman cross-sections. A number of other experimental and theoretical studies of preresonance and resonance interference effects have been reported the literature.[21,23,25,27,28]

In this work we present a relatively high resolution preresonance Raman excitation profile for the strongest symmetric stretching mode of all-trans diphenyldecapentaene, $C_6H_5\{CH=CH\}_5C_6H_5$ (structure shown in Figure 7), in solution.

Figure 2. Three Raman scattering processes as a function of incident radiation:

1. Ordinary Stokes Raman scattering $\omega_0 << \omega_\ell$
2. Preresonance Raman scattering $\omega_0 < \omega_\ell$
3. Resonance Raman scattering $\omega_0 \approx \omega_\ell$

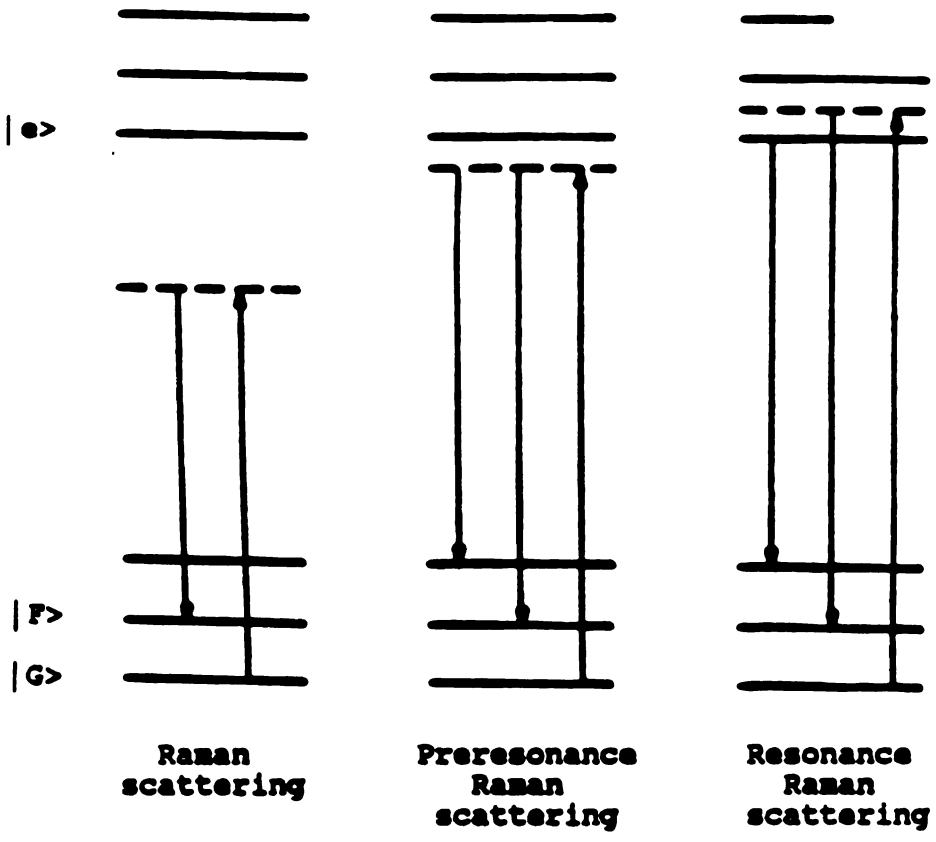
|e>
|F>
|G>
Raman scattering
Preresonance Raman scattering
Resonance Raman scattering

Figure 2.

The diphenyldecapentaene (DPDP) molecule was selected for this study primarily because data for the 2^1A_g and 1^1B_u excited states are available from high resolution absorption, as well as from two-photon and conventional fluorescence excitation spectra.[9,29] We demonstrate a one-to-one correspondence between the predictions of the theoretical excitation profile and the features of the experimental REP, through the utilization of parameters obtained from the one-photon spectra. This enables us to propose an interpretation for the preresonanace Raman excitation features in terms of the underlying hidden electronic state.

CHAPTER II

EXPERIMENTAL

Pure samples of all-trans diphenyldecapentaene, prepared according to procedures refined by Spangler,[30,31] were kindly supplied by Professors R. R. Birge and C. W. Spangler. Samples were further purified to remove undissolved residue by filtering DPDP crystal flakes in hot cyclohexane solution, first through a paper filter and then through a syringe filter (0.25 μm pores) until all undissolved particles were removed. The solvent employed for the Raman measurements was a mixture of cyclohexane and chloroform at a volume ratio of 10:1, where the sole purpose of the chloroform was to keep the ~10^{-4}M DPDP in solution. Equally important, chloroform has no Raman spectral features in the region of interest. The Raman spectrum of the DPDP solution is shown in Figure 3. UV-visible absorption spectra of the samples, such as that shown in Figure 4, were obtained with a Perkin-Elmer Lambda 5 scanning spectrophotometer; no changes in the electronic absorption were discerned from spectra obtained prior and subsequent to each Raman excitation profile measurement.

Figure 3. The Raman spectrum of diphenyldecapentaene (DPDP) in cyclohexane/chloroform solution at room temperature obtained with excitation frequency 21720 cm^{-1}. The solvent lines of cyclohexane and chloroform are identified by * and +, respectively. The DPDP lines at 1160 cm^{-1} and 1565 cm^{-1} are unmarked.

Figure 4. Absorption spectrum of diphenyldecapentaene (DPDP) of ~$1x10^{-4}$M in a 0.5 cm cell at room temperature. The 0-0 band is at 419 nm (~23800 cm^{-1}). The 0-1 band at 394 nm is not resolved to its vibronic components as it is at 77K in Figure 18.

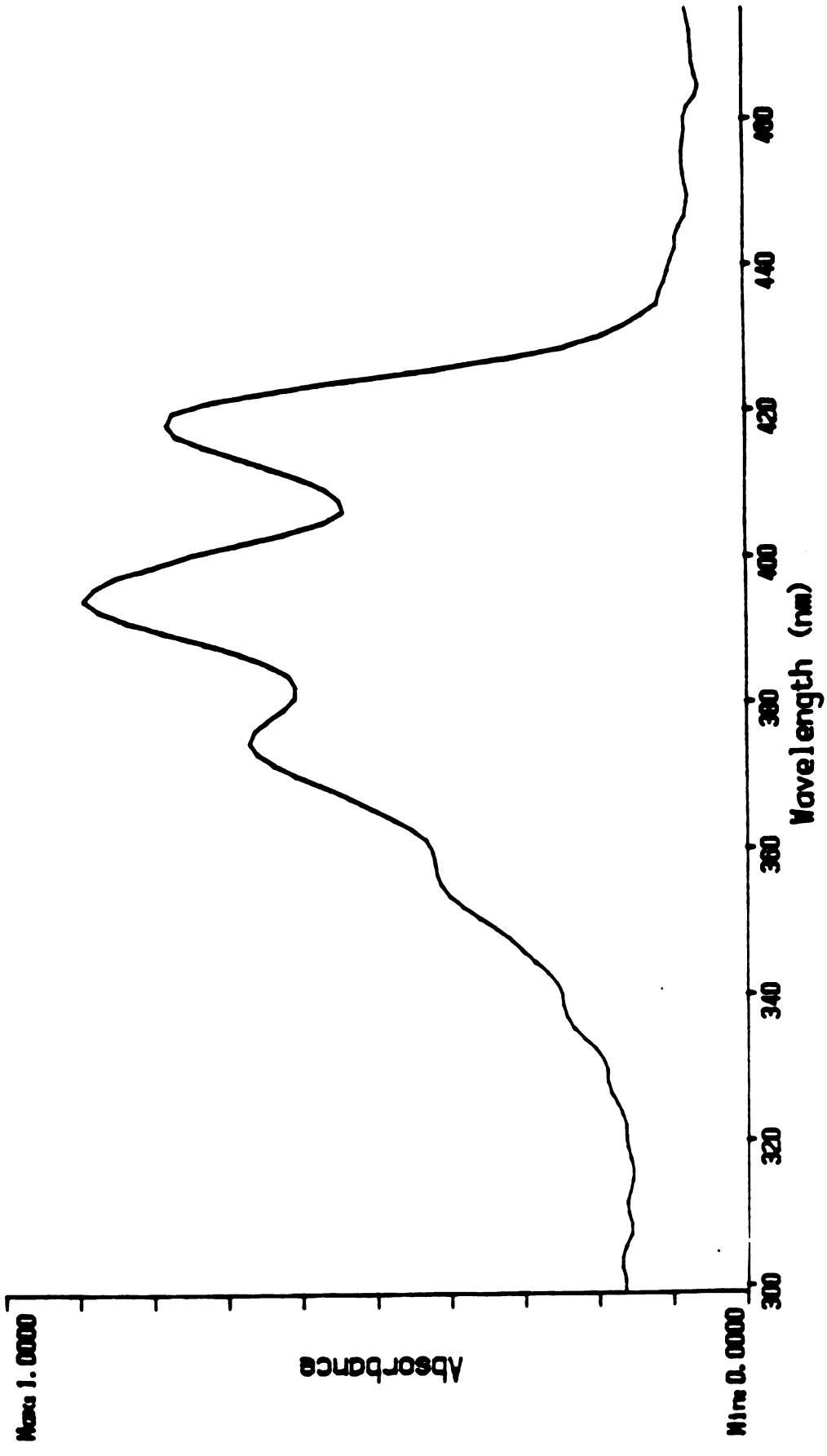
Max 1.0000
Absorbance
Min 0.0000
300
320
340
360
380
400
420
440
460
Wavelength (nm)

Figure 4.

A Coherent model 100 Argon ion laser, operating in the multiline UV (MLUV) mode (essentially 363.8 nm and 351.1 nm), was used to pump a Coherent model CR-599 cw dye laser. Dyes used were stilbene 420 and coumarin 480, to cover the excitation range: 20000-22700 cm^{-1}. The dye laser output power was kept constant at 45 mW and recorded to be 20 mW at the sample site.

A concentration of 1.5 x 10^{-3}M of stilbene 420 (also known as stilbene 3) dissolved in ethylene glycol had minimum lasing power output of 25 mW within the range 21400-24080 cm^{-1} when pumped by 3.5 Watts MLUV from the Ar^{+} laser. The maximum power output was measured at 22700 cm^{-1}, where the dye laser power exceeded 200 mW. A significant drop in laser power output ocurred within approximately 50 hours, indicating a chemical decomposition of the dye.

Coumarin 480 (also known as coumarin 102) does not absorb well at 364 nm or 351 nm. However, an energy transfer from stilbene 420 to coumarin 480 can be employed, where the emission of stilbene 420 will be absorbed by coumarin 480 whose fluorescence is utilized to initiate the lasing process. To a liter of stilbene 420 solution 0.75 grams of coumarin 480 dissolved in 75 ml of benzyl alcohol is added (Final solution concentration of ~2.9 x 10^{-3}M).[32] Pumped by ~4 Watts of MLUV the available range with a minimum power output of 45 mW began at 19960 cm^{-1}; the maximum power peaked at 21400 cm^{-1}, (The power output of various dyes generally has a Gaussian like shape as shown in

Figure 5. The power output of several dyes, pumped by a cw Ar^+ laser, as a function of the dye laser output wavelength (nm) range.[32]

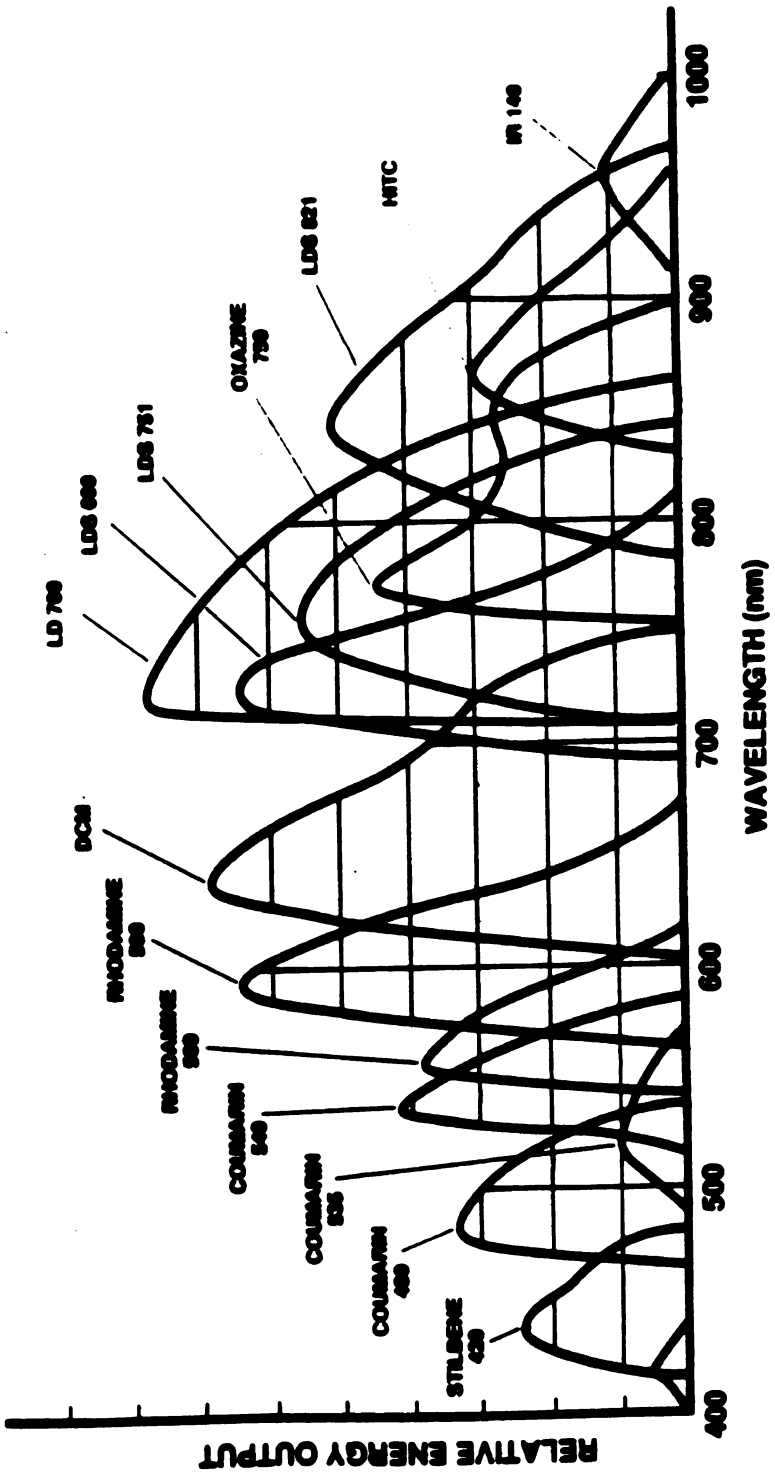
RELATIVE ENERGY OUTPUT
WAVELENGTH (nm)
400
500
600
700
800
900
1000
STILBENE 420
COUMARIN 480
COUMARIN 535
COUMARIN 540
RHODAMINE 590
RHODAMINE 640
DCM
LD 700
LDS 698
LDS 751
OXAZINE 750
LDS 821
HITC
IR 140

Figure 5.

Figure 6. A schematic diagram of the apparatus utilized in obtaining the Raman spectrum.

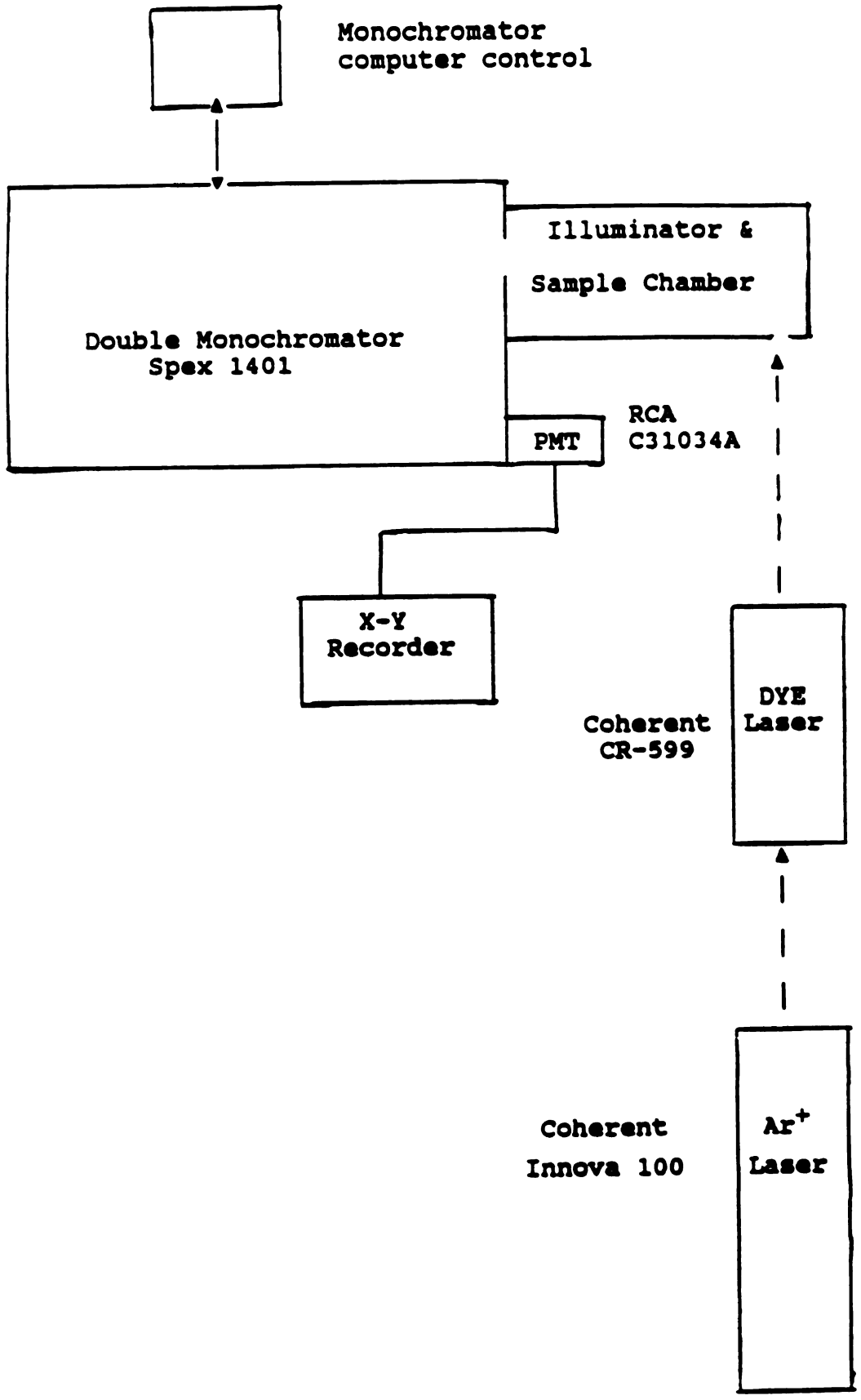
Monochromator
computer control
Illuminator &
Sample Chamber
Double Monochromator
Spex 1401
PMT
RCA
C31034A
X-Y
Recorder
DYE
Laser
Coherent
CR-599
Ar+
Laser
Coherent
Innova 100

Figure 6.

Figure 5. Thus it follows that the total available range from coumarin 480 under our experimental conditions is from ~20000 - 22800 cm^{-1}).

The Raman scattered radiation from room-temperature samples was collected at 90° to the incident laser beam, passed through a computer-controlled Spex 1401 double monochromator, and detected by an RCA C31034A photomultiplier tube cooled to -20°C. A schematic diagram of the apparatus utilize to obtain the Raman spectra is shown in Figure 6.

Each Raman excitation profile data point, which is an average of several measurements, was determined by obtaining the ratio of the area of the C=C symmetric stretch of DPDP at 1565 cm^{-1} to the area of the 1445 cm^{-1} band of cyclohexane. This can be done since the 0-0 absorption band for cyclohexane is at ~40000 cm^{-1}. Thus being far from resonance for cylclohexane or chloroform the preresonance REP range of 20000-22700 cm^{-1} corresponds to ordinary Raman scattering. Therefore by taking the ratio of the two peaks the $[(\nu-\nu_{GF})^4 / (\nu-\nu_{G'F'})^4] \sim 1$, canceling the ν^4 effect does cancel. Consequently the Raman intensity of the REP is entirely due to DPDP. The ratio is obtained by first drawing, a base line connecting both peaks, this is followed by enlarging the peaks, (using a Xerox copier with no distortion), to minimize the associated error in the cutting and weighing. Each individual peak is then cut out and weighed with an analytical balance. Since the paper density

is essentially constant, the weight ratio will be identical to the ratio of the corresponding peak areas. Figure 7 and Figure 8 shows such a typical Raman spectrum. The points in regions where the REP showed intensity ratios departing from the expected monotonic preresonance increase were repeated with several different samples on different occasions; each time these interference features were confirmed.

The Raman excitation profile of DPDP over the range 20000-22700 cm^{-1} was obtained in several overlapping segments. The DPDP concentration at the lower end, the 20000-21000 cm^{-1} region, was adjusted to be slightly higher than its concentration at the upper end; however for all segments it was maintained in the $\sim 10^{-4}M$ range. Concentration adjustment was necessary for otherwise the height of the Raman-active ground state C=C symmetric stretch would be either too intense or too weak relative to the nearby cyclohexane reference band, which was used as an internal standard. All REP segments were then scaled to the concentration of a central segment in the 21200-21700 cm^{-1} range. As an example the segment identified by Δ-Δ in Figure 9 is multiplied by a factor of 0.1825 and the segment identified as []-[] is scaled by a factor of 1.28. The central segment o-o is left unchanged. Data points of an REP segment which were not reproducible in the REP segments, such as the ones labeled by X, were not utilized in the final composite preresonance REP. Once normalized, an

Figure 7. A typical Raman spectrum of DPDP in cyclohexane /chloroform solution at an excitation frequency of 22200 cm^{-1}. The more intense band at 1565 cm^{-1} is the symmetric C=C stretch and the cyclohexane peak at 1445 cm^{-1} is used as an internal standard. The structure of DPDP is also shown.

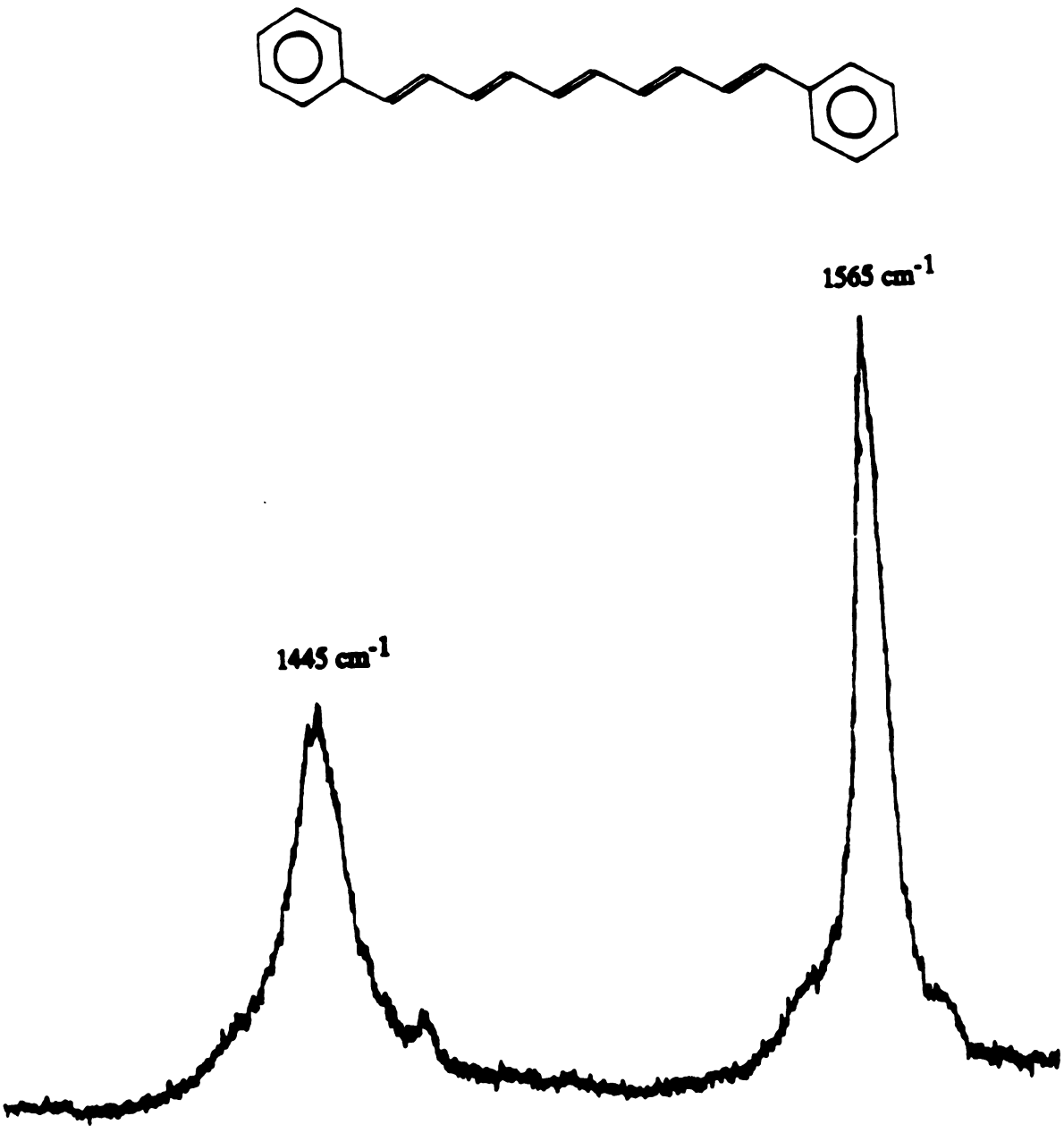

Figure 7.

Figure 8. A typical Raman spectrum of DPDP in cyclohexane /chloroform solution at various excitation frequencies. At ~2000 cm^{-1} below the 1^1B_u state, the cyclohexane peak at 1445 cm^{-1} is of greater intensity (bottom). At 21650 cm^{-1} both peaks are of approximately equal intensity (center). The DPDP 1565 cm^{-1} band is most intense for the excitation frequency of 22200 cm^{-1} (top).

Figure 9. A sample of the preresonance REP segments after adjustment were made to compensate for differences in concentration. Each segment other than the central segment was multiplied by an appropriate value. Points marked X, which were not reproducible in all overlapping segments, were not included in the the final composite spectrum.

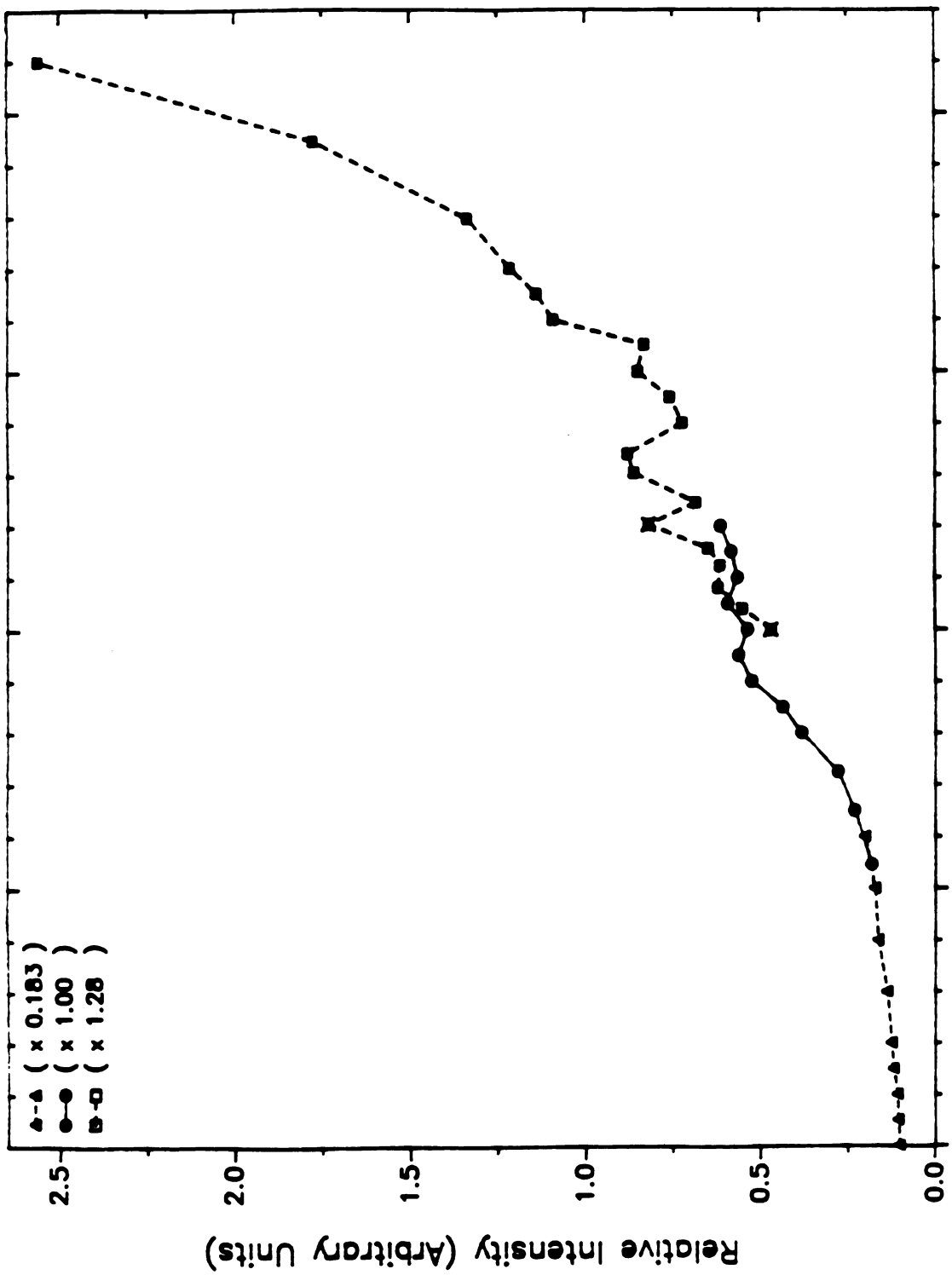
Relative Intensity (Arbitrary Units)
2.5
2.0
1.5
1.0
0.5
0.0
20400
20900
21400
21900
22400
wavenumbers (cm−1)
(x 0.183)
(x 1.00)
(x 1.28)

Figure 9.

averag

profil

obtain

compos

excita

Co

analyti

develop

prograr

These

disper

(equat

The re

harmor

formul

vibrat

state

the e

profi

average relative scattering intensity for each excitation profile point and its corresponding error distribution were obtained from the repeated measurements. The final composite REP, the intensity ratio $I_{C=C}/I_{ref}$ vs. dye laser excitation energy, is shown in Figure 10.

Computer programs for determining, graphically and analytically, the REP and the absorption cross-section, were developed for an IBM AT personal computer. (The detailed program listing is given in part B of the appendix I.) These programs are based on the Kramers-Heisenberg dispersion relation and the absorption cross-section (equations (4) and (11), respectively, in the next Chapter.) The requisite Franck-Condon integrals were calculated using harmonic oscillator eigenfunctions in the multimode formulation (three or four modes). A total of 23 vibrational states, 7 for the 2^1A_g state and 16 for the 1^1B_u state, were found necessary for an adequate description of the experimental spectra, both for the Raman excitation profile of DPDP and its absorption cross-section.

Figure 10. The experimental ([]-[]) preresonance Raman excitation profile of the symmetric C=C band of DPDP. The vertical bars correspond to the deviation error associated with each point of the REP.

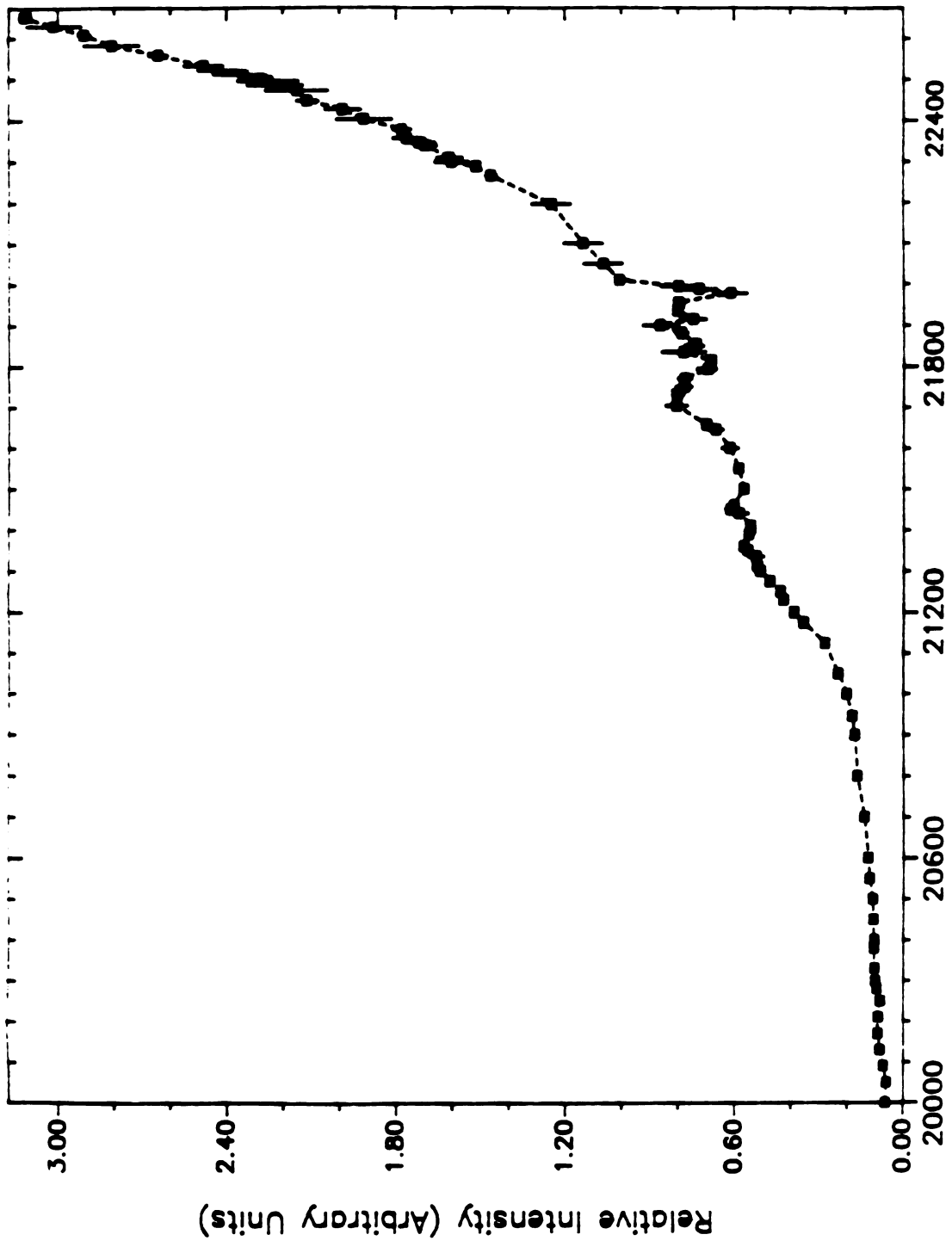
Relative Intensity (Arbitrary Units)
3.00
2.40
1.80
1.20
0.60
0.00
20000
20600
21200
21800
22400
wavenumbers (cm−1)

Figure 10.

T

transi

excite

molecu

where

scatte

fine

compor

T

Krame

$$\alpha_{\rho\sigma} =$$

where

vibror

incide

operat

CHAPTER III

THEORY

The Raman scattering cross-section for the Stokes transition from an initial vibronic state $|G\rangle$ to a final excited state $|F\rangle$, for a system of randomly oriented molecules, is given by[33]

$$\sigma_{GF} = \frac{2^5\pi^3}{3^2}\left[\frac{e^2}{\hbar c}\right]^2(\nu_0 - \nu_{GF})^4 \sum_{\rho,\sigma} |(\alpha_{\rho\sigma})_{GF}|^2 \qquad (1)$$

where ν_0 is the incident wavenumber and $(\nu_0 - \nu_{GF})$ is the scattered wavenumber (in cm^{-1}), respectively, $(e^2/\hbar c)$ is the fine structure constant, and ρ,σ = x,y,z designate the components of the molecular polarizability tensor.

The polarizability tensor may be expressed by the Kramers-Heisenberg dispersion relation[34,35]

$$\alpha_{\rho\sigma} = \frac{1}{\hbar}\sum_{\ell}\left[\frac{\langle F|\mu_\rho|\ell\rangle\langle\ell|\mu_\sigma|G\rangle}{\omega_\ell - \omega_0 + i\Gamma_\ell} + \frac{\langle F|\mu_\sigma|\ell\rangle\langle\ell|\mu_\rho|G\rangle}{\omega_\ell + \omega_0 + i\Gamma_\ell}\right] \qquad (2)$$

where $i\Gamma_\ell$ is the complex damping factor associated with the vibronic state $|\ell\rangle$ of energy $\hbar\omega_\ell$, $\hbar\omega_0$ is the energy of the incident radiation, $\mu_{\rho(\sigma)}$ is the total dipole moment operator (nuclear and electronic) in the $\rho(\sigma)$ direction, and

$\langle 1|\mu_0$

momen

vibra

excite

compon

the tr

final

Moreov

an al

(2) d

secon

appro

init

fina

of t

where

respe

momen

μ =

$\langle \ell | \mu_\sigma | G \rangle$ is the σth component of the transition dipole moment associated with the transition from the initial vibrational level of the ground electronic state $|G\rangle$ to the excited vibronic state $|\ell\rangle$. Similarly $\langle F | \mu_\rho | \ell \rangle$ is the ρth component of the transition dipole moment associated with the transition from the $|\ell\rangle$ excited vibronic state to the final vibrational level of the ground electronic state, $|F\rangle$. Moreover, in the near preresonance and resonance region of an allowed electronic transition the first term in equation (2) dominates and we may neglect the contribution from the second term, the antiresonance term.

We next apply the adiabatic Born-Oppenheimer approximation. The wavefunctions corresponding to the initial ground state, G, the intermediate state, ℓ, and the final excited state, F, may then be expressed as the product of the nuclear and electronic wavefunctions.

$$\Psi_G(r,R) = \Phi_g(r)\theta_0(R) \quad \leftrightarrow \quad |G\rangle = |g\rangle|0\rangle$$

$$\Psi_\ell(r,R) = \Phi_e(r)\theta_v(R) \quad \leftrightarrow \quad |\ell\rangle = |e\rangle|v\rangle$$

$$\Psi_F(r,R) = \Phi_g(r)\theta_n(R) \quad \leftrightarrow \quad |F\rangle = |g\rangle|n\rangle$$

where r, R are the electronic and nuclear coordinates respectively. We now write the total transition dipole moment as :

$$\mu = \mu_{nuc} + \mu_e$$

The transition moment in the numerator of equation (2) becomes:

$$\langle F|\mu_\rho|\ell\rangle = \langle F|\mu_{nuc}|\ell\rangle + \langle F|\mu_e|\ell\rangle \qquad (2a)$$

$$= \langle g|\{\langle 0|\mu_{nuc}|\upsilon\rangle\}|e\rangle + \langle g|\{\langle 0|\mu_e|\upsilon\rangle\}|e\rangle$$

or

$$\langle F|\mu_\rho|\ell\rangle = \langle g|e\rangle\langle 0|\mu_{nuc}|\upsilon\rangle + \langle 0|\{\langle g|\mu_e|e\rangle\}|\upsilon\rangle \qquad (2b)$$

Since the electronic eigenfunctions are orthonormal, that is

$$\int \Phi^*_g(r)\Phi_e(r)\, d^3r = \delta_{ge}$$

where δ_{ge} is the Kronecker delta, the first term in equation (2b) will vanishe for g≠e and the above reduces to

$$\langle F|\mu_\rho|\ell\rangle = \langle 0|\{\langle g|\mu_e|e\rangle\}|\upsilon\rangle$$

Similarily for $\langle\ell|\mu_\sigma|G\rangle$.

Thus the first term of the polarizability tensor, $\alpha_{\rho\sigma}$, in expression (2) becomes

$$\alpha_{\rho\sigma} = \frac{1}{\hbar} \sum_{\upsilon,e} \frac{\langle n|[\mu_\rho]_{ge}|\upsilon\rangle\langle\upsilon|[\mu_\sigma]_{eg}|0\rangle}{\omega_\upsilon - \omega_0 + i\Gamma_\upsilon} \qquad (3)$$

where $[\mu_\rho]_{ge} \equiv \langle g|\mu_\rho|e\rangle$ and $[\mu_\sigma]_{eg} \equiv \langle e|\mu_\sigma|g\rangle$ are components of the pure electronic transition moment, and where $|0\rangle$ and $|n\rangle$ are the initial and final electronic ground state

vibrational levels, respectively. For a totally symmetric vibration of a centrosymmetric linear polyene, only one diagonal element of the polarizability tensor, $\alpha_{\rho\rho}$, need be evaluated.[36]

Since the electronic transition moment is a slowly varying function of the internuclear distances, it may be expressed as a rapidly converging power series expanded about the equilibrium position in the normal coordinate Q_0.[27]

$$\langle g|\mu|e\rangle = [\mu_{ge}]_{Q_0} + \sum_{\kappa} \left[\frac{\partial \mu_{ge}}{\partial Q_\kappa}\right]_{Q_0}(Q_\kappa - Q_0) + \ldots \qquad (3a)$$

The numerator of equation (3), $\langle n|[\mu_\rho]_{ge}|v\rangle\langle v|[\mu_\sigma]_{eg}|0\rangle$, then becomes

$$= \left\{ \langle n| \left[[\mu_{ge}]_{Q_0} + \sum_{\kappa} \left[\frac{\partial \mu_{ge}}{\partial Q_\kappa}\right]_{Q_0}(Q_\kappa - Q_0) + \ldots \right] |v\rangle \right.$$

$$\left. \times \langle v| \left[[\mu_{eg}]_{Q_0} + \sum_{\kappa} \left[\frac{\partial \mu_{eg}}{\partial Q_\kappa}\right]_{Q_0}(Q_\kappa - Q_0) + \ldots \right] |0\rangle \right\}$$

or

$$= \left\{ \left[\langle n|[\mu_{ge}]_{Q_0}|v\rangle + \sum_{\kappa} \left[\frac{\partial \mu_{ge}}{\partial Q_\kappa}\right]_{Q_0} \langle n|(Q_\kappa - Q_0)|v\rangle + \ldots \right] \right.$$

$$\left. \times \left[\langle v|[\mu_{eg}]_{Q_0}|0\rangle + \sum_{\kappa} \left[\frac{\partial \mu_{eg}}{\partial Q_\kappa}\right]_{Q_0} \langle v|(Q_\kappa - Q_0)|0\rangle + \ldots \right] \right\}$$

The first term in each factor simplifies, giving

$$= \left\{ \left[[\mu_{ge}]_{Q_0} \langle n|v\rangle + \sum_{\kappa} \left[\frac{\partial \mu_{ge}}{\partial Q_\kappa}\right]_{Q_0} \langle n|(Q_\kappa - Q_0)|v\rangle + \ldots \right] \right.$$

$$\left. \times \left[[\mu_{eg}]_{Q_0} \langle v|0\rangle + \sum_{\kappa} \left[\frac{\partial \mu_{eg}}{\partial Q_\kappa}\right]_{Q_0} \langle v|(Q_\kappa - Q_0)|0\rangle + \ldots \right] \right\}$$

After expansion, the product

$$= \left\{ |\mu_{ge}|^2_{Q_0} \langle n|v\rangle\langle v|0\rangle \right. \tag{3b}$$

$$+ [\mu_{ge}]_{Q_0} \sum_{\kappa} \left[\frac{\partial \mu_{ge}}{\partial Q_\kappa}\right]_{Q_0} \langle n|(Q_\kappa - Q_0)|v\rangle\langle v|0\rangle$$

$$\left. + [\mu_{eg}]_{Q_0} \sum_{\kappa} \left[\frac{\partial \mu_{eg}}{\partial Q_\kappa}\right]_{Q_0} \langle n|v\rangle\langle v|(Q_\kappa - Q_0)|0\rangle \right\}$$

where the high order terms has been neglected.

For a single normal coordinate, Q_κ, the product

$$= \left\{ |\mu_{ge}|^2_{Q_0} \langle n|v\rangle\langle v|0\rangle \right.$$

$$+ [\mu_{ge}]_{Q_0} \left[\frac{\partial \mu_{ge}}{\partial Q_\kappa}\right]_{Q_0} \langle n|(Q_\kappa - Q_0)|v\rangle\langle v|0\rangle$$

$$\left. + [\mu_{eg}]_{Q_0} \left[\frac{\partial \mu_{eg}}{\partial Q_\kappa}\right]_{Q_0} \langle n|v\rangle\langle v|(Q_\kappa - Q_0)|0\rangle \right\} \tag{3c}$$

For a given excited electronic state e, equation (3) becomes

$$\alpha_{\rho\rho} = \frac{1}{\hbar}\left\{ |\mu_{ge}|^2_{Q_0} \sum_{\upsilon_e} \frac{\langle n|\upsilon\rangle\langle\upsilon|0\rangle}{\omega_\upsilon - \omega_0 + i\Gamma_\upsilon} + [\mu_{ge}]_{Q_0} \left[\frac{\partial \mu_{ge}}{\partial Q_\kappa}\right]_{Q_0} \sum_{\upsilon_e} \frac{\langle n|(Q_\kappa - Q_0)|\upsilon\rangle\langle\upsilon|0\rangle}{\omega_\upsilon - \omega_0 + i\Gamma_\upsilon} + [\mu_{eg}]_{Q_0} \left[\frac{\partial \mu_{eg}}{\partial Q_\kappa}\right]_{Q_0} \sum_{\upsilon_e} \frac{\langle n|\upsilon\rangle\langle\upsilon|(Q_\kappa - Q_0)|0\rangle}{\omega_\upsilon - \omega_0 + i\Gamma_\upsilon} \right\} \quad (3d)$$

The first term in the series (known also as the A-term) will dominate provided that the magnitude $|(\partial\mu_{ge}/\partial Q)_0| << |(\mu_{ge})_0|$. This will be valid for a centrosymmetric linear polyene in the preresonance or resonance region for a totally symmetric vibrational mode.[37] In addition, for the case of a dipole forbidden state, the need for the second term (the B-term) in the expansion can be avoided by introducing an empirical value for the forbidden transition moment.[19]

Under these conditions, the polarizability expression for such a system with two excited electronic states, e and s, reduces to

$$\alpha_{\rho\rho} = \frac{1}{\hbar}\left[|\mu_{ge}|^2 \sum_{\upsilon_e} \frac{\langle \bar{n}|\bar{\upsilon}_e\rangle\langle\bar{\upsilon}_e|\bar{0}\rangle}{\omega_\upsilon - \omega_0 + i\Gamma_\upsilon} + |\mu_{gs}|^2 \sum_{\upsilon_s} \frac{\langle \bar{n}|\bar{\upsilon}_s\rangle\langle\bar{\upsilon}_s|\bar{0}\rangle}{\omega_\upsilon - \omega_0 + i\Gamma_\upsilon} \right] \quad (4)$$

where the coefficients $|\mu_{ge}|^2$, $|\mu_{gs}|^2$ are proportional to the corresponding oscillator strengths for the transition from the ground state to the electronic states e and s, respectively. Namely, $f_{eg} = [(8\pi mc)/(6\hbar e^2)]\nu|\mu_{eg}|^2$, where ν is the wavenumber of the transition and $|\mu|$ is the electronic transition moment.[38]

In the limit of no Duschinsky mixing (normal coordinate rotation), the multidimensional Franck-Condon integral $\langle\bar{n}|\bar{v}_e\rangle$ can be factored into products of one-dimensional integrals[39-41]

$$\langle\bar{n}|\bar{v}_e\rangle = \prod_{i=1}^{m} \langle n_{ig}|v_{ie}\rangle \tag{5}$$

where m is the number of normal modes.

In particular, for Raman scattering arising from the ath, totally symmetric fundamental mode, the multimode expression becomes

$$\langle\bar{1}_g|\bar{v}_e\rangle\langle\bar{v}_e|\bar{0}_g\rangle = \langle 1_{ag}|v_{ae}\rangle\langle v_{ae}|0_{ag}\rangle \prod_{i\neq a} \langle 0_{ig}|v_{ie}\rangle\langle v_{ie}|0_{ig}\rangle \tag{6}$$

For example, in the case where the ath mode corresponds to ν_1, in a multimode formulation involving only three modes: ν_1, ν_2, ν_3 and for excitation in resonance with the vibrational fundamental ν_2 in the excited state, equation (6) reduces to

$$\begin{aligned}\langle\bar{1}_g|\bar{v}_e\rangle\langle\bar{v}_e|\bar{0}_g\rangle = {} & [\langle 1_g|0_e\rangle\langle 0_e|0_g\rangle]_{\nu_1}[\langle 0_g|1_e\rangle\langle 1_e|0_g\rangle]_{\nu_2} \\ & \times [\langle 0_g|0_e\rangle\langle 0_e|0_g\rangle]_{\nu_3}\end{aligned} \tag{7}$$

The Raman Franck-Condon integrals utilized in the REP model are shown in Appendix II, Table A.

We may describe the Franck-Condon factors by the harmonic oscillator eigenfunction basis. These overlap integrals are a function of the displacement of the excited state potential curve for each normal coordinate from the corresponding ground state position, $\Delta_a = (Q_{ag}-Q_{ae})_0$, and of the corresponding vibrational frequencies in the ground $(\nu_g)_a$ and excited $(\nu_e)_a$ electronic states.[39,41-43] The relationship of ground and excited electronic potential curves to one another is exemplified in Figure 11.

The one-dimensional overlap integrals may be evaluated by using the Manneback recurrence relations:[26,44,45]

$$\langle 0|0\rangle = \frac{2(\nu_e\,\nu_g)^{1/4}}{\nu_e+\nu_g}\exp\left[-\frac{\pi c}{\hbar}\,\frac{\nu_e\,\nu_g}{\nu_e+\nu_g}\,\Delta^2_{eg}\right] \tag{8}$$

$$\langle \upsilon_e|m_g+1\rangle = \left[\frac{m}{m+1}\right]^{1/4}\frac{\nu_g-\nu_e}{\nu_e+\nu_g}\langle \upsilon_e|m_g-1\rangle + \left[\frac{\upsilon}{m+1}\right]^{1/4}\frac{2(\nu_e\,\nu_g)^{1/4}}{\nu_e+\nu_g}\langle \upsilon_e-1|m_g\rangle$$
$$+ \left[\frac{1}{m+1}\right]^{1/4}\left[\frac{4\pi c}{\hbar}\right]^{1/4}\frac{\nu_e\,\nu_g^{1/4}}{\nu_e+\nu_g}\Delta_{eg}\langle \upsilon_e|m_g\rangle \tag{9}$$

$$\langle \upsilon_e+1|m_g\rangle = -\left[\frac{\upsilon}{\upsilon+1}\right]^{1/4}\frac{\nu_g-\nu_e}{\nu_e+\nu_g}\langle \upsilon_e-1|m_g\rangle + \left[\frac{m}{\upsilon+1}\right]^{1/4}\frac{2(\nu_e\,\nu_g)^{1/4}}{\nu_e+\nu_g}\langle \upsilon_e|m_g-1\rangle$$
$$- \left[\frac{1}{\upsilon+1}\right]^{1/4}\left[\frac{4\pi c}{\hbar}\right]^{1/4}\frac{\nu_g\,\nu_e^{1/4}}{\nu_e+\nu_g}\Delta_{eg}\langle \upsilon_e|m_g\rangle \tag{10}$$

Figure 11. A two electronic state system with a displacement parameter shift, Δ_{eg}. The electronic transition moments associated with the Raman process and the harmonic oscillator wave functions representing the ground and fundamental modes are illustrated. {Some authors express Δ^2 by multiplying it by $(\pi c/\hbar)\nu$; this results in a unitless expression with a numerical value greater by a factor of 10 than that given in $(amu)^{1/2}$Å }.[43,45]

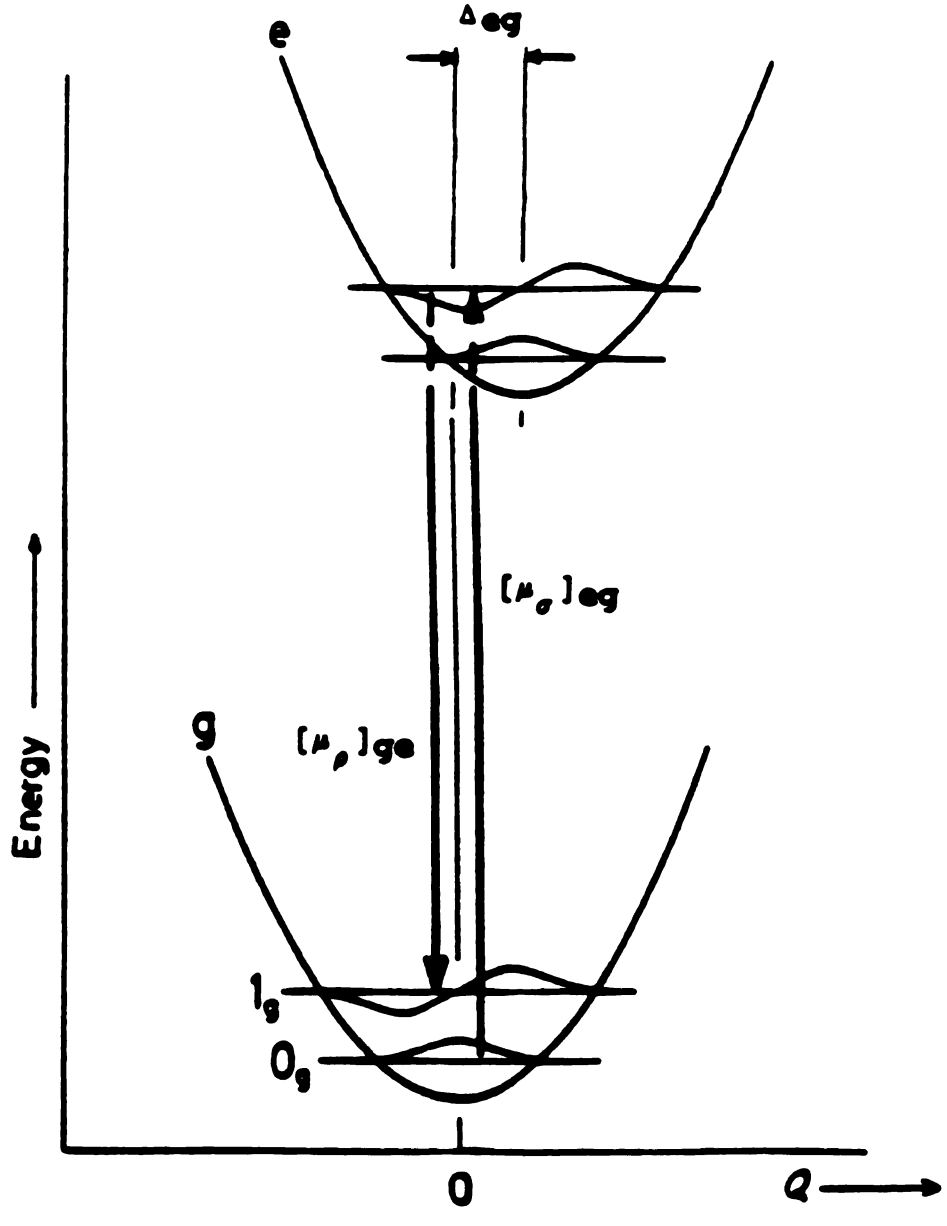

Figure 11.

Thus the Franck-Condon integrals which constitute the 2^1A_g vibrational states utilized in the model (Plus the overtone, shown here for completeness only) are:

$$\langle 0|0\rangle = \frac{2(\nu_e \nu_g)^{1/2}}{\nu_e + \nu_g} \exp\left[-\frac{\pi c}{\hbar} \frac{\nu_e \nu_g}{\nu_e + \nu_g} \Delta^2 eg\right] \tag{8}$$

From equation (9)

$$\langle 0_e|1_g\rangle = 2\left[\frac{\pi c}{\hbar}\right]^{1/2} \frac{\nu_e (\nu_g)^{1/2}}{(\nu_e + \nu_g)} \Delta_{eg} \langle 0|0\rangle \tag{9a}$$

From equation (10)

$$\langle 1_e|0_g\rangle = -2\left[\frac{\pi c}{\hbar}\right]^{1/2} \frac{\nu_g (\nu_e)^{1/2}}{(\nu_e + \nu_g)} \Delta_{eg} \langle 0|0\rangle \tag{10a}$$

From equation (9)

$$\langle 1_g|1_e\rangle = \left[\frac{2(\nu_g \nu_e)^{1/2}}{\nu_e + \nu_g} - \left[\frac{4\pi c}{\hbar}\right] \frac{(\nu_g \nu_e)^{3/2}}{(\nu_e + \nu_g)^2} \Delta_{eg}^2 \right] \langle 0|0\rangle \tag{9b}$$

From equation (10

$$\langle 0_g|2_e\rangle = \frac{1}{\sqrt{2}} \left[\frac{\nu_g - \nu_e}{\nu_e + \nu_g} + \left[\frac{4\pi c}{\hbar}\right] \frac{\nu_e (\nu_g)^2}{(\nu_e + \nu_g)^2} \Delta_{eg}^2 \right] \langle 0|0\rangle \tag{10b}$$

$$\langle 1_g|2_e\rangle = \frac{\left[\frac{2\pi c}{\hbar}\right]^{1/2} \left[\nu_e \nu_g\right]^{1/2}}{(\nu_e + \nu_g)^2} \left\{ \left[\frac{4\pi c}{\hbar}\right] \frac{(\nu_g)^{3/2} (\nu_e)^{4/2}}{\nu_e + \nu_g} \Delta_{eg}^2 \right.$$

$$\left. -[\nu_e]^{1/2}[\nu_g - \nu_e] - 4[\nu_e]^{1/2}[\nu_g] \right\} \Delta_{eg}^2 \langle 0|0\rangle \tag{10c}$$

In the specific case of the linear polyenes, for the electronic transition from the 1^1A_g ground state to the 1^1B_u excited state we may take $\nu_e \cong \nu_g$, where ν_e, ν_g are the vibrational frequencies of a given mode for the corresponding electronic states. [Of course, this approximation does not apply to the $1^1A_g \rightarrow 2^1A_g$ (hidden) transition, because of large frequency differences, as much as 250 cm^{-1},[6] associated with vibrational modes of linear polyenes in the 2^1A_g excited state.] This leads to considerable simplification in the above recurrence relations, equations (8)-(10)

$$\langle 0|0\rangle = \exp\left[-\frac{\pi c}{\hbar}\frac{\nu}{2}(\Delta_{eg})^2\right] \qquad (8')$$

$$\langle v_e|m_g+1\rangle = \left[\frac{v}{m+1}\right]^{1/2}\langle v_e-1|m_g\rangle + \left[\frac{1}{m+1}\right]^{1/2}\left[\frac{4\pi c}{\hbar}\right]^{1/2}\frac{\nu^{1/2}}{2}\Delta_{eg}\langle v_e|m_g\rangle \qquad (9')$$

$$\langle v_e+1|m_g\rangle = \left[\frac{m}{v+1}\right]^{1/2}\langle v_e|m_g-1\rangle - \left[\frac{1}{v+1}\right]^{1/2}\left[\frac{4\pi c}{\hbar}\right]^{1/2}\frac{\nu^{1/2}}{2}\Delta_{eg}\langle v_e|m_g\rangle \qquad (10')$$

Thus the Franck-Condon integrals utilized for the REP model are:

$$\langle 0|0\rangle = \exp\left[-\frac{\pi C}{\hbar}\frac{\nu}{2}(\Delta_{eg})^2\right] \tag{8'}$$

From 9'

$$\langle 0_e|1_g\rangle = 2\left[\frac{\pi C}{\hbar}\right]^{1/2}\frac{\nu^{1/2}}{2}\Delta_{eg}\langle 0|0\rangle \tag{9a'}$$

From 10'

$$\langle 1_e|0_g\rangle = -2\left[\frac{\pi C}{\hbar}\right]^{1/2}\frac{\nu^{1/2}}{2}\Delta_{eg}\langle 0|0\rangle \tag{10a'}$$

$$\langle 1_g|1_e\rangle = \left[1 - \frac{\pi C}{\hbar}\nu(\Delta_{eg})^2\right]\langle 0|0\rangle \tag{9b'}$$

$$\langle 0_g|2_e\rangle = \left[\frac{\pi C}{\hbar}\right]\nu(\Delta_{eg})^2\langle 0|0\rangle \tag{10b'}$$

$$\langle 1_g|2_e\rangle = \left[\frac{2\pi C}{\hbar}\right]^{1/2}\nu^{1/2}\left[\left[\frac{\pi C}{2\hbar}\right](\Delta_{eg})^2 - 1\right](\Delta_{eg})\langle 0|0\rangle \tag{10c'}$$

$$\langle 0_g|3_e\rangle = \frac{-1}{\sqrt{3}}\left[\frac{\pi C\nu}{\hbar}\right]^{3/2}(\Delta_{eg})^3\langle 0|0\rangle \tag{10d'}$$

$$\langle 1_g|3_e\rangle = \left\{1 - \sqrt{2}\left\{\left[\frac{\pi C\nu}{2\hbar}\right](\Delta_{eg})^2 - 1\right\}\right\}\frac{-1}{\sqrt{3}}\left[\frac{\pi C\nu}{\hbar}\right](\Delta_{eg})^2\langle 0|0\rangle \tag{10e'}$$

$$\langle 0_g | 4_e \rangle = \frac{-1}{2} \left[\frac{\pi C \nu}{\hbar}\right]^{1/2} (\Delta_{eg}) \langle 3_e | 0_g \rangle \qquad (10f')$$

$$\langle 1_g | 4_e \rangle = \frac{1}{2}\left[\langle 4_e | 0_g \rangle - \frac{1}{2} \left[\frac{\pi C \nu}{\hbar}\right]^{1/2} (\Delta_{eg}) \langle 3_e | 1_g \rangle \right] \qquad (10g')$$

The absorption cross-section[39,40,46,47] is given by

$$\sigma_{abs} \simeq \sum_{\upsilon} \frac{|\langle \bar{0} | \bar{\upsilon} \rangle|^2 \Gamma_\upsilon \omega_\upsilon}{(\omega_\upsilon - \omega_0)^2 + \Gamma_\upsilon^2} \qquad (11)$$

$$\text{where} \quad \langle \bar{0} | \bar{\upsilon} \rangle = \prod_{i=1}^{m} \langle 0_{ig} | \upsilon_{ie} \rangle$$

Γ_υ is the homogeneous linewidth of the vibronic state $|\upsilon\rangle$ having energy $\hbar\omega_\upsilon$, and $\hbar\omega_0$ is the energy of the incident radiation. The Franck-Condon integrals utilized for the model absorption spectrum are collected in Appendix II, Table B (The Raman Franck-Condon integrals differs from ordinary Franck-Condon integrals in being a product of two Franck-Condon integrals rather than a single integral). As with the Raman cross-section, the sum is over the vibronic subspace associated with the electronic state e.

CHAPTER IV

RESULTS

4.1 Vibronic Features of the Preresonanace Raman Excitation Profile

The experimental REP for the symmetric C=C stretch (hereafter designated ν_1) of DPDP in cyclohexane at room temperature in the preresonance region from 20000-22700 cm^{-1} is shown in Figure 10 on page 22. A vertical line designates the reproducibility of each data point. As the incident radiation is tuned towards the 1^1B_u dipole-allowed excited state, for which the 0-0 absorption maximum lies at 23,750 cm^{-1} in cyclohexane, it is expected that the Raman intensity would continue to increase monotonically,[27] if the 1^1B_u state was the lowest excited singlet state. (This is simulated in Figure 12 by a calculated excitation profile for which the 2^1A_g oscillator strength is chosen to be vanishingly small.) Instead, we observe spectroscopic features which result from constructive and destructive interference between an underlying, weakly-allowed state and the nearby 1^1B_u excited state.

The departure from the smooth intensity increase in the preresonance REP of DPDP shown in Figure 12 manifests itself

Figure 12. Experimental preresonanace REP ([]-[]) and the calculated preresonanace REP (——) (fourth ν_8 mode is included).

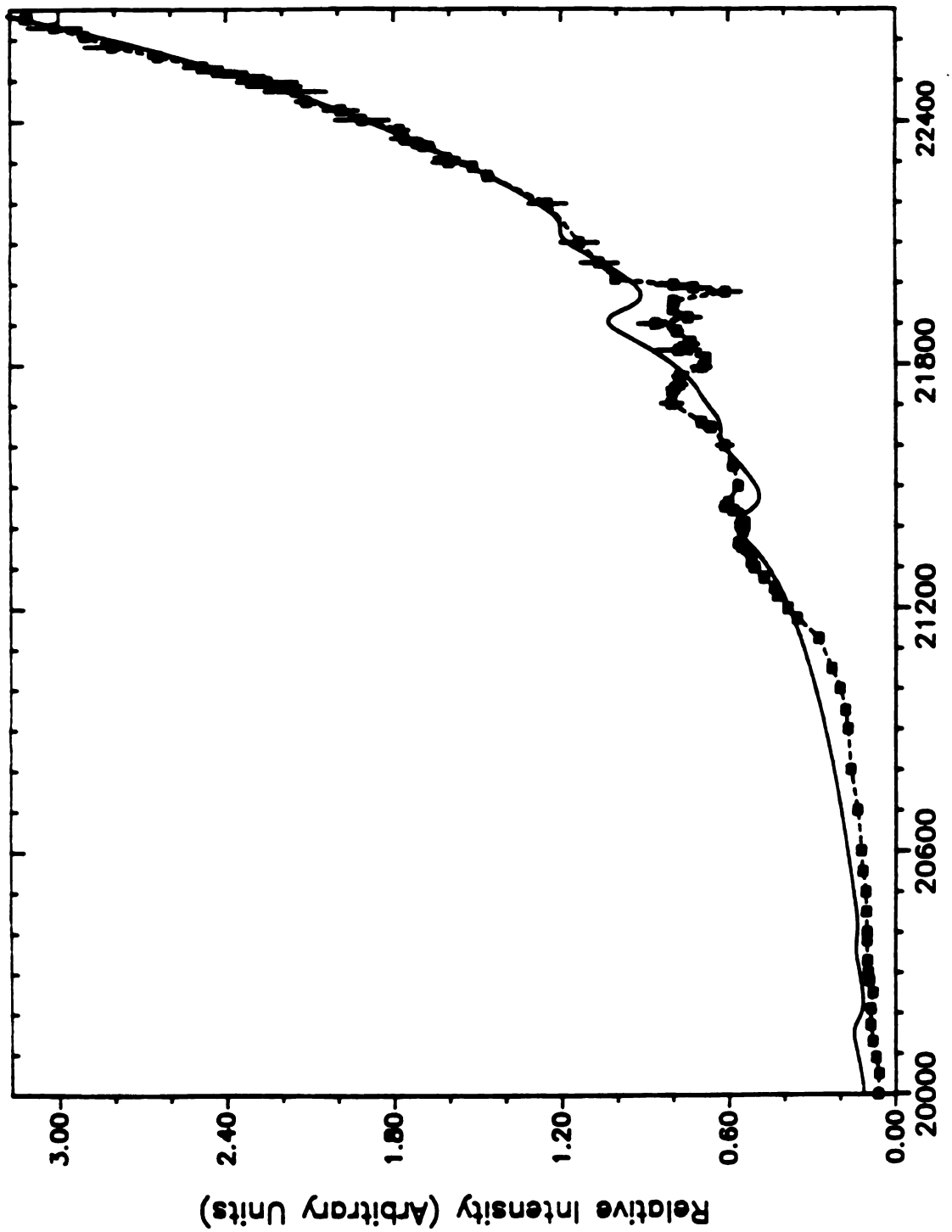
Relative Intensity (Arbitrary Units)
3.00
2.40
1.80
1.20
0.60
0.00
20000
20600
21200
21800
22400
wavenumbers (cm-1)

Figure 12.

initially as a steep ascent which begins at ~21100 cm^{-1} and continues to ~21300 cm^{-1}, where it culminates in a plateau on which there are several undulations. The lower energy features, at approximately 21350 cm^{-1}, and 21425 cm^{-1}, as well as the higher energy components at approximately 21700 cm^{-1} and 21900 cm^{-1}, dominate the preresonanace region. A relatively sharp drop in intensity is measured near 21975 cm^{-1}, before the excitation profile resumes its monotonic increase in intensity as the strongly allowed 1^1B_u state is approached. From the experimental data, the depth of this fairly sharp dip appears to be a function of solvent polarizability (i.e. concentration of chloroform in cyclohexane). Moreover, it seems to be part of the vibronic pattern associated with the feature at ~21900 cm^{-1}. Unlike peaks in fluorescence or absorption spectra, due to the overlapping interference effects of several vibrations the structure in the Raman excitation profile is not easily directly associated with the 2^1A_g vibrational modes. Consequently the interpretation of the preresonance Raman excitation region requires additional analysis, which is provided by a theoretical approach.

In general, for linear polyenes the C-C and C=C vibrational modes dominate in fluorescence, fluorescence excitation, and absorption, for both the 2^1A_g and the 1^1B_u excited states.[11,48] For DPDP, the most intense band seen in high resolution fluorescence excitation of the 2^1A_g state is assigned by Horwitz et al.[9] to the symmetric C=C stretch,

at a 1750 cm^{-1} shift from the electronic origin (The fluorescence excitation spectrum from reference 9 was manually fit and digitized; it was then simulated by a theoretical model as shown in Figure 13. The absorption cross-section expression of equation (11) is employed for this purpose. A quick look at the fluorescence excitation spectrum for the 1^1B_u state of reference 9 and the 77K absorption spectrum in Figure 18 will convince the reader of this.) It seems reasonable to assign by direct comparison the strongest feature in the preresonance Raman excitation profile, at approximately 21900 cm^{-1}, to the same C=C vibration.

A similar comparison for the remaining spectroscopic features is not as straightforward, primarily due to the presence of the interference effects. It is here that the Raman excitation model is of paramount importance. The interference features generated by the model on the basis of very few parameters, obtained *without adjustment* from other sources, replicate the experimental Raman excitation spectral data as illustrated in Figure 14 . Although the simplified model does not account for all the details, it does satisfy our primary objective by providing an interpretation for the salient aspects of the excitation profile. It enables us to establish a one-to-one correspondence between the prominent Raman interference features, belonging to the hidden 2^1A_g excited state, and the vibrational frequencies previously determined by various

Figure 13. High resolution fluorescence excitation of the 2^1A_g state. The digitized data points were obtained from reference 9. The effect of including (——) and excluding (- - -) the ν_8 mode from the multimode formulation in the best fit model is shown. Although this effect is easilly seen here, it is not as apparent in the preresonance REP shown in Figure 12 and Figure 14.

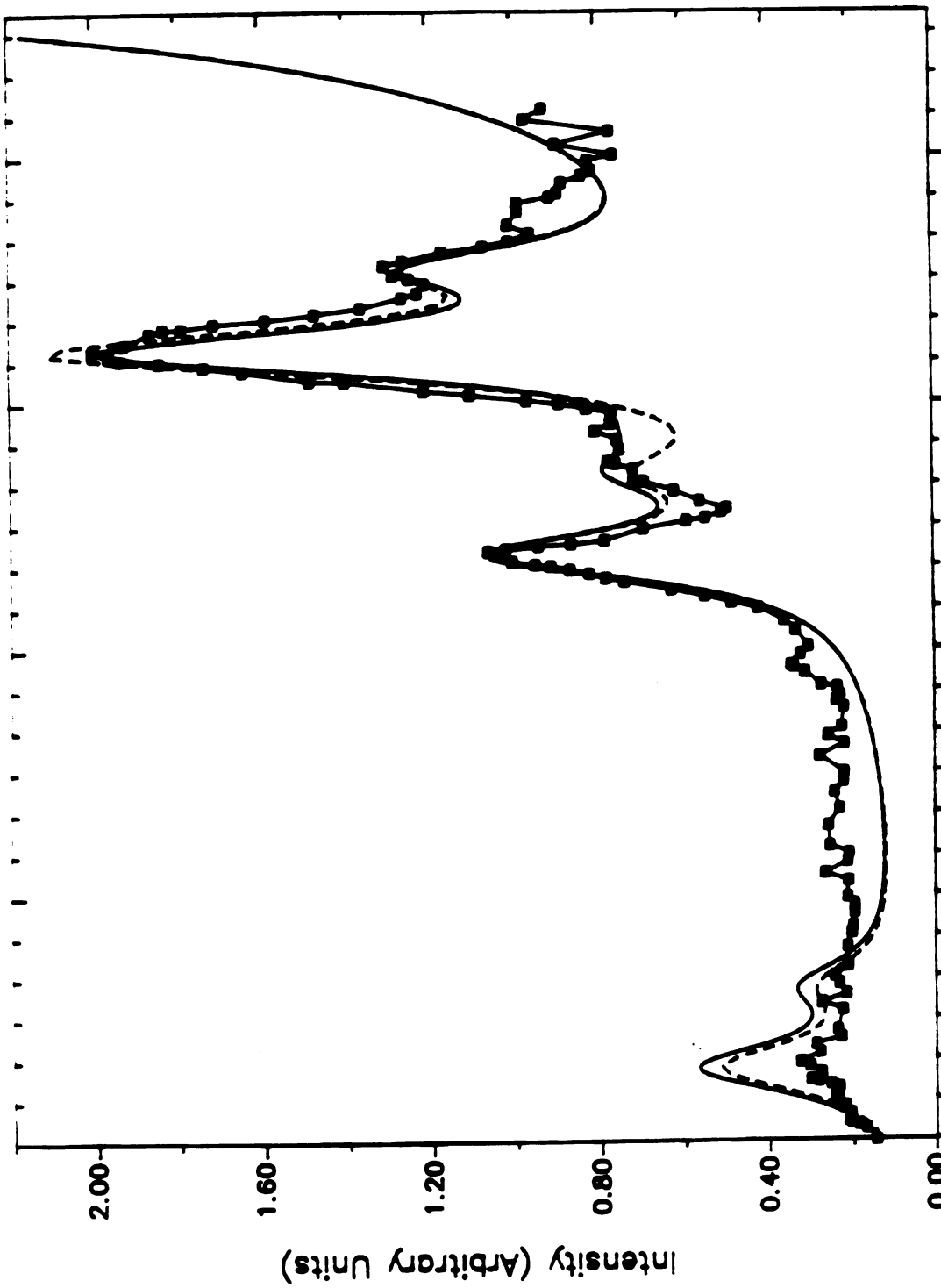
Intensity (Arbitrary Units)
2.00
1.60
1.20
0.80
0.40
0.00
20000
20600
21200
21800
22400
wavenumbers (cm−1)

Figure 13.

spectroscopic techniques. Thus the vibrational mode identified as the C-C stretch in the fluorescence excitation spectrum[9] of Figure 13 is manifested in the REP as an interference feature on the plateau at approximately 21425 cm^{-1}, as seen in Figure 14. This corresponds to a vibrational frequency of 1250 cm^{-1}. (A number of fundamental vibrational frequencies are observed in the 1000-1400 cm^{-1} region for a typical linear polyene;[49,50] such modes may account for some of the additional structure observed in the vicinity of 21425 cm^{-1}.) The remaining prominent interference features can be interpreted in terms of combination bands of only three polyene fundamental modes, which we will call ν_1 (symmetric C=C stretch), ν_2 (symmetric C-C stretch) and ν_3 (symmetric bend). [A fourth mode, assigned as a phenyl vibration (ν_8) in the fluorescence excitation,[9] is included for completeness. Although its presence is clearly observed in the fluorescence excitation model, it has very little effect on the preresonance REP.]

4.2 The 2^1A_g Electronic Origin

The electronic origin for the 2^1A_g excited state, being of gerade vibronic symmetry, is inaccessible by a one-photon process from the ground state. However, such origins have been detected by high resolution fluorescence excitation when the guest molecule is situated in a symmetry-perturbing

Figure 14. The calculated preresonance Raman excitation profile of DPDP (——) and an REP for which the 2^1A_g oscillator strength is chosen to be vanishingly small (—— ——). The effect of excluding the ν_8 mode from the multimode formulation for the REP (- - -) is also shown.

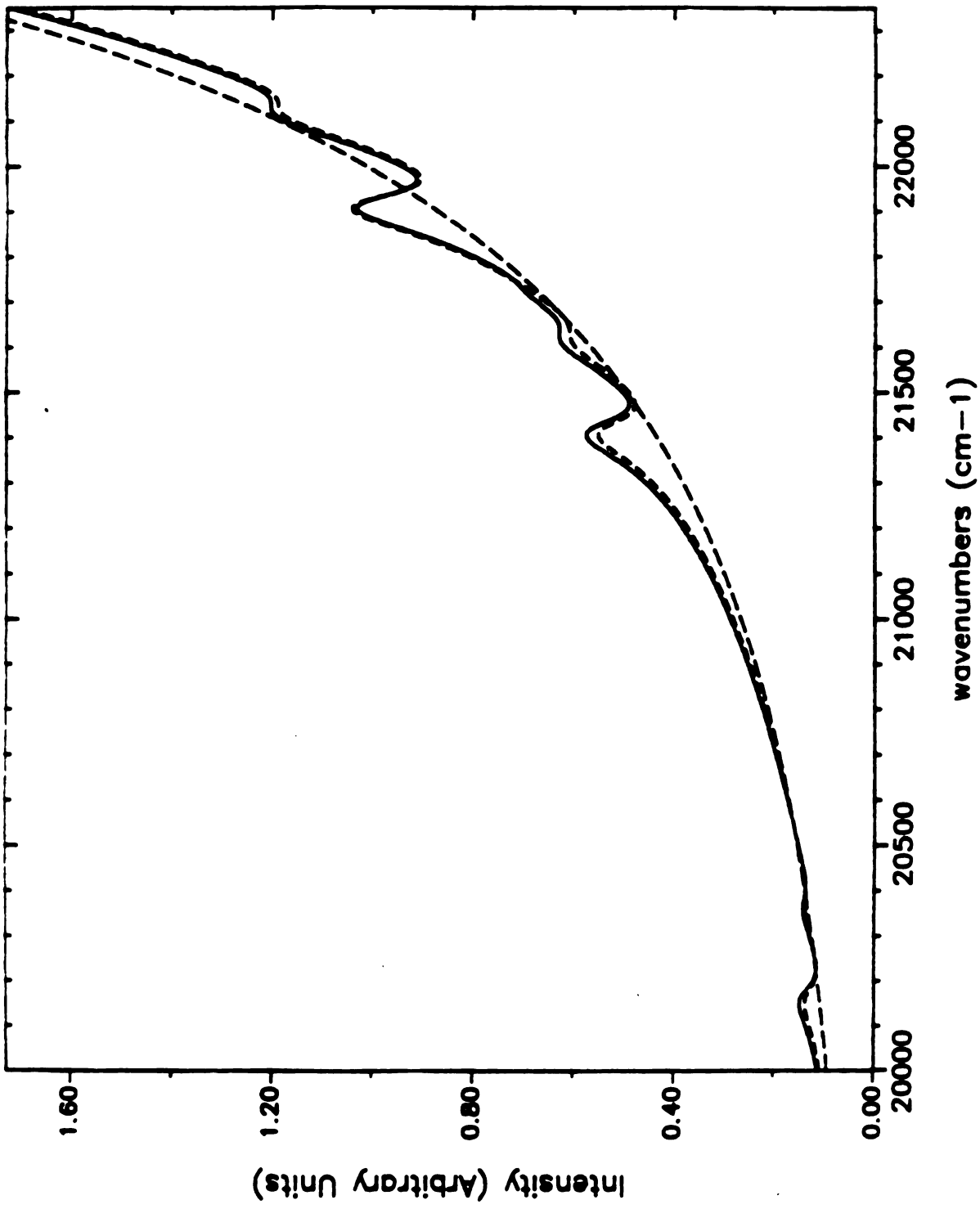
Intensity (Arbitrary Units)
0.00
0.40
0.80
1.20
1.60
20000
20500
21000
21500
22000
wavenumbers (cm-1)

Figure 14.

environment, such as a Shpolskii matrix.[7,10] The electronic origin of the 2^1A_g state of DPDP has been observed at 20130 cm^{-1} via absorption and fluorescence excitation measurements on the molecule isolated in an n-decane host at 4.2 K.[9] (In hosts where polyenes retain their center of symmetry the origin is absent, yet strong spectroscopic progressions built on a low-frequency promoting mode are observed.[51])

In the preresonance Raman excitation of DPDP, two weak features separated by ~200 cm^{-1} are observed in an otherwise featureless region in the vicinity of the reported origin, one at 20175 cm^{-1} and the other at 20375 cm^{-1}. An expanded view of this region of the REP is shown in Figure 15 . Two possible interpretations are:

(1) Two low-frequency vibrational modes, and

(2) The 2^1A_g electronic origin and a nearby low-frequency vibrational mode.

Low energy vibrational modes are commonly observed for polyenes in the 50-300 cm^{-1} range;[6,49,51] the first interpretation would thus place the 2^1A_g origin below 20175 cm^{-1}. However we favor the second possiblity. A low-frequency vibrational mode at 210 cm^{-1}, assigned to a symmetric bending motion, is seen in fluorescence excitation of DPDP[9] and it may correspond to the second feature (with the higher intensity) in the REP. The first feature would then correspond to the 2^1A_g electronic origin; this assignment cannot be ruled out, because even if it is assumed that the electronic transition moment $\mu_{ge}(Q_0)=0$ at

Figure 15. Expanded view in the region of the electronic origin. The lower REP curve (- - -) correpsond to the experimental data points and its corresponding error. The REP model (——) is situated immediately above.

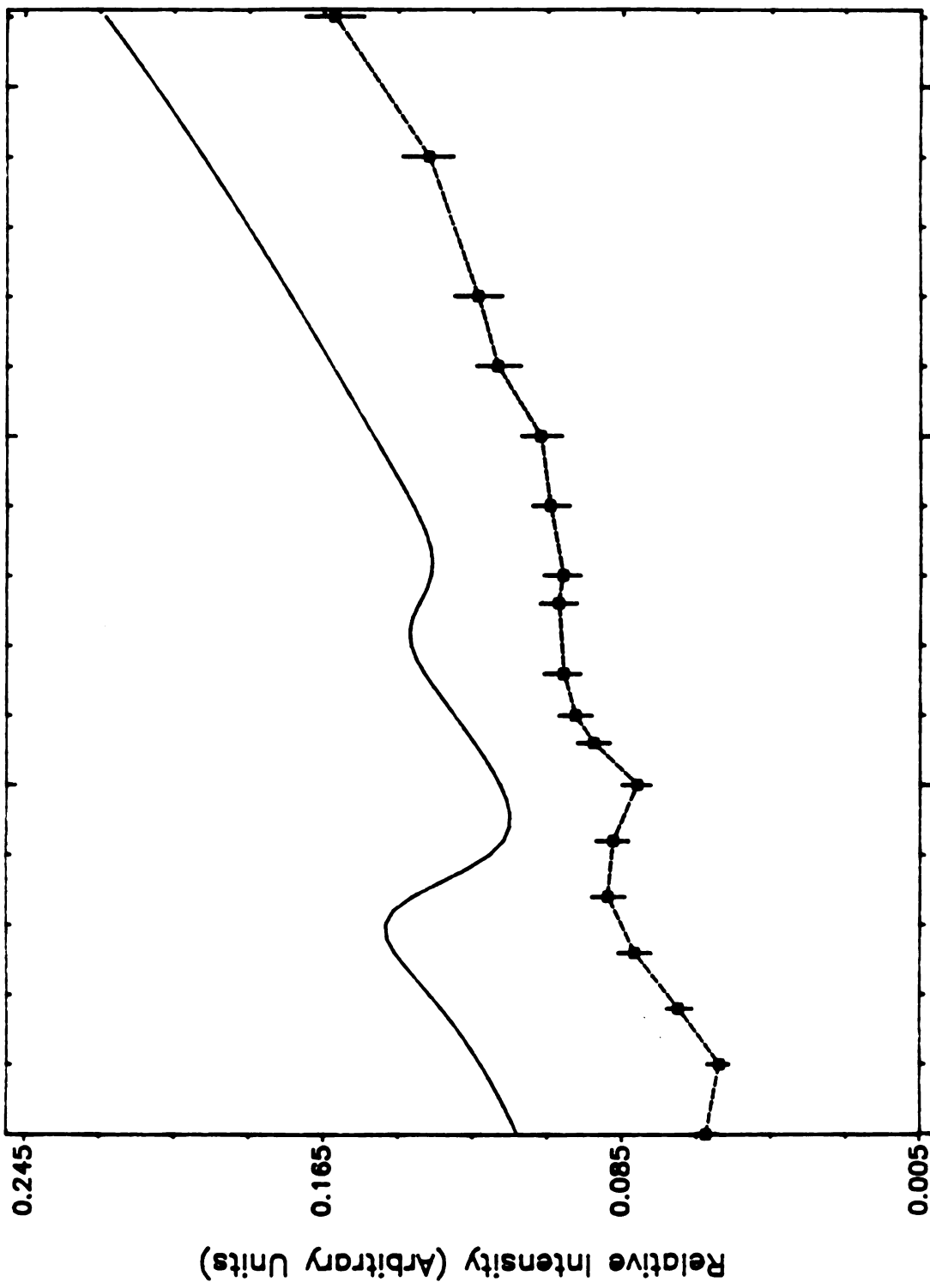
Relative Intensity (Arbitrary Units)
0.245
0.165
0.085
0.005
20000
20250
20500
20750
wavenumbers (cm−1)

Figure 15.

equilibrium, vibrationally-induced intensity will occur because of the fluctuation in μ_{ge} due to zero-point vibrations of the nuclei.[52] The extreme sensitivity of this forbidden transition to small perturbations is demonstrated by polyenes for which the origin is absent in one-photon spectra in a particular, matched n-alkane host, but is observed in other n-alkane hosts differing by only one or two carbon atoms.[11] Thus small static distortions give visibility to the 2^1A_g origin; so might small dynamic distortions due to asymmetric vibrations and collisions in solution. We therefore assign the weak peak at 20,175 cm^{-1} to the origin of the 2^1A_g state of DPDP in cyclohexane solution at room temperature.

CHAPTER V

DISCUSSION

5.1 The Raman Interference Effect

The contribution of weakly allowed states to the Raman excitation profile intensity may be understood by considering the Raman scattering intensity, which is proportional to $|\alpha_{\rho\sigma}|^2$, where $\alpha_{\rho\sigma}$ is the polarizability tensor. When $\alpha_{\rho\sigma}$ is expressed by the Kramers-Heisenberg dispersion relation of equation (4), it is seen that "mixing" cross terms arise, which may reduce or enhance the Raman intensity. This is due, in part, to the Franck-Condon factors, for which the sign is a function of the displacement parameter, Δ_i. In sharp contrast to Raman excitation, each term of the absorption cross-section, given by equation (11), contributes solely to the intensity of a single state, since the absolute square of the overlap integral leads only to the enhancement of its intensity; hence, there is no "mixing" of states.

As an illustration, consider $|\alpha_{\rho\rho}|^2$ obtained from expression (4) which is given by[53]

$$|\alpha_{\rho\rho}|^2 = \sum_{i=1} \frac{A_i^2}{\delta\omega_i^2 + \Gamma_i^2}$$

$$+ \sum_{i=1} \sum_{j=1}^{j<i} \frac{2A_jA_i(\delta\omega_j\,\delta\omega_i + \Gamma_j\,\Gamma_i)}{(\delta\omega_j^2 + \Gamma_j^2)(\delta\omega_i^2 + \Gamma_i^2)} \qquad (12)$$

where the sum extends over all vibrational states i, $\delta\omega_i \equiv \omega_i - \omega_0$ and A_i and A_j are proportional to the oscillator-strengths and to the Raman Franck-Condon factors defined by equation (6) for states i and j respectively.

Furthermore, consider a system with two electronic excited states, e and s, where the oscillator strength for state s is much greater than that of state e; that is $\mu_{gs} >> \mu_{ge}$. For a given vibrational mode j of the weakly allowed electronic state e, A_j will be very small. Its contribution to the first term of equation (12) may therefore be neglected. The Raman cross terms will then be the only measurable contribution to the Raman intensity, which otherwise may not be detectable within the signal-to-noise limits of the experiment. The interferences in the preresonace REP of DPDP, shown in Figures 7 and 9, demonstrate this effect.

The proximity of the two electronic excited states is a crucial factor in the determination of the intensity level for the interference features in the REP. This is easily seen from the cross term expression of equation (12). If the incident radiation ω_0 is in resonance with state j then

$\delta\omega_j=0$ and the maximum contribution of the cross terms will occur when the separation between the two coupled electronic excited states is at a minimum, since then $\delta\omega_i$ will also be smallest.

Symmetry-forbidden transitions generally have oscillator strengths in the 10^{-3} to 10^{-2} range,[10] in comparison to ~10^{-6} for a singlet-triplet transition.[23] Strong dipole-allowed states, on the other hand, have oscillator strengths of 1.0-1.5.[10,38] For example, the $1^1A_g \rightarrow 1^1B_u$ oscillator strength for DPO in EPA at 77K is 1.5;[2,10-12] for the $1^1A_g \rightarrow 2^1A_g$ transition it is 0.05.[10] The ratio of the 2^1A_g transition oscillator strength to that of the 1^1B_u state is thus 0.03. The value which best fits our experimental data is 0.04 (This would approximately correspond to the ratio of $|\mu_{ge}|^2$ and $|\mu_{gs}|^2$ in equation 4 of the polarizability tensor, $\alpha_{\rho\rho}$); this ratio is the *only* parameter which was allowed to vary in our treatment of the DPDP preresonance REP. The value is obtained by taking the ratio of the multiplicative constant 425 and 10225 in program lines 24020 and 24060, respectively of Appendix I part B.

From the argument already introduced that g→g transitions are parity forbidden it would seem natural to assume that the preresonance Raman excitation profile structure would be of ungerade character. Then the overlap integrals for the Raman scattering arising from the ground state ν_1, in a multimode formulation involving four modes:

ν^{s}_{1}, ν^{a}_{1}, ν^{a}_{2}, ν^{a}_{3} and for excitation in resonance with the vibrational fundamental ν_2 in the excited state would be given by:

$$\langle \bar{1}_g | \bar{\upsilon}_e \rangle \langle \bar{\upsilon}_e | \bar{0}_g \rangle = [\langle 1_g | 0_e \rangle \langle 0_e | 0_g \rangle]^{s}_{\nu_1} [\langle 0_g | 0_e \rangle \langle 0_e | 0_g \rangle]^{a}_{\nu_1}$$

$$\times [\langle 0_g | 1_e \rangle \langle 1_e | 0_g \rangle]^{a}_{\nu_2} [\langle 0_g | 0_e \rangle \langle 0_e | 0_g \rangle]^{a}_{\nu_3} \quad (13)$$

where the superscripts s and a are the symmetric and asymmetric vibronic modes, respectively.

This results in a preresonance Raman excitation profile whose features, as shown in Figure 16, are weaker than those in Figure 10, where it was assumed that the associated vibrational level in the 2^1A_g state are totally symmetric. Moreover, for the best fit value the oscillator strength ratio is about 0.08, a significant deviation from DPO. The arguments employed to account for the observation of the 2^1A_g origin in the REP apply as well to the intensity of symmetric fundamental modes in the hidden electronic state. Consequently the vibrational modes which are associated with the electronic 2^1A_g state, which give rise to the preresonance REP features are assumed to be of totally symmetric character.

Figure 16. The experimental preresonance Raman excitation profile, and predicted excitation profiles for symmetric 2^1A_g modes (——) and for asymmetric modes (- - -).

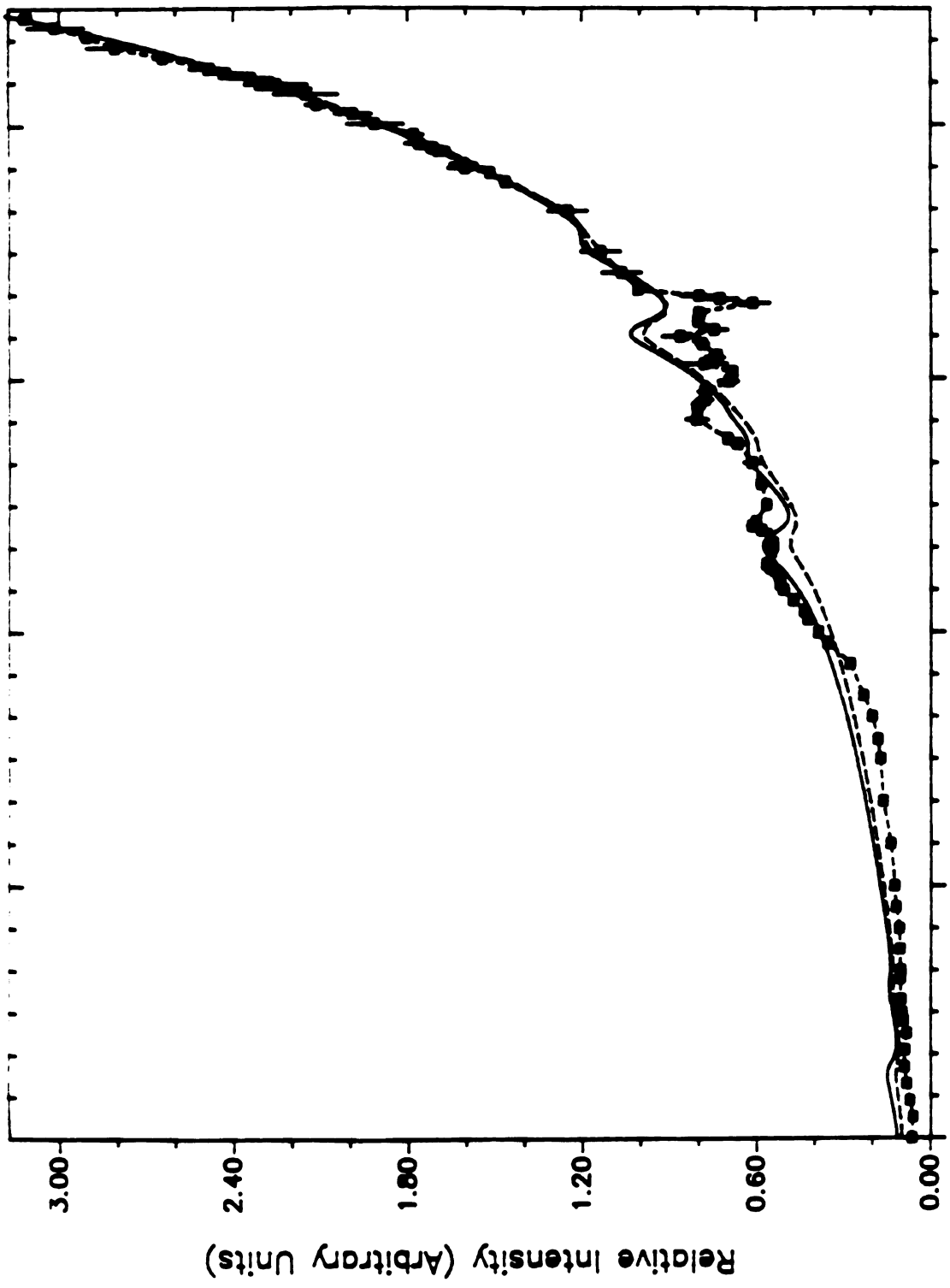
Relative Intensity (Arbitrary Units)
3.00
2.40
1.80
1.20
0.60
0.00
20000
20600
21200
21800
22400
wavenumbers (cm−1)

Figure 16.

5.2 Solvent Polarizability Effect

As the solvent polarizability increases, the absorption band for the strongly-allowed polyene 1^1B_u state shifts to lower energy.[10,12,54,55] The wavenumber shift is given by[10,11] $\delta\nu = k\, f_{eg}[(n^2-1)/(n^2+2)]$, where $\delta\nu$ is the shift in cm^{-1}, n is the refractive index of the solvent, f_{eg} is the oscillator strength for the g→e transition, and k is a molecular constant. This effect is illustrated by the DPDP molecule, where the 1^1B_u electronic origin is shifted from 23050 cm^{-1} in EPA at 77K[29] to 23750 cm^{-1} in cyclohexane at 300K. The 2^1A_g state, however, is in general little affected by solvent polarizability. In fact, a plot of the emission band of DPO as a function of the effective polarizability, $(n^2-1)/(n^2+2)$, reproduced in Figure 17 from reference 10 reveals that the slope is nearly horizontal (only 0.1 times that of a similar plot for the strong $1^1A_g \rightarrow 1^1B_u$ absorption).[10] The 1^1B_u state shift from 23068 cm^{-1}, reported by Horowitz et al.,[9] to 23750 cm^{-1} for DPDP in cyclohexane at room temperature. Thus the corresponding predicted shift for the 2^1A_g state origin will be (0.10)(682) ≈ 50 cm^{-1}. Therefore, to account for the differences in solvent and temperature, the 77K fluorescence excitation spectrum reported in reference 9 was shifted 50 cm^{-1} higher before it was employed in the interpretation of the preresonance REP of DPDP in cyclohexane.

Figure 17. A plot of the position of the first absorption (upper) and emission (lower) peaks of DPO as a function of the effective polarizability, $(n^2-1)/(n^2+2)$, where n is the solvent index of refraction.[10]

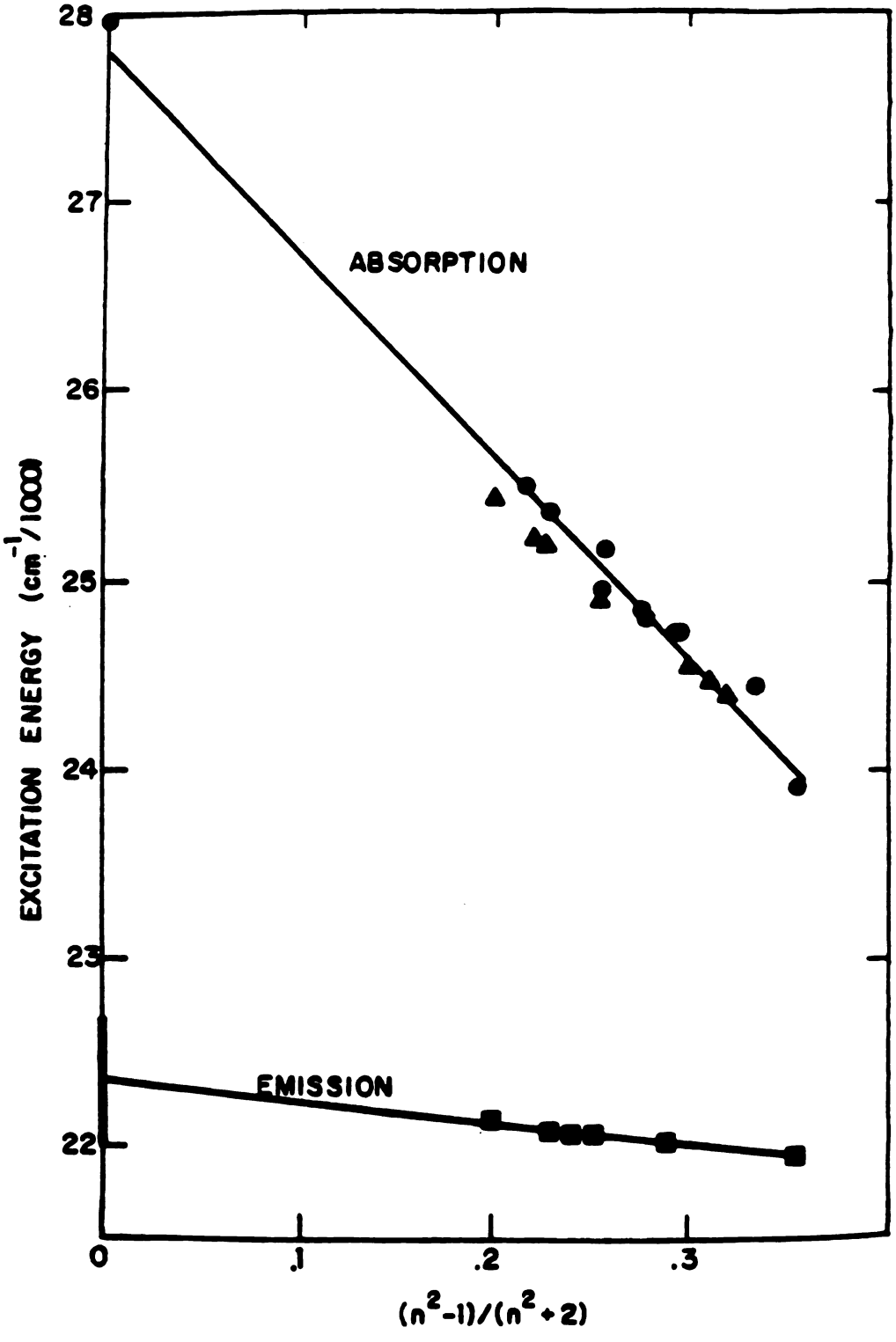
28
27
26
25
24
23
22
EXCITATION ENERGY (cm^{-1}/1000)
ABSORPTION
EMISSION
0
.1
.2
.3
$(n^2-1)/(n^2+2)$

Figure 17.

5.3 The Semi-Analytical Transform from Absorption to Raman Excitation

5.3.1 Franck-Condon Factors

The theoretical REP is obtained from magnitude square of the diagonal of the polarizability tensor, which are written in terms of the Kramers-Heisenberg dispersion relation of equation (4). The Franck-Condon integrals are expressed in terms of harmonic oscillator eigenfunctions, which require experimental values of the following parameters: ν_{gi}, and ν_{ei}, the ground and excited state vibrational frequencies for mode i, and $|\Delta_i|$, the shift in the potential minimum between the ground and the excited state for that vibrational mode. The vibrational modes and displacement parameters utilized for the 2^1A_g and 1^1B_u excited states of DPDP are listed in Tables I-III.

The values of ν_i required to calculate the Franck-Condon parameters for the 11Bu excited state were obtained directly from the absorption and fluorescence excitation spectra of DPDP shown in Figures 3 and 15.9,29 The mode displacement parameters listed in Table I for the 11Bu excited state were obtained by "fitting" the absorption cross-section of equation (11) to the experimental absorption spectrum of DPDP in EPA glass at 77K,29 as shown

TABLE I. Displacement parameters, Δ_i ±0.005, in units of $(amu)^{1/2}$Å, obtained by fitting the absorption spectra to equation (11).

Parameter	2^1A_g		1^1B_u	
	4-mode	3-mode	3-mode	2-mode
Δ_{ν_1}	0.36	0.40	0.17	0.11
Δ_{ν_2}	0.30	0.32	0.15	0.24
Δ_{ν_3}	0.37	0.35	0.10	-
Δ_{ν_8}	0.11	-	-	-

TABLE II. The 1^1B_u excited state vibrational modes (cm^{-1}) and their corresponding Raman Franck-Condon integrals for the C=C symmetric mode used in the Raman excitation model.

Assignment	ν	$\Delta\nu$	F-C integral x 10^{-3}
ν_{00}	23750	-	274
ν_3	23950	200	8.11
ν_2	24950	1200	109
$\nu_2 + \nu_3$	25150	1400	3.24
ν_1	25300	1550	-92.3
$\nu_1 + \nu_3$	25500	1750	-2.73
$2\nu_2$	26150	2400	43.7
$2\nu_2 + \nu_3$	26350	2600	1.30
$\nu_1 + \nu_2$	26500	2750	-36.9
$2\nu_1$	26850	3100	-171
$2\nu_1 + \nu_3$	27050	3300	-5.06
$2\nu_2 + \nu_1$	27700	3950	-14.7
$2\nu_1 + \nu_2$	28050	4300	-68.3
$3\nu_1$	28400	4650	-77.8
$2\nu_1 + 2\nu_2$	29250	5500	-27.3
$3\nu_1 + \nu_2$	29600	5850	-31.1

TABLE III. The 2^1A_g excited state vibrational modes (cm^{-1}) and their corresponding Raman Franck-Condon integrals for the C=C symmetric mode used in the Raman excitation model.

Assignment	ν	$\Delta\nu$	F-C integral x 10^{-3}
ν_{00}	20175	-	7.70
ν_3	20375	200	3.12
ν_2	21425	1250	12.3
$\nu_2 + \nu_3$	21625	1450	4.98
ν_8	21725	1550	2.14
ν_1	21925	1750	15.6
$\nu_1 + \nu_3$	22125	1950	6.31

in Figure 18. A two-mode model inadequately reproduces the structure at higher energies (see Figure 18); addition of the low-frequency bending mode provided satisfactory simulation. Each Δ_i was varied until the following best-fit values were obtained: $\Delta_{C=C}$=0.17 (amu)$^{1/2}$Å, Δ_{C-C} =0.15 (amu)$^{1/2}$Å, and Δ_{ν_s} =0.10 (amu)$^{1/2}$Å. These mode displacements compare closely to those of octatetraene, for which Δc=c = 0.14 (amu)$^{1/2}$Å and Δc-c = 0.13 (amu)$^{1/2}$Å, respectively,[56] for the only two modes reported.

Similarly, for the 2^1A_g excited state we use the relative peak intensities from the experimental DPDP fluorescence excitation spectrum,[9] reconstructed in Figure 13, to determine the Δ_i given in Table I. Both three-mode and four-mode models were employed. The electronic origin, ν_{00}, and the low frequency vibrational mode, ν_s, are the least intense among the prominent vibrational states. To simulate this condition for the 2^1A_g "absorption" model, the polyene mode displacements must have values greater than those of the 1^1B_u excited state, since for the latter the origin is the most intense peak. These larger values of the 2^1A_g displacement parameters can be understood on the basis of a plot of Δ_i as a function of the Franck-Condon amplitude, which shows that as the value of the displacement parameter increases, the intensity of the electronic origin decreases from its peak value, while that of fundamental

Figure 18. Visible-UV absorption spectrum of DPDP in EPA at 77 K ([]-[]) and the calculated absorption cross-section (——). The effect of deleting the combination band $3\nu_1+\nu_2$ (---) from the calculated absorption cross-section is also shown.

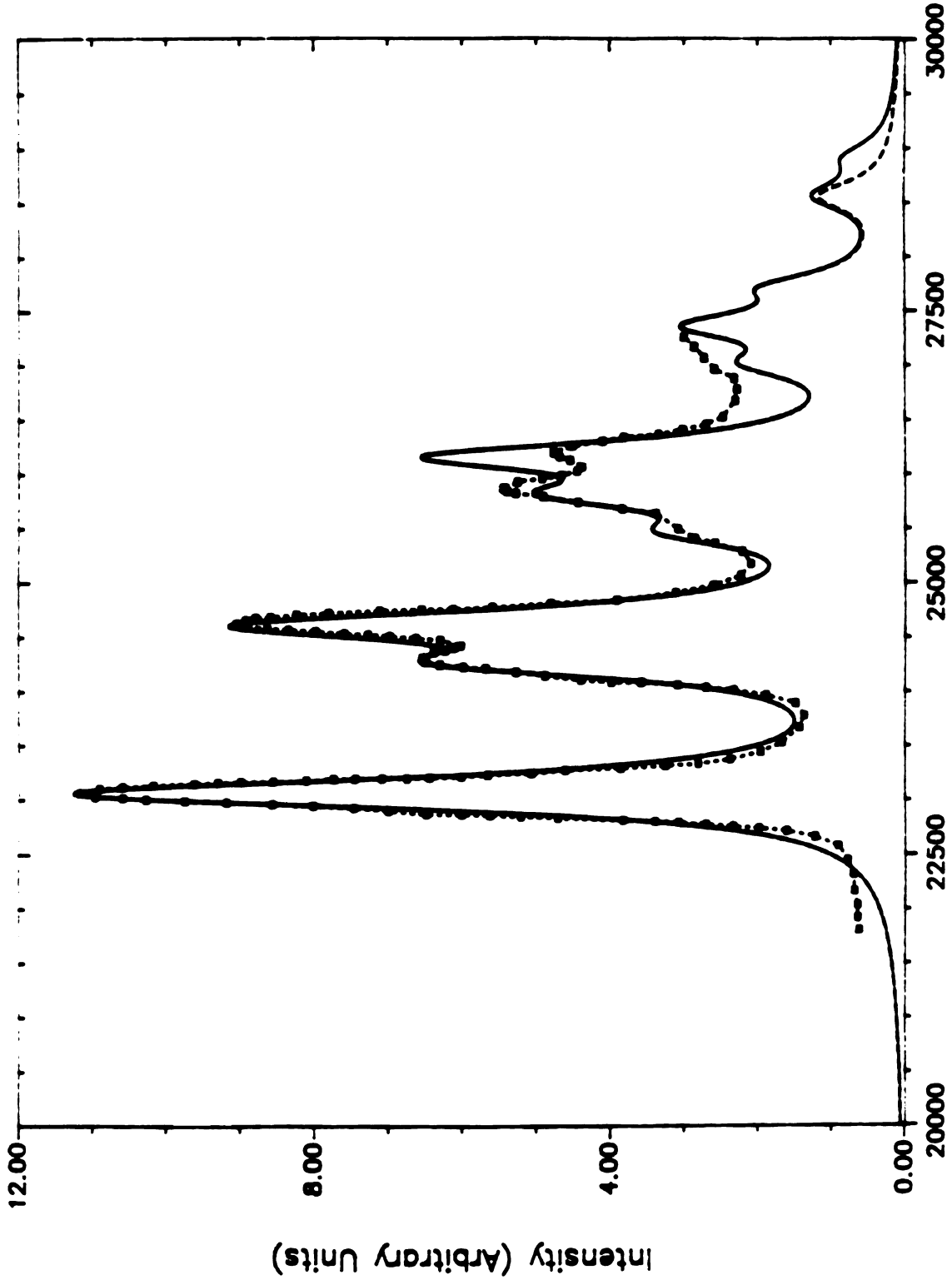
Intensity (Arbitrary Units)
12.00
8.00
4.00
0.00
20000
22500
25000
27500
30000
wavenumbers (cm−1)

Figure 18.

vibrational modes increases. In Figure 19a, where the overlap integrals for a 3-mode model are plotted, the ν_{00} formulation, namely $[\langle 1_g|0_e\rangle\langle 0_e|0_g\rangle]_{\nu_1}[\langle 0_g|0_e\rangle\langle 0_e|0_g\rangle]_{\nu_2}$ x $[\langle 0_g|0_e\rangle\langle 0_e|0_g\rangle]_{\nu_3}$, peaks at 0.15 $(amu)^{1/2}$Å and then begins a steep decline; that for ν_1 that is, $[\langle 1_g|1_e\rangle\langle 1_e|0_g\rangle]_{\nu_1}$ $x[\langle 0_g|0_e\rangle\langle 0_e|0_g\rangle]_{\nu_2}[\langle 0_g|0_e\rangle\langle 0_e|0_g\rangle]_{\nu_3}$ peaks at 0.30 $(amu)^{1/2}$Å, for ν_2 namely $[\langle 1_g|0_e\rangle\langle 0_e|0_g\rangle]_{\nu_1}[\langle 0_g|1_e\rangle\langle 1_e|0_g\rangle]_{\nu_2}$ $x[\langle 0_g|0e\rangle\langle 0_e|0_g\rangle]_{\nu_3}$ peaks at 0.24 $(amu)^{1/2}$Å, and for ν_3 the product peaks at 0.55 $(amu)^{1/2}$Å. Since the overtones $2\nu_1$ and $3\nu_1$ are shifted relative to ν_1 as illustrated in Figure 19b, a large Δ_i will result for these modes in acquiring significant intensity. For completeness Franck-Condon integrals of various combination modes are illustrated in Figure 19c and Figure 19d. The values selected for DPDP are supported by results for diphenylhexatriene, for which the displacement parameters Δ_{ν_1} and Δ_{ν_2} are significantly smaller in the 1^1B_u state than in the 2^1A_g excited state.[55] Moreover, for the dipole-forbidden $^1B_{2u}$ electronic state of benzene, the Δ-value found[19] for the symmetric ring breathing mode (992 cm^{-1}) is 0.33 $(amu)^{1/2}$Å, which agrees well with the values listed for DPDP in Table I.

The overlap integrals are not as sensitive to ν_i as they are to Δ_i. A plot of the overlap integrals as a function of ν_i will show a curve that is nearly a constant. Therefore the experimental frequency differences for the 1^1A_g and 1^1B_u states of DPDP, about 50 cm^{-1} for both the symmetric C-C and the symmetric C=C stretches,[57] may be

Figure 19a. The three fundamental Franck-Condon integrals ν_1, ν_2, ν_3. Only ν_1 has negative values. The F-C origin peaks first for a given displacement paramenter Δ_i. The amplitude of all except for ν_3 approaches zero for $\Delta_i > 0.4$

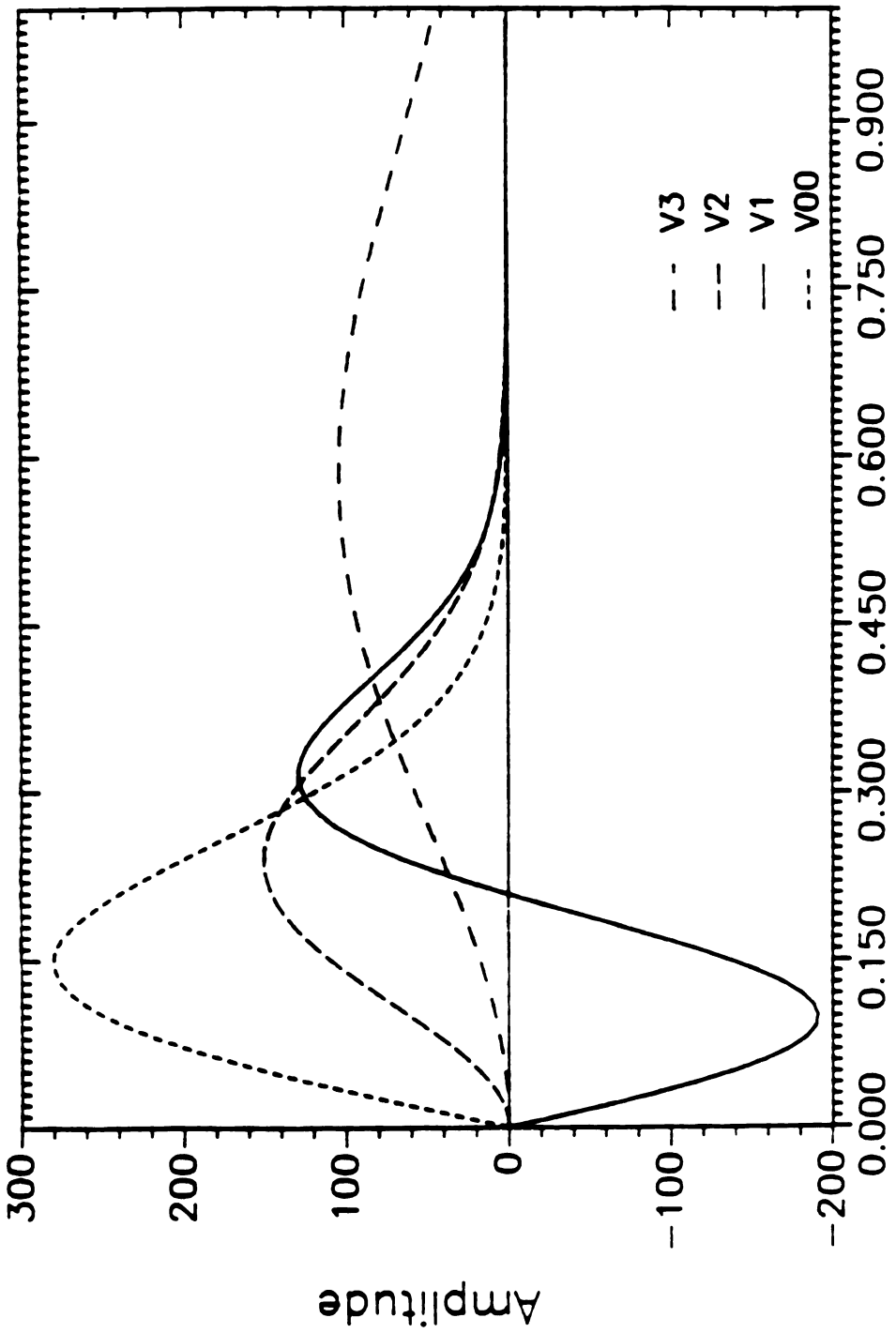
Amplitude
300
200
100
0
−100
−200
0.000
0.150
0.300
0.450
0.600
0.750
0.900
displacement parameter
V3
V2
V1
V00

Figure 19a.

Figure 19b. The Franck-Condon integral ν_1 and its overtones $2\nu_1$, and $3\nu_1$. The relative shift between the F-C integrals is most apparent. It is clear that as Δ_i increases (at $\Delta_i > 0.3$) these overtone amplitudes increases, but the fundamental ν_1 decreases.

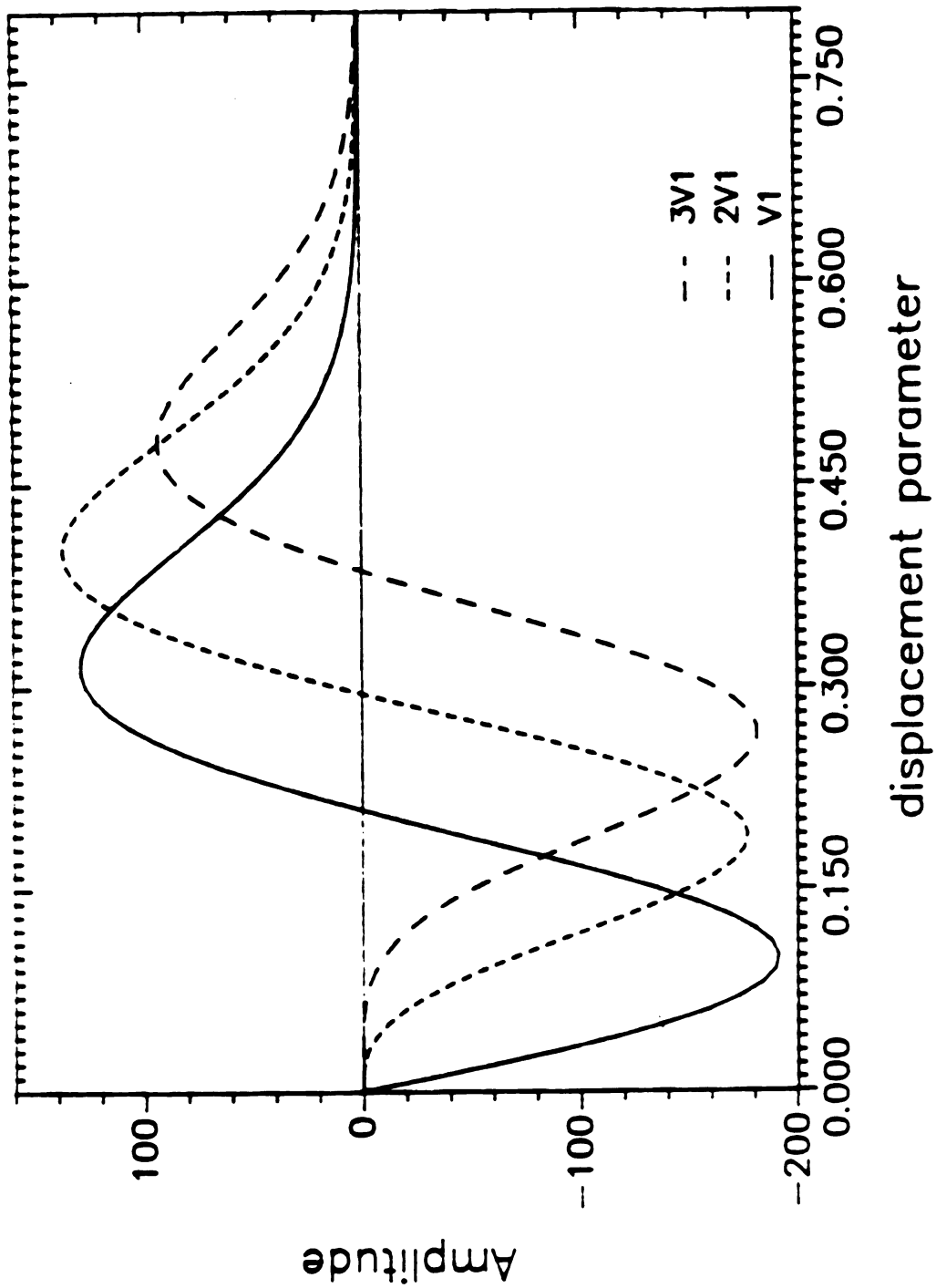
Amplitude
100
0
-100
-200
0.000
0.150
0.300
0.450
0.600
0.750
displacement parameter
3V1
2V1
V1

Figure 19b.

Figure 19c. The Franck-Condon integral amplitude as a function of Δ_i for several combinations of ν_1, ν_2, and ν_3.

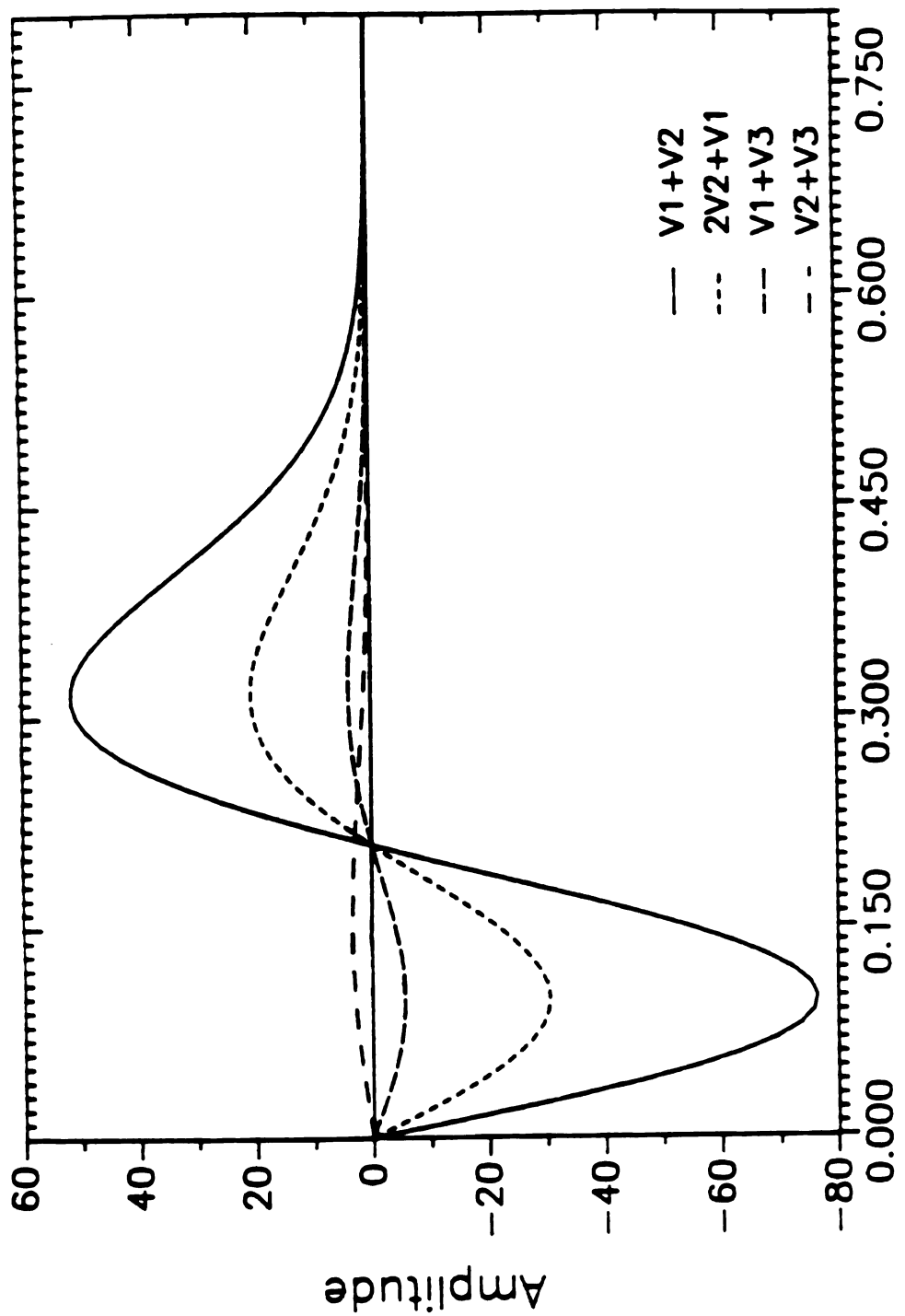
Amplitude
displacement parameter
V1+V2
2V2+V1
V1+V3
V2+V3
60
40
20
0
-20
-40
-60
-80
0.000
0.150
0.300
0.450
0.600
0.750

Figure 19c.

Figure 19d. The Franck-Condon integral amplitude as a function of Δ_i for combinations of ν_1 with ν_2.

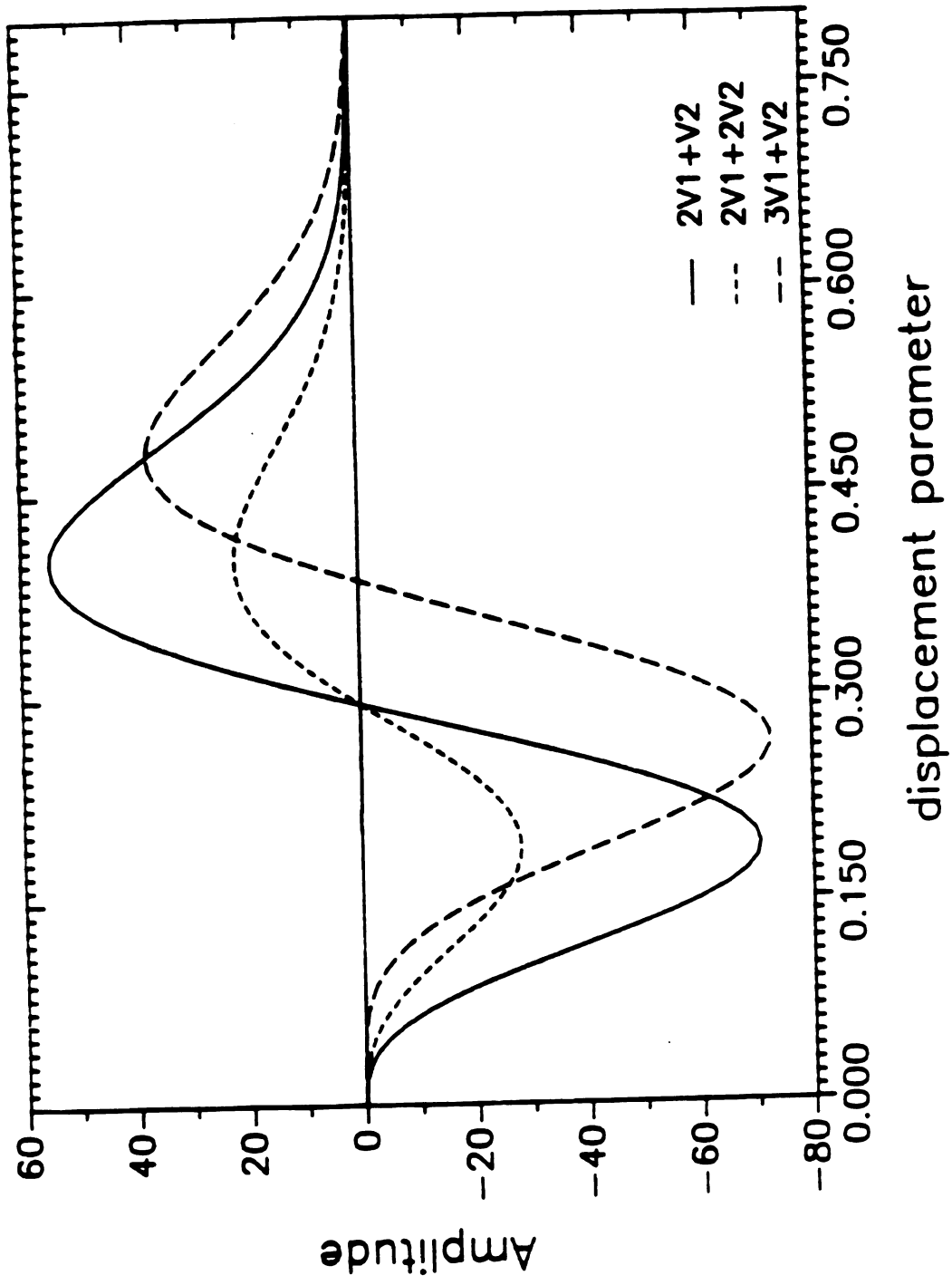
Amplitude
displacement parameter
2V1+V2
2V1+2V2
3V1+V2
60
40
20
0
-20
-40
-60
-80
0.000
0.150
0.300
0.450
0.600
0.750

Figure 19d.

neglected for the purpose of determining the Franck-Condon integrals. As a result, the recurrence relations of equations (8)-(10) simplify considerably, as shown by equations (8')-(10'). However, for the transition to the 2^1A_g excited state a similar approximation would result in significant error, because of the expected large change in the C=C symmetric stretching frequency. For DPDP this mode is observed at 1750 cm^{-1},[9] 200 cm^{-1} higher than the ground state value. Such a large increase for the C=C stretching mode in the 2^1A_g excited state is typical for linear polyenes;[6,7,9,58] as the chain length increases so does the frequency of this vibration. Theoretical results initially predicted a slight decrease in frequency.[59] Among possible explanations,[6,7,60,61] the unexpected increase has been attributed to vibronic coupling between the 1^1Ag ground state and the 2^1Ag excited state.

5.3.2 Bandwidth

A linewidth value (HWHM) of Γ_i = 500 cm^{-1} for the vibrational modes in the 1^1B_u state was obtained by fitting the model absorption cross-section of equation (11) to the room temperature experimental absorption spectrum of DPDP in cyclohexane (Figure 4). Confirmation was provided by fitting the upper end of the experimental preresonance profile to the tail of the calculated REP; a lower limit of

500 cm^{-1} for the linewidth was determined. This seems reasonable, since a Γ_i value of 650 cm^{-1} has been measured for the REP of β-carotene in cyclohexane.[62] A narrower linewidth (250 cm^{-1}) was reported by the same authors for β-carotene in isopentane.[62]

For each vibrational band of the 2^1A_g excited state a half bandwidth value of 50 cm^{-1}, typical of vibrational linewidths in solution, was selected. For the purpose of mathematical simplicity the damping parameters, Γ_i, were all assigned the same numerical value within a given electronic excited state.

5.3.3 Combinations and Overtones

By including combinations and overtone bands in the model for the 1^1B_u excited state, not only did the absorption spectrum of the model improve, but the calculated preresonance Raman excitation profile also better fit the experimental spectrum of Figure 10. The omission of the three highest energy absorption bands (see Figure 20), comprised of overtones and combinations of the 11Bu excited state fundamentals, would cause the low-energy preresonance REP tail in the 2^1A_g region, 20000-21000 cm^{-1}, to be significantly misaligned, and would predict a curvature which does not coincide with the experimental data.

Figure 20. The predicted resonance Raman excitation profile (——) and the REP with the combination band $3\nu_1+\nu_2$ deleted (---). The deletion of this band affects the entire REP spectrum, in sharp contrast to the effect on the calculated absorption spectrum of Figure 18.

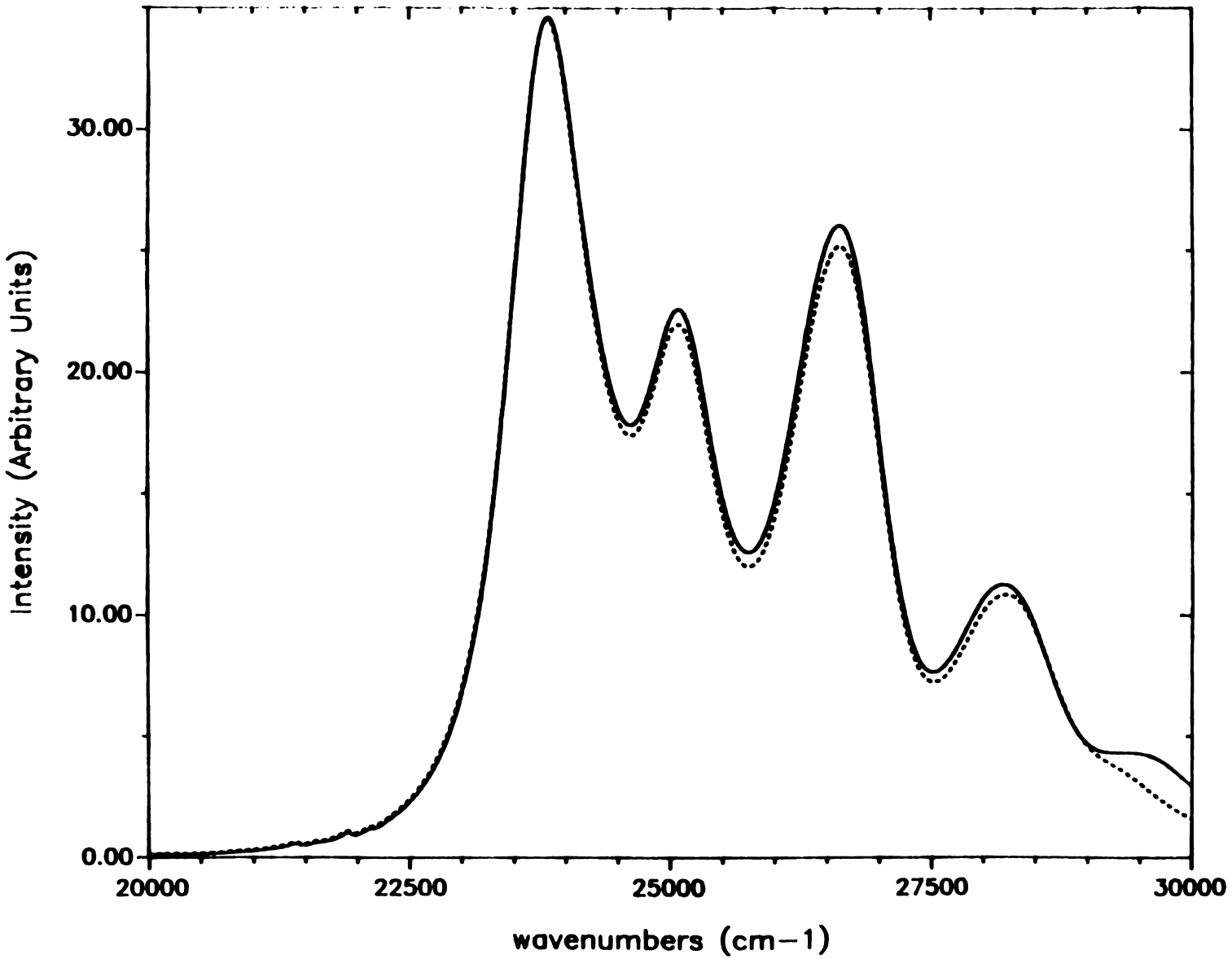
30.00
20.00
10.00
0.00
Intensity (Arbitrary Units)
20000
22500
25000
27500
30000
wavenumbers (cm−1)

Figure 20.

Figure 21. Expanded view of the 20000-22500 cm^{-1} region. for the REP shown in Figure 20.

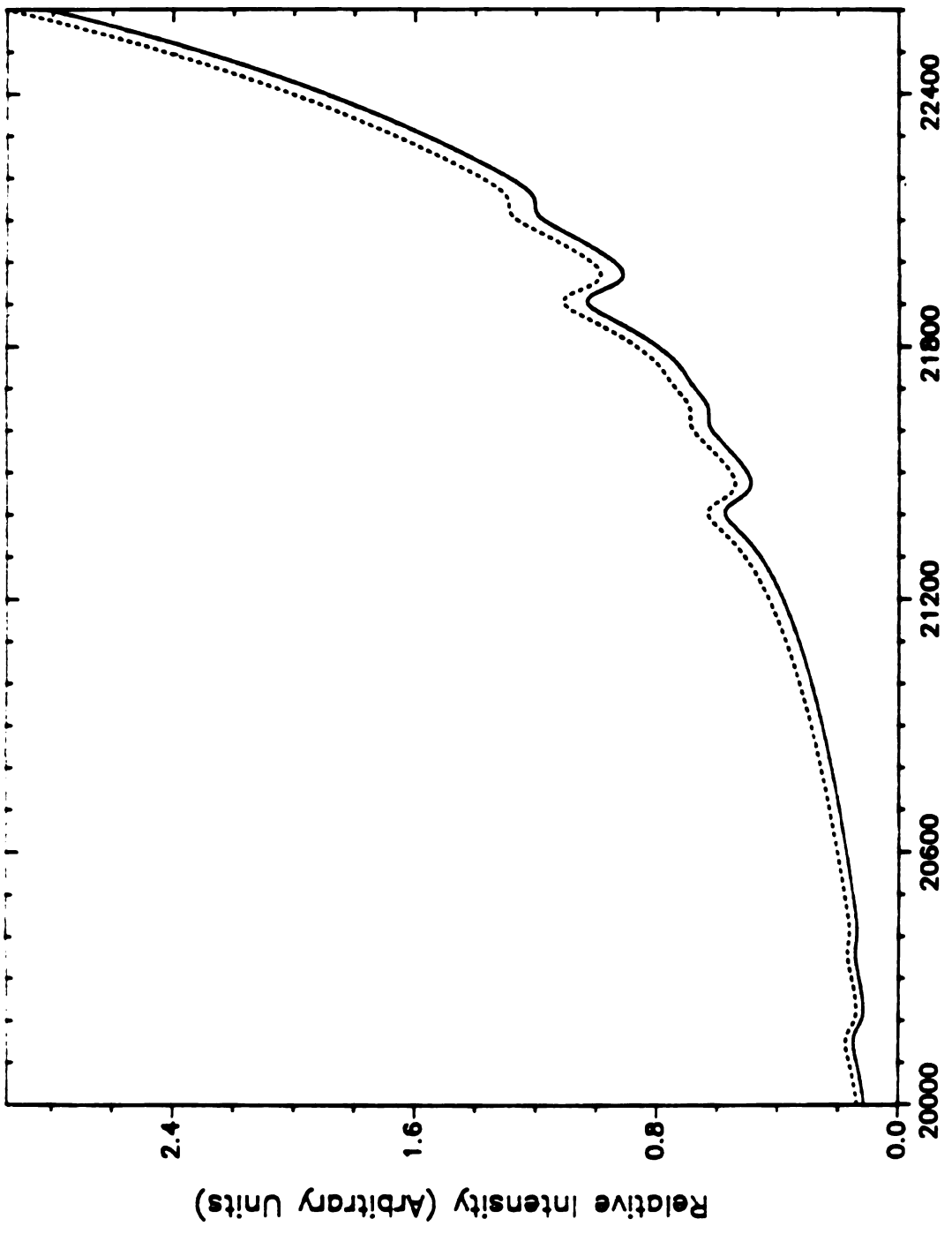
Relative Intensity (Arbitrary Units)
2.4
1.6
0.8
0.0
20000
20600
21200
21800
22400
wavenumbers (cm−1)

Figure 21.

This is interesting, since these 1^1B_u states modes are at least 4000 cm^{-1} from the nearest prominent 2^1A_g vibronic feature. Their effect on the preresonance region of the calculated REP given in Figure 20 appears to be negligible. However, on the expanded scale shown in Figure 21 it is clear that the model does not coincide as well with the experimental data when even the single highest energy combination band ($3\nu_1+\nu_2$) considered in our analysis is deleted from the calculated REP. The preresonance intensity calculated with the truncated model is higher than the prediction shown in Figure 12, which is already higher than the experimental observations. The overlap integrals for the 1^1B_u C=C stretch, its overtones and combinations are negative for the corresponding Δ_i value (Tables I-II, and clearly seen in Figures 16a-16d), which has the effect of lowering the model excitation profile curve. The antiresonance term in the Kramers-Heisenberg dispersion relation of equation (2) has a similar effect; however it was sufficiently small in this case to be neglected.

From the tabulated parameters and the Kramers-Heisenberg expression the "best fit" calculated REP was obtained. In principle we could have solved the absorption cross-section equation (11) for Δ_i (taking ν_i and Γ_i directly from the absorption spectrum), and then inserted these expressions into equation (4) to obtain the Raman polarizability. In practice, however, obtaining the Δ_i graphically by fitting the absorption equation to the

experimental absorption spectrum at 77K (Figure 18) was found to be more appropriate.

5.3.4 Multimode Formulation

The multidimensional Franck-Condon integrals of equation (5) involve all of the 3N-6 vibrational modes. However, the absorption spectrum of DPDP, like those of other linear polyenes, is dominated by two symmetric carbon-carbon stretching modes, ν_1 (C=C) and ν_2 (C-C), and their progressions, where the remaining fundamental vibrations are much weaker. A two-mode model, $\langle 1_1 0_2 | \nu_1 \nu_2 \rangle \langle \nu_1 \nu_2 | 0_1 0_2 \rangle$, may therefore be expected to offer a reasonable description of such spectra. In fact, for the 1^1Bu absorption two fundamental modes describe the 0-0 and 0-1 band systems adequately, but not the higher energy transitions. For the two-mode model as well as well as for the three-mode model, only the 0-0 and the 0-1 bands of Figure 18 are utilized to determine the "best" fit and hence Δ_i (The fit for the higher energy bands are incidental). The inadequacy of this two-mode approximation is also apparent in the values for the displacement modes obtained: $\Delta\nu_1$ = 0.11 (amu)$^{1/2}$Å, and $\Delta\nu_2$ = 0.24 (amu)$^{1/2}$Å, which deviate significantly from the values, $\Delta\nu_1$ = 0.14 (amu)$^{1/2}$Å and $\Delta\nu_2$ = 0.13 (amu)$^{1/2}$Å, obtained for octatetraene.[56]

However, when a three-mode model, $\langle 1_1 0_2 0_3 | \nu_1 \nu_2 \nu_3 \rangle$x $\langle \nu_1 \nu_2 \nu_3 | 0_1 0_2 0_3 \rangle$, is employed, the description of the absorption and Raman excitation spectra improves for both excited states. Moreover, enhanced intensity in the 2^1Ag REP near 20350 cm^{-1}, 21600 cm^{-1} and 22100 cm^{-1} can be accounted for by the low-frequency mode ν_3 and combination bands, $\nu_2+\nu_3$ and $\nu_1+\nu_3$, respectively. Horwitz et al. interpreted a band in the fluorescence excitation profile of DPDP, shifted from the 2^1A_g origin by 1550 cm^{-1}, as the benzene ν_8 mode, belonging to the phenyl end groups.[9] Inclusion of this mode in the calculated preresonance REP provided only slight improvement to the experimental fit, as noted in Figure 14, although for the model fluorescence excitation spectrum of Figure 13 the improvement is clearly noticeable. All calculated model spectra for the 11Bu excited state were determined by using three modes in the multimode formulation; a four-mode model was utilized for the 2^1A_g state.

The mode displacements, Δ_i, in the three-mode model were consistent with values presented in the literature, as already noted. Interestingly, increasing the multimode formulation to include four vibrational modes, namely C-C, C=C, and two low-frequency vibrations or one low frequency mode and another higher frequency fundamental, did not improve significantly the excitation profile for the preresonance region nor did it considerably affect the calculated resonance REP. It follows that for further

significant improvement in the theoretical description of the DPDP spectra, all 3N-6 normal modes should be included in the multimode formulation.

5.4 Resonance Region

On the basis of the previous analysis the resonance REP of DPDP, which has not been obtained experimentally to date, can be predicted. If one employs the Δs and νs given for the 1^1B_u state in Tables I and II, the resonance REP shown in Figure 20 is obtained. The vibronic structure in the REP in resonance with the 1^1B_u state for polyenes in general is also governed by Franck-Condon progressions formed by two dominating totally symmetric modes: the more prominent being the C=C stretch at ν_{00}+1550 cm^{-1}, and a slightly less intense C-C stretch at ν_{00}+1200 cm^{-1}.[11,48] For DPDP both fundamental modes fall within the 0-1 band. The electronic origin at 23750 cm^{-1} is the most intense band. The overtones and combinations which comprise the remaining bands are listed in Table II. The inclusion of the ν_3 mode not only gives structure to the expected REP at high energies, but as noted earlier it also improves the fit of the experimental data in the preresonance region.

The calculated resonance REP intensity of the 0-1 band of DPDP is slightly weaker than the 0-2 band, which is contrary to the observed REPs of the longer chain

polyenes,[63-65] such as β-carotene. This discrepancy may be due to the unadjusted displacement parameters, which were not optimized to the experimental DPDP REP solvent environment; it may also be due to the CH_3 bending fundamental of β-carotene, which is not present in DPDP. A 10% reduction in the Δ_i values will remove this discrepancy, as is seen clearly in Figure 22, and slightly improve the fit at the tail of the experimental preresonance REP of DPDP. On the other hand, using lower Δ_i values than those obtained from the absorption spectrum of DPDP at 77K will result in an inaccurate prediction of the room temperature absorption spectrum, as illustrated in Figure 23. Measurement of the resonance REP of DPDP would resolve this question.

Figure 22. (a) The REP of DPDP with unadjusted displacement parameters (——). (b) The REP with the adjusted parameters(- -).

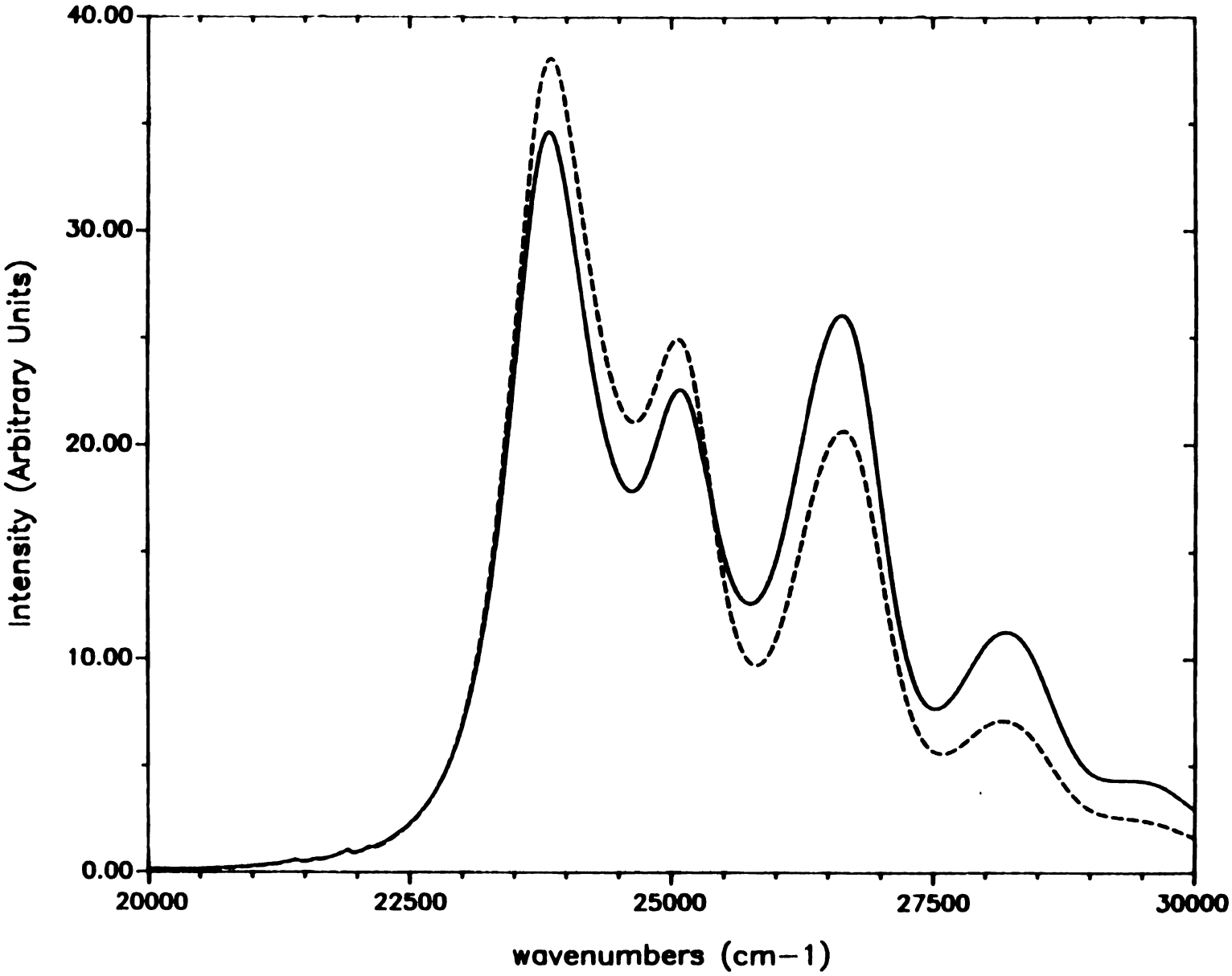
40.00
30.00
20.00
10.00
0.00
Intensity (Arbitrary Units)
20000
22500
25000
27500
30000
wavenumbers (cm−1)

Figure 22.

Figure 23. (a) The effect of adjusting the displacement parameters (- -) on the calculated room temperature absorption spectrum of DPDP. (b) The spectrum with the unadjusted parameters (——) is consistent with that expected from Figure 4.

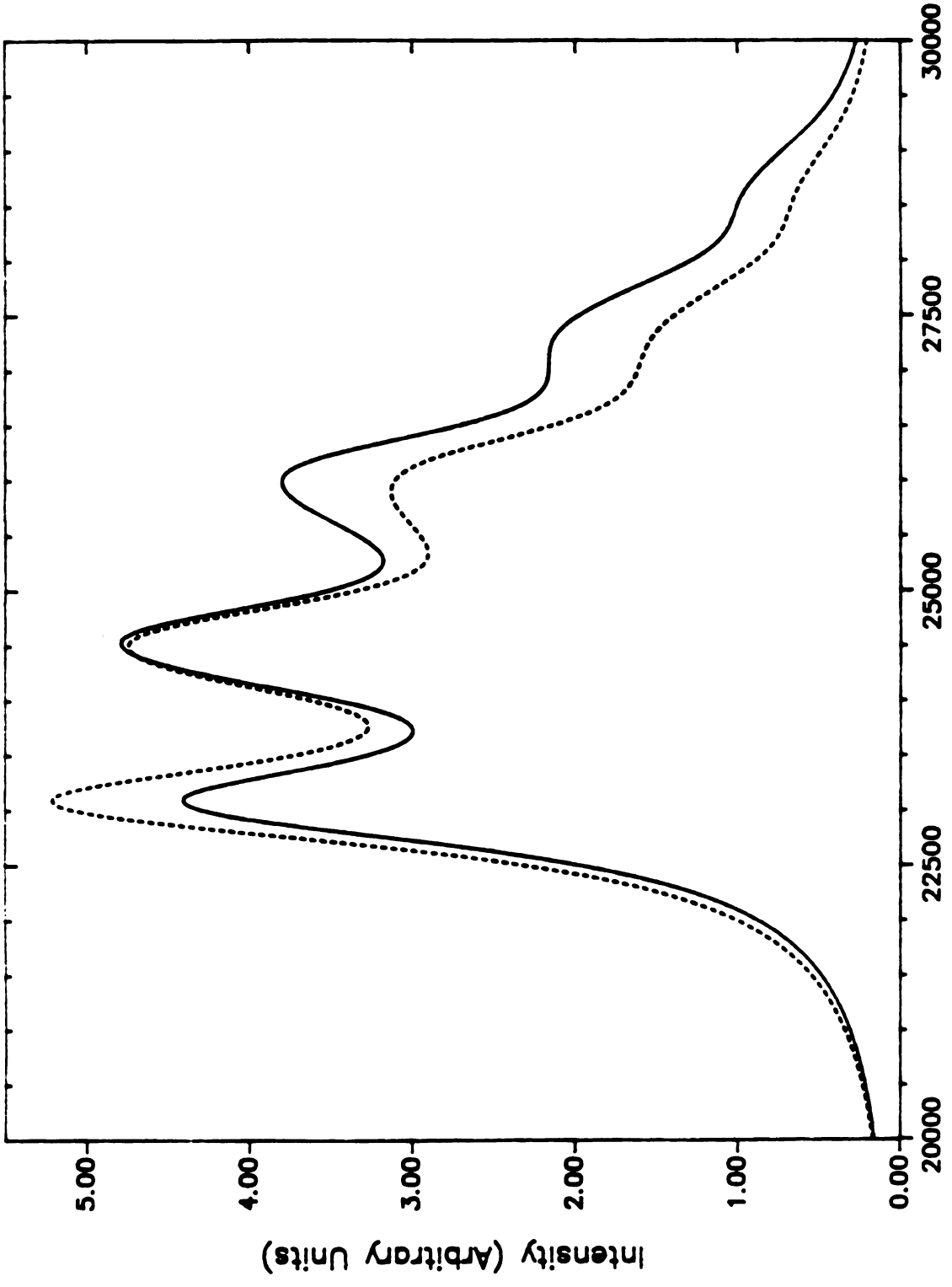
Intensity (Arbitrary Units)
0.00
1.00
2.00
3.00
4.00
5.00
20000
22500
25000
27500
30000
wavenumbers (cm-1)

Figure 23.

CHAPTER VI

Conclusions

Evidence of the low-lying 2^1A_g excited state of the DPDP molecule has been observed in the preresonance Raman excitation profile. Moreover, a one-to-one correspondence between interference features in an experimental Raman excitation profile and the vibrational modes of a dipole-forbidden state has been established for the first time. Preresonance Raman excitation thus promises to be suitable for the detection of weakly allowed states in molecules having low fluorescence quantum yield.

Raman excitation profiles might be exploited to help resolve the excited state level ordering of the 2^1A_g and 1^1B_u states for diphenylhexatriene[55] and diphenylbutadiene.[66] The locations of these states have differing dependence on the solvent polarizability, which can account for the inconclusiveness of their relative positions for the diphenyl polyenes and for their unsubstituted counterparts.[67,68] The shapes and intensities of interferences in the REP due to the presence of a dipole-forbidden state depend strongly on the proximity of the coupled allowed state, and a solvent mixture might be "tuned" to highlight the presence of the hidden state.

For β-carotene and other biological polyenes, firm establishment of the 2^1A_g excited state energy may help answer crucial questions regarding energy transfer processes in photosynthetic systems.[16,18,69] As noted earlier,a detailed report of the preresonance Raman scattering from β-carotene is to be published shortly.[24]

The manuscripts which describes this research project has had an excellent reception. A. C. Albrecht of Cornell stated that my "A-state Raman studies are already an impressive contribution." A similar response came from Z. G. Soos at Princeton, R. M. Hochstrasser at Pennsylvania, and others (including B. E. Kohler of Riverside who refereed the paper). At present, obtaining a high resolution Raman excitation profile point by point is both laborious and time consuming. We have established, the preresonance REP as a viable technique for the detection of dipole forbidden states; however, for it to be regularly and practicaly useful, computerization of the REP apparatus and the data analysis will be required.

APPENDICES

APPENDIX I

A complete listing of the program written in Basic for an IBM compatible computer, which was utilized to calculate the Franck-Condon factors, REPs, and the Absorption Cross-Section, is given in Appendix I part B. A flow diagram of the program is also included.

In order that an interested reader may better follow the rationale under which the REP portion of the program was developed, the discussion in Appendix I part A is offered.

APPENDIX I

PART A

Program lines 25295-27400 (labeled as the first equation) determine the Raman excitation profile, based on the Kramers-Heisenberg dispersion relation (see Theory Chapter III). Initially the program was written for six energy levels (ε_1-ε_6). It became apparent that six terms are inadequate to represent the excitation profile of the 2^1A_g and 1^1B_u excited states; consequently it was necessary to increase the number of terms from six to a yet undetermined number, n. This was done not by reworking the REP model for n terms, but by developing an algorithm which made it possible to build on the existing expression. The mathematical expressions utilized are shown in this section.

Past the sixth term, one term at a time was added until the model REP, consisting of 23 terms, gave an adequate description of the experimental data. Although an algorithm consisting of a loop program would have been more efficient than this approach, the calculation time and memory capacity was not a problem. Thus there was little incentive for a major mid-course correction (minimizing the risk of errors was also a factor). Nevertheless, had a large number of terms for the REP model, been anticipated a more efficient program would have been written.

To extend the number of terms from m to k we may use the following approach (the use of brute force is lengthy and prone to errors).

Let

$$S_m = \left[\sum_j^m C_j \right] \left[\sum_j^m C_j^* \right] \tag{1}$$

we wish to evaluate

$$S_k = \left\{ \sum_j^m C_j + C_k \right\} \left\{ \sum_j^m C_j^* + C_k^* \right\} \tag{2}$$

$$= \left[\sum_j C_j \right] \left[\sum_j C_j^* \right] + \left[\sum_j C_j \right] C_k^* + C_k \left[\sum_j C_j^* \right] + (Ck)(C_k^*)$$

$$= S_m + \left[\sum_j C_j \right] C_k^* + C_k \left[\sum_j C_j^* \right] + (C_k)(C_k^*) \tag{3}$$

where S_m has aready been determined.

As an illustration, for 7 terms (k=7) and the center expressions for

K=m+1 becomes.

$$S_7 = S_6 + \left[\sum_j^6 C_j \right] C_7^* + C_7 \left[\sum_j^6 C_j^* \right] + (C_7)(C_7^*) \tag{4}$$

or

$$(c_1 + c_2 + c_3 + c_4 + c_5 + c_6)c_7^* = c_1c_7^* + c_2c_7^* + c_3c_7^* + c_4c_7^* + c_5c_7^* + c_6c_7^*$$

similarly

$$c_7(c_1^* + c_2^* + c_3^* + c_4^* + c_5^* + c_6^*) = c_7c_1^* + c_7c_2^* + c_7c_3^* + c_7c_4^* + c_7c_5^* + c_7c_6^*$$

Let $c_j = \left[\frac{A_j}{(\Delta\varepsilon_j + i\Gamma_j)}\right]$

$$c_jc_7^* = \left[\frac{A_j}{(\Delta\varepsilon_j + i\Gamma_j)}\right]\left[\frac{A_7^*}{(\Delta\varepsilon_7 - i\Gamma_7)}\right]$$

we combine $c_jc_7^*$ and $c_7c_j^*$ and if $A_j^* = A_j$

using the result from equation (9) the expression for 7 terms becomes

$$S_{1-7} = S_6 + 2\sum_j^6 A_jA_7\left[\frac{(\Delta\varepsilon_j\,\Delta\varepsilon_7 + \Gamma_j\,\Gamma_7)}{(\Delta\varepsilon_j^2 + \Gamma_j^2)(\Delta\varepsilon_7^2 + \Gamma_7^2)}\right] + \frac{(A_7)^2}{\Delta\varepsilon_7^2 + \Gamma_7^2} \quad (5)$$

Thus to the existing S_6 we add the above expressions to obtain S_7.

To determine S_6 we begin with S_3

$$R_{123} = \sum_{j}^{3} \frac{A_j}{\Delta\varepsilon_j + i\Gamma_j} \tag{6}$$

Evaluating $|R_{123}|^2$ is straightforward thus

$$S_3 = \left[\sum_{j}^{3} \frac{A_j}{\Delta\varepsilon_j + i\Gamma_j}\right] \left[\sum_{j}^{3} \frac{A_j^*}{\Delta\varepsilon_j - i\Gamma_j}\right] \tag{7}$$

Taking the product and if A_j is real we have

$$= A_2A_1\left[\frac{1}{(\Delta\varepsilon_2 + i\Gamma_2)(\Delta\varepsilon_1 - i\Gamma_1)} + \frac{1}{(\Delta\varepsilon_1 + i\Gamma_1)(\Delta\varepsilon_2 - i\Gamma_2)}\right] \tag{8}$$

$$+ A_2A_3\left[\frac{1}{(\Delta\varepsilon_3 + i\Gamma_3)(\Delta\varepsilon_2 - i\Gamma_2)} + \frac{1}{(\Delta\varepsilon_2 + i\Gamma_2)(\Delta\varepsilon_3 - i\Gamma_3)}\right]$$

$$+ A_3A_1\left[\frac{1}{(\Delta\varepsilon_3 + i\Gamma_3)(\Delta\varepsilon_1 - i\Gamma_1)} + \frac{1}{(\Delta\varepsilon_1 + i\Gamma_1)(\Delta\varepsilon_3 - i\Gamma_3)}\right]$$

$$+ \left[\frac{(A_1)^2}{(\Delta\varepsilon_3 + i\Gamma_3)(\Delta\varepsilon_1 - i\Gamma_1)} + \frac{(A_2)^2}{(\Delta\varepsilon_1 + i\Gamma_1)(\Delta\varepsilon_3 - i\Gamma_3)}\right.$$

$$\left. + \frac{(A_3)^2}{(\Delta\varepsilon_3 + i\Gamma_3)(\Delta\varepsilon_1 - i\Gamma_1)}\right]$$

Each of the above pairs can be further simplified if we note that

$$\left[\frac{1}{(\Delta\varepsilon_k + i\Gamma_k)(\Delta\varepsilon_j - i\Gamma_j)} + \frac{1}{(\Delta\varepsilon_j + i\Gamma_j)(\Delta\varepsilon_k - i\Gamma_k)}\right]$$

$$= \frac{(\Delta\varepsilon_j + i\Gamma_j)(\Delta\varepsilon_k - i\Gamma_k) + (\Delta\varepsilon_k + i\Gamma_k)(\Delta\varepsilon_j - i\Gamma_j)}{(\Delta\varepsilon_k + i\Gamma_k)(\Delta\varepsilon_k - i\Gamma_k)(\Delta\varepsilon_j - i\Gamma_j)(\Delta\varepsilon_j + i\Gamma_j)}$$

$$= \frac{(\Delta\varepsilon_j\Delta\varepsilon_k - i\Delta\varepsilon_j\Gamma_k + i\Delta\varepsilon_k\Gamma_j + \Gamma_k\Gamma_j) + (\Delta\varepsilon_j\Delta\varepsilon_k - i\Delta\varepsilon_j\Gamma_k + i\Delta\varepsilon_k\Gamma_j + \Gamma_k\Gamma_j)}{(\Delta\varepsilon_k + i\Gamma_k)(\Delta\varepsilon_k - i\Gamma_k)(\Delta\varepsilon_j - i\Gamma_j)(\Delta\varepsilon_j + i\Gamma_j)}$$

$$= \frac{(2\Delta\varepsilon_j\Delta\varepsilon_k + 2\Gamma_k\Gamma_j + (-i\Delta\varepsilon_j\Gamma_k + i\Delta\varepsilon_j\Gamma_k) + (i\Delta\varepsilon_k\Gamma_j - i\Delta\varepsilon_k\Gamma_j)}{[(\Delta\varepsilon_k)^2 + (\Gamma_k)^2][(\Delta\varepsilon_j)^2 + (\Gamma_j)^2]}$$

$$= \frac{2(\Delta\varepsilon_j\Delta\varepsilon_k + \Gamma_k\Gamma_j)}{[(\Delta\varepsilon_k)^2 + (\Gamma_k)^2][(\Delta\varepsilon_j)^2 + (\Gamma_j)^2]} \qquad (9)$$

Therefore

$$|R_{123}|^2 = \left\{ \frac{2A_3}{(\Delta\varepsilon_3^2 + \Gamma_3^2)} \left[\frac{A_1(\Delta\varepsilon_1\ \Delta\varepsilon_3 + \Gamma_1\ \Gamma_3)}{\Delta\varepsilon_1^2 + \Gamma_1^2} \right] \right. \tag{10}$$

$$+ \frac{2A_1}{(\Delta\varepsilon_1^2 + \Gamma_1^2)} \left[\frac{A_2(\Delta\varepsilon_2\ \Delta\varepsilon_1 + \Gamma_2\ \Gamma_1)}{\Delta\varepsilon_1^2 + \Gamma_1^2} \right]$$

$$+ \frac{2A_2}{(\Delta\varepsilon_2^2 + i\Gamma_2^2)} \left[\frac{A_3(\Delta\varepsilon_3\ \Delta\varepsilon_2 + \Gamma_3\ \Gamma_2)}{\Delta\varepsilon_3^2 + i\Gamma_3^2} \right]$$

$$\left. + \sum_{s=1}^{3} \frac{(A_s)^2}{\Delta\varepsilon_s^2 + \Gamma_s^2} \right\}$$

Renaming the indices 456 instead 123, $|R_{456}|$ is similarly defined (to be used below).

Thus to increase $|R_{123}|^2$ to six terms we may write

$$I_6 = \left\{ R_{123} + \left[\frac{A_4}{\Delta\varepsilon_4 + i\Gamma_4} + \frac{A_5}{\Delta\varepsilon_5 + i\Gamma_5} + \frac{A_6}{\Delta\varepsilon_6 + i\Gamma_6} \right] \right\} \qquad (11)$$

$$\times \left\{ R^*_{123} + \left[\frac{A^*_4}{\Delta\varepsilon_4 - i\Gamma_4} + \frac{A^*_5}{\Delta\varepsilon_5 - i\Gamma_5} + \frac{A^*_6}{\Delta\varepsilon_6 - i\Gamma_6} \right] \right\}$$

$$= \left\{ |R_{123}|^2 + |R_{456}|^2 + R_{123} \left[\frac{A^*_4}{\Delta\varepsilon_4 - i\Gamma_4} + \frac{A^*_5}{\Delta\varepsilon_5 - i\Gamma_5} + \frac{A^*_6}{\Delta\varepsilon_6 - i\Gamma_6} \right] \right.$$

$$\left. + R^*_{123} \left[\frac{A_4}{\Delta\varepsilon_4 + i\Gamma_4} + \frac{A_5}{\Delta\varepsilon_5 + i\Gamma_5} + \frac{A_6}{\Delta\varepsilon_6 + i\Gamma_6} \right] \right\} \qquad (12)$$

The first two terms already have been evaluated (For $|R_{456}|$ just exchange 123 for 456 in the final expression of $|R_{123}|$).

Expanding the remaining two terms, namely

$$\left\{ \left[\frac{A_1}{\Delta\varepsilon_1 + i\Gamma_1} + \frac{A_2}{\Delta\varepsilon_2 + i\Gamma_2} + \frac{A_3}{\Delta\varepsilon_3 + i\Gamma_3} \right] \right.$$

$$x \left[\frac{A_4^*}{\Delta\epsilon_4 - i\Gamma_4} + \frac{A_5^*}{\Delta\epsilon_5 - i\Gamma_5} + \frac{A_6^*}{\Delta\epsilon_6 - i\Gamma_6} \right] \Bigg\} \tag{13}$$

and

$$\left\{ \left[\frac{A_1^*}{\Delta\epsilon_1 - i\Gamma_1} + \frac{A_2^*}{\Delta\epsilon_2 - i\Gamma_2} + \frac{A_3^*}{\Delta\epsilon_3 - i\Gamma_3} \right] \right.$$

$$x \left[\frac{A_4}{\Delta\epsilon_4 + i\Gamma_4} + \frac{A_5}{\Delta\epsilon_5 + i\Gamma_5} + \frac{A_6}{\Delta\epsilon_6 + i\Gamma_6} \right] \Bigg\} \tag{14}$$

For clarity consider only one of the possible nine terms of the products above

$$\left[\frac{A_i}{\Delta\epsilon_i + i\Gamma_i} + \frac{A_j}{\Delta\epsilon_j + i\Gamma_j} + \frac{A_k}{\Delta\epsilon_k + i\Gamma_k} \right] \frac{A_r^*}{\Delta\epsilon_r - i\Gamma_r} \tag{15}$$

and its complement (equation 14)

$$\left[\frac{A_i^*}{\Delta\epsilon_i - i\Gamma_i} + \frac{A_j^*}{\Delta\epsilon_j - i\Gamma_j} + \frac{A_k^*}{\Delta\epsilon_k - i\Gamma_k} \right] \frac{A_r}{\Delta\epsilon_r + i\Gamma_r} \tag{16}$$

For each two corresponding pair of terms in equation 15 and 16 we obtain the following expressions

$$\left[\frac{A_i}{\Delta\epsilon_i + i\Gamma_i} \right] \left[\frac{A_r^*}{\Delta\epsilon_r - i\Gamma_r} \right] + \left[\frac{A_i^*}{\Delta\epsilon_i - i\Gamma_i} \right] \left[\frac{A_r}{\Delta\epsilon_r + i\Gamma_r} \right] \tag{17}$$

which reduces to

$$= \left[\frac{(A_i)(A_r^*)}{(\Delta\epsilon_i + i\Gamma_i)(\Delta\epsilon_r - i\Gamma_r)} \right] + \left[\frac{(A_i^*)(A_r)}{(\Delta\epsilon_i - i\Gamma_i)(\Delta\epsilon_r + i\Gamma_r)} \right] \quad (18)$$

The numerator above can be factored out provided A_i and A_r are real

$$= (A_i)(A_r) \left[\frac{1}{(\Delta\epsilon_i + i\Gamma_i)(\Delta\epsilon_r - i\Gamma_r)} + \frac{1}{(\Delta\epsilon_i - i\Gamma_i)(\Delta\epsilon_r + i\Gamma_r)} \right] \quad (19)$$

or (as done earlier)

$$= (A_i)(A_r) \left[\frac{2(\Delta\epsilon_i \, \Delta\epsilon_r + \Gamma_i \, \Gamma_r)}{(\Delta\epsilon_i^2 + i\Gamma_i^2)(\Delta\epsilon_r^2 + i\Gamma_r^2)} \right] \quad (20)$$

Repeating the same for each pair,

therefore

$$\left\{\left[\frac{A_1}{\Delta\varepsilon_1 + i\Gamma_1} + \frac{A_2}{\Delta\varepsilon_2 + i\Gamma_2} + \frac{A_3}{\Delta\varepsilon_3 + i\Gamma_3}\right]\frac{A_4^*}{\Delta\varepsilon_4 - i\Gamma_4}\right.$$

$$\left.\left[\frac{A_1^*}{\Delta\varepsilon_1 - i\Gamma_1} + \frac{A_2^*}{\Delta\varepsilon_2 - i\Gamma_2} + \frac{A_3^*}{\Delta\varepsilon_3 - i\Gamma_3}\right]\frac{A_4}{\Delta\varepsilon_4 + i\Gamma_4}\right\} \qquad (21)$$

$$+\left\{\left[\frac{A_1}{\Delta\varepsilon_1 + i\Gamma_1} + \frac{A_2}{\Delta\varepsilon_2 + i\Gamma_2} + \frac{A_3}{\Delta\varepsilon_3 + i\Gamma_3}\right]\frac{A_5^*}{\Delta\varepsilon_5 - i\Gamma_5}\right.$$

$$\left.\left[\frac{A_1^*}{\Delta\varepsilon_1 - i\Gamma_1} + \frac{A_2^*}{\Delta\varepsilon_2 - i\Gamma_2} + \frac{A_3^*}{\Delta\varepsilon_3 - i\Gamma_3}\right]\frac{A_5}{\Delta\varepsilon_5 + i\Gamma_5}\right\}$$

$$+\left\{\left[\frac{A_1}{\Delta\varepsilon_1 + i\Gamma_1} + \frac{A_2}{\Delta\varepsilon_2 + i\Gamma_2} + \frac{A_3}{\Delta\varepsilon_3 + i\Gamma_3}\right]\frac{A_6^*}{\Delta\varepsilon_6 - i\Gamma_6}\right.$$

$$\left.\left[\frac{A_1^*}{\Delta\varepsilon_1 - i\Gamma_1} + \frac{A_2^*}{\Delta\varepsilon_2 - i\Gamma_2} + \frac{A_3^*}{\Delta\varepsilon_3 - i\Gamma_3}\right]\frac{A_6}{\Delta\varepsilon_6 + i\Gamma_6}\right\}$$

From each of the expressions in the large braces we obtain

$$\left\{\left[\frac{2A_1A_4(\Delta\varepsilon_1\ \Delta\varepsilon_4 + \Gamma_1\ \Gamma_4)}{(\Delta\varepsilon_1^2 + \Gamma_1^2)(\Delta\varepsilon_4^2 + \Gamma_4^2)}\right] + \left[\frac{2A_2A_4(\Delta\varepsilon_2\ \Delta\varepsilon_4 + \Gamma_2\ \Gamma_4)}{(\Delta\varepsilon_2^2 + \Gamma_2^2)(\Delta\varepsilon_4^2 + \Gamma_4^2)}\right]\right.$$

$$\left. + \left[\frac{2A_3A_4(\Delta\varepsilon_3\ \Delta\varepsilon_4 + \Gamma_3\ \Gamma_4)}{(\Delta\varepsilon_3^2 + \Gamma_3^2)(\Delta\varepsilon_4^2 + \Gamma_4^2)}\right]\right\} \tag{22}$$

or

$$= \frac{2A_4}{(\Delta\varepsilon_4^2 + \Gamma_4^2)} \sum_{s=1}^{3} \frac{A_s(\Delta\varepsilon_s\ \Delta\varepsilon_4 + \Gamma_s\ \Gamma_4)}{\Delta\varepsilon_s^2 + \Gamma_s^2} \tag{23}$$

The same is done with the remaining two terms in the large braces on the previous page. Thus the final expression is

$$\left[\frac{2A_4}{(\Delta\varepsilon_4^2 + \Gamma_4^2)} \sum_{s=1}^{3} \frac{A_s(\Delta\varepsilon_s\ \Delta\varepsilon_4 + \Gamma_s\ \Gamma_4)}{\Delta\varepsilon_s^2 + \Gamma_s^2}\right. \tag{24}$$

$$\frac{2A_5}{(\Delta\varepsilon_5^2 + \Gamma_5^2)} \sum_{s=1}^{3} \frac{A_s(\Delta\varepsilon_s\ \Delta\varepsilon_5 + \Gamma_s\ \Gamma_5)}{\Delta\varepsilon_s^2 + \Gamma_s^2}$$

$$\left.\frac{2A_6}{(\Delta\varepsilon_6^2 + \Gamma_6^2)} \sum_{s=1}^{3} \frac{A_s(\Delta\varepsilon_s\ \Delta\varepsilon_6 + \Gamma_s\ \Gamma_6)}{\Delta\varepsilon_s^2 + \Gamma_s^2}\right] + |R_{123}|^2 + |R_{456}|^2$$

To expand to n>6 we proceed as prescribed on the second page.

APPENDIX I

PART B

A flow diagram of the program

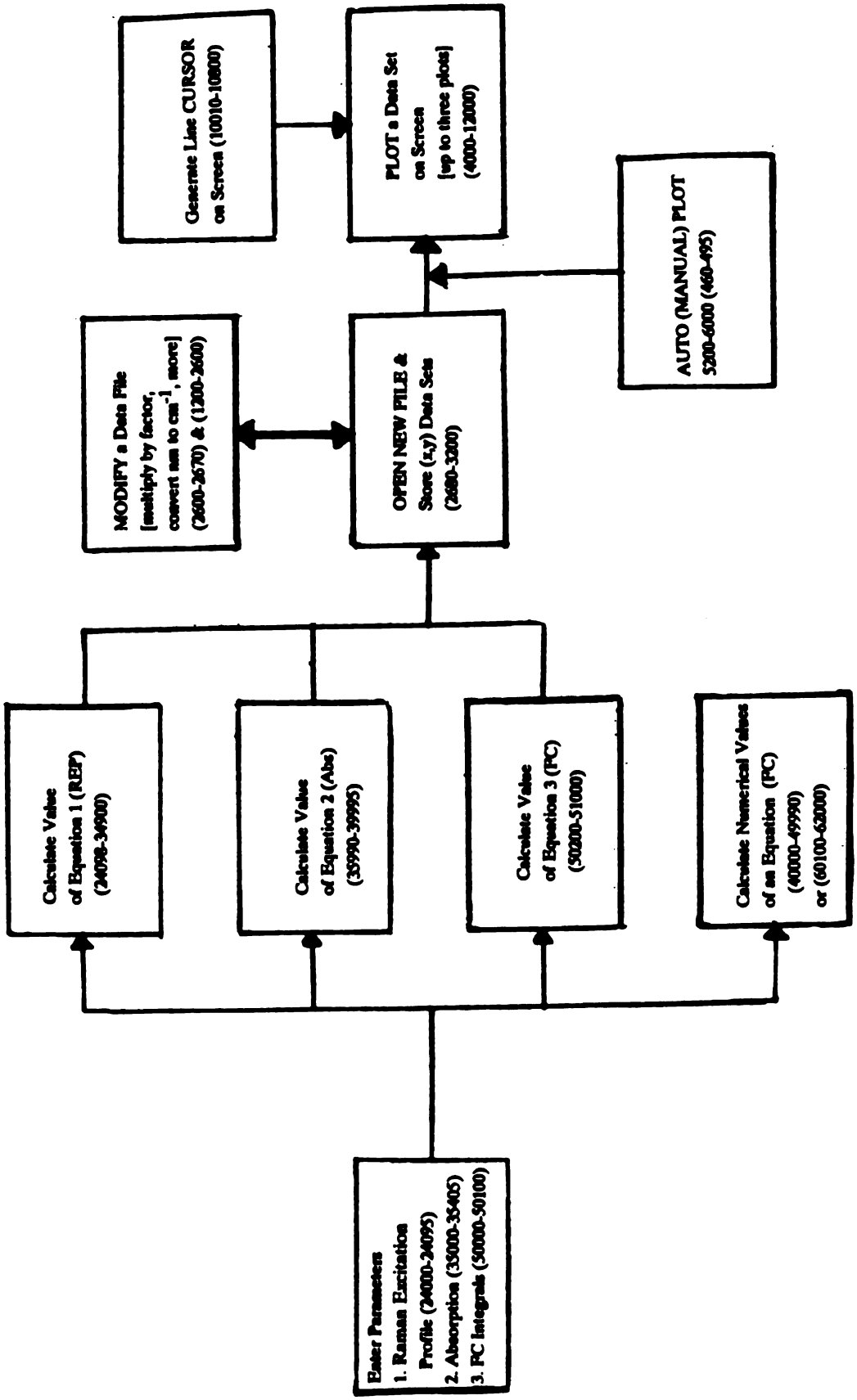
Enter Parameters
1. Raman Excitation Profile (24000-24095)
2. Absorption (33000-35405)
3. FC Integrals (50000-50100)
Calculate Value of Equation 1 (REP) (24098-34900)
Calculate Value of Equation 2 (Abs) (35990-39995)
Calculate Value of Equation 3 (FC) (50200-51000)
Calculate Numerical Values of an Equation (FC) (40000-49990) or (60100-62000)
OPEN NEW FILE & Store (x,y) Data Sets (2680-3200)
MODIFY a Data File [multiply by factor; convert nm to cm^{-1}, more] (2600-2670) & (1200-2600)
AUTO (MANUAL) PLOT 5200-6000 (460-495)
PLOT a Data Set on Screen [up to three plots] (4000-12000)
Generate Line CURSOR on Screen (10010-10800)

TABLE IV.

APPENDIX I

PART B††

```
100 REM *------* lines 110-140 set up the screen *--------*
110 CLS
120 SCREEN 9 : REM ==== EGA ======
130 PALETTE 0,3 :REM ==== Blue background =====
200 CLS:LOCATE 6,10

205 PRINT "---- PLOTTING AND DATA MANIPULATION PROGRAM ----
                        BY ISAAC SZTAINBUCH       "

210 LOCATE 10,10

215 PRINT  "Program to create and modify data points (x,y).
            Lines 2635 and 2655 are for performing
            calculation on x and y.  Press [enter] for a
            default step.  Respond to questions in ( )."
220 PRINT  "Equations of lines 24000- or 35000- or 50000
            will be plotted and its points will be stored
            in a file (If out of memory delete equations
            50000-, temporarily)"

225  PRINT "------   PRESS * TO START OR STOP   --------"


230 B$=INKEY$
235 IF B$="*" THEN GOTO 245
240 GOTO 230
245 CLS:LOCATE 10,10


250  PRINT " (1) Create a NEW FILE
              (2) MODIFY an existing file
              (3) Create and Plot a New File by Equations
                   [lines 24K, 35K, 50K]"
255  PRINT " (4) Same as 3 but graph points are CONNECTED
              (5) Plot a Data File
              (6) Plot TWO Files simultaneously (x,y scale
                  of file 1) "
260  PRINT " (7) Same as 6 but points NOT CONNECTED
              (8) Plot TWO files but NOT AUTOSCALE (+ for a
                  3rd file, * to end)
              (9) Plot THREE Files (otherwise it is same as 6)"
265  INPUT " (10) Perform calculation on equations [line
                  40000-]
              (11) Perform calculation on equations [line
                  60000-] ";Y
```

```
270 GOTO 1140
295 REM *-------* Lines 300-380 sets-up a table *-------*
300 LOCATE 6,11
310 LINE (35,90)-(530,65),12,B
320 LINE (75,65)-(75,170),5
330 LINE (178,65)-(178,170),10
340 LINE (285,65)-(285,170),5
350 LINE (287,65)-(287,170),5
360 LINE (410,65)-(410,170),10
370 LOCATE 6,7:PRINT "N":LOCATE 6,15:PRINT "X":LOCATE
    6,31:PRINT
    "Y":LOCATE 6,43:PRINT "X'":LOCATE 6,59:PRINT "Y'"
380 RETURN
400 REM -- 400-450 determines max.,min of x,y in the file --
410 IF N=1 THEN LET Q=U
420 IF ABS(U)>M THEN LET M=U
425 IF ABS(T)>K1 THEN LET K1=T
430 IF T<K2 THEN LET K2=T
440 L=(M-Q)/100
450 RETURN
460 REM -------- When auto scale is not needed ---------
470 LOCATE 7,8 : INPUT "Enter min range for x in f(x) ";Q
475 LOCATE 8,8 : INPUT "Enter max range for x in f(x) ";M
480 LOCATE 9,8 : INPUT "Enter min range for y ";K2
485 LOCATE 10,8 : INPUT "Enter max range for y ";K1
490 IF K1=0 THEN GOTO 480 : REM ****to be sure that value
    <>0,error otherwise ****
495 RETURN : REM ** ( to line 4005 ) **
499 REM --- 545-560 places a numerical value at tick mark --
500 LOCATE 25,2 :PRINT Q
510 LOCATE 25,38:PRINT ((M-Q)/2)+Q
515 LOCATE 25,71:PRINT USING "##.###^^^^";M
520 LOCATE 3,4:PRINT USING  "##.###^^^^";K1
530 REM --- 530-550 generates tick marks on the x,y-axis ---
532 T1=10 : REM ---- This is the number of tick marks -----
535 FOR N=0 TO T1
540 F=26+N*((619-26)/T1)
545 F2=26+N*((324-26)/T1)
550 LINE (F,330)-(F,320),15
555 LINE (20,F2)-(30,F2),15
560 NEXT N
570 IF K2=0 THEN GOTO 600
580 LINE (25,25)-(620,176),4,B : REM *** DRAW CENTER LINE
                                 IF K2<0 ***
590 LOCATE 23,5:PRINT USING "##.##^^^^";K2
600 RETURN : REM *---* see line 9175 *---*
1140 IF  3=Y  OR 4=Y OR 1=Y THEN GOTO  2700 :REM see line
270
1150 IF 10=Y THEN GOTO 40000
1160 IF 11=Y THEN GOTO 60000
1180  IF  5=Y OR 6=Y OR 7=Y OR 8=Y OR 9=Y THEN GOTO  4000
1195 REM ---- 1200-2600 for modifing existing file, Z$ ----
1200 CLS : LOCATE 8,8 : INPUT "Existing file name";Z$
1250 LOCATE 10,8 : INPUT "New modified file name";A$
```

```
1400 LOCATE 12,8 : INPUT "Enter New Text";T$
1410 LOCATE 13,8 : PRINT T$
1440 LOCATE 15,8 : INPUT  "Enter value to screen ";B :
     REM *---* See 1690,92 *---*
1445 GOSUB 2600
1450 OPEN "I",#1,Z$
1500 FOR N=0 TO 10000
1550 IF N=0 THEN GOTO 2300
1565 IF "n"=F$ THEN GOTO 1675
1575 LOCATE 3,7 : INPUT "Modify manually (n)";F$ : CLS
1585 IF "n"=F$ THEN GOTO 1675
1600 LOCATE 6,8 : INPUT "Insert Line (i)";H$
1650 IF "i"=H$ THEN GOTO 1850
1675 INPUT #1,W
1680 ON ERROR GOTO 2530
1690 REM *-* Numerical values in the original TITLE must be
     deleted (e.g. date) *-*
1692 B2=88 : REM *------* If more than one value is to be
             deleted enter a value for B2(next step) *-----*
1700 IF W=0 OR W=B OR W=B2 THEN GOTO 1675
1725 INPUT #1,S
1740 IF "n"=F$ THEN GOTO 1785
1750 LOCATE 8,32:PRINT  N,W,S
1785 IF "n"=F$ THEN GOTO 2150
1800 LOCATE 8,8 : INPUT "Delete Line (d)";G$
    :IF "d"=G$ THEN GOTO 2520
1850 LOCATE 10,25 : INPUT "New X Value";P
1900 LOCATE 10,50 : INPUT "New Y Value";Q1 : CLS
1950 IF P=0 THEN GOTO 2050
2000 IF P<>0 THEN LET W=P
2050 IF Q1=0 THEN GOTO 2150
2100 IF Q1<>0 THEN LET S=Q1
2150 GOSUB 2635
2250 IF N<>0 THEN GOTO 2360
2295 REM *=*=*=* Modified file is stored in A$ *=*=*=*=*
2300 OPEN "o",#2,A$
2350 PRINT #2,T$:GOTO 2520
2360 GOSUB 300
2400 LOCATE 8,6: PRINT N :LOCATE 8,13: PRINT W:LOCATE
     8,25:PRINT
     USING "##.###^^^^";S:LOCATE 8,39:PRINT USING
    "##.###^^^^";U:LOCATE 8,54:PRINT USING "##.###^^^^";T
2450 GOSUB 400
2500 PRINT #2,U,T
2510 IF EOF(1) THEN GOTO 2530
2520 NEXT N
2530 LOCATE  15,28:INPUT "Plot this file ( y or n )";C$
2540 IF "y"<>C$ THEN  GOTO 11000
2550 REM - lines 2560-2590 prepares the file to be plotted -
2560 CLOSE #2
2570 CLS:OPEN "I", #2,A$
2580  V=2
2590 GOTO 9150
2595 END
```

```
2600 REM ---- 2600-2670 For modification of data points ----
2605 CLS
2610 LOCATE 8,8 : INPUT " Enter new slope ";A2
2615 LOCATE 10,8: INPUT " Enter new vertical shift
     ( intercept )";A3
2620 LOCATE 12,8: INPUT " Change nm to cm-1";Q$
2625 CLS
2630 RETURN : REM ----- To 1445 -------
2635 A1=1E+07  : U=(1/W)*A1 :REM -*- Change nm to cm-1 -*-
2640 IF "y" = Q$  THEN GOTO 2650
2645 A1=1  : U=W*A1 :REM -*- ENTER X VALUE CHANGES IN A1 -*-
2650 IF A2=0  THEN GOTO 2660
2655 T=(S*A2)+A3
2660 IF A2<>0 THEN GOTO 2680: REM*2640 & this leaves T
     unchanged by default**
2670 T=S+A3
2680 RETURN : REM ----- To 2150 ------
2698 REM*** STEPS 2700-3200 ARE FOR CREATING A NEW FILE ***
2700 CLS : LOCATE 10,10 : INPUT "File Name";Z$
2750 LOCATE 12,10 : INPUT "Text";T$
2800 OPEN "O",#1,Z$
2825 PRINT #1,T$ : LOCATE 13,10 : PRINT T$
2860 IF  3=Y OR 4=Y THEN GOTO 5000
2900 FOR N=0 TO 10000
2950 LOCATE 16,15 : INPUT "X value";W
3000 LOCATE 16,35 : INPUT "Y value";S
3050 LOCATE 18,15 : PRINT N,W,S
3100 PRINT #1,W,S
3125 REM IF W=0 AND S=0 THEN GOTO 12000 :
     REM -- To terminate a new file --
3150 NEXT N
3200 GOTO 9000
3995 REM -*-*-*-*-*-* 4000-4475 plots file 1 -*-*-*-*-*-*-
4000 CLS: LOCATE 4,8: INPUT "File 1 to be plotted";Z$
4005 IF 8=Y THEN GOSUB 470
4010 IF Y=5 THEN GOTO 4050
4025 LOCATE 12,8 :INPUT "File 2 to be plotted";P$
4030 IF Y<>9 AND Y<>8 THEN GOTO 4050
4040 LOCATE 20,8 :INPUT "File 3 to be plotted";SZ$
4045 IF 8=Y THEN GOTO 9000
4050 CLS:OPEN "I",#1,Z$
4100 INPUT "Enter value to screen" ;B
4125 REM IF 8=Y THEN GOTO 4370
4150  FOR N=1 TO 100000!
4200  INPUT #1,U
4250 IF U=0 OR U=89 OR U=88 OR U=87 OR U=90 OR U=B THEN
     GOTO 4200 : REM *-* Number (U) in the title that needs
     to be screened -*-*-
4300 INPUT #1,T
4320  IF EOF(1) THEN GOTO 9000
4350 GOSUB 400
4400 PRINT U,T
4450 NEXT N
4475 END
```

```
4495 REM -*-*- 4500-4750 file 2 to be plotted -*-*-
4500 CLOSE #1: V=1
4550 OPEN "I",#1,P$
4600 J=1 : H=4 :REM *-* J=1 prevents first & second graph
from being connected ( H sets the graph color to brown ) *-*
4650 KZ=9 :REM ---- To get it to plot file 3 after
          plotting file 2 ----
4700 GOTO 9300
4750 END
4780 REM *--------* 4800-4950 file 3 to be plotted *------*
4790 IF Y<>9  THEN GOTO 11200
4800 CLOSE #1: V=1
4825 OPEN "I",#1,SZ$
4850 J=1 : H=1 :REM *-------* J=1 prevents first & second
graph from being connected   ( H sets the graph color to
blue ) *-----*
4870 KZ=99 :REM -- To get to end after plotting file 3 ---
4900 GOTO 9300
4950 END
4995 REM -------- 5000-6000 Plots the equation -------
5000 LOCATE 14,10 : INPUT "Plot Equation (0), (1), or (2)
[ENTER for 0]  ";HH
5025 LOCATE 16,10 : INPUT "Enter min range for x in f(x) ";Q
5050 LOCATE 18,10 : INPUT "Enter max range for x in f(x) ";M
5075 LOCATE 20,10 : INPUT "Enter incremental steps for x";L
5100 FOR W=Q TO M STEP L
5125 IF HH=0 THEN GOSUB 24000
5150 IF HH=1 THEN GOSUB 35000
5175 IF HH=2 THEN GOSUB 50000
5200 REM ---- 5225 determines max y value for auto plot ----
5225 IF ABS(S)> K1 THEN LET K1=S
5250 IF S< K2 THEN LET K2=S
5300 PRINT W,S
5400 PRINT #1,W,S
5600 NEXT W
5800 GOTO 9000
6000 END
9000 CLOSE #1
9100 V=1
9125 CLS: OPEN "I",#1,Z$
9150 REM LINE (25,25)-(620,325),7,BF
9175 GOSUB 500
9200 H=10:REM - This determines the color of graph (green) -
9225 C=Z:W0=W1
9250 IF KZ<>9  THEN GOTO 9275:REM ** kz presence of file 3
     (Also in line 4650)**
9265 IF EOF(1) THEN GOTO 4790:REM *** file 2 completed start
     plotting 3 ***
9275 IF KZ<>99  THEN GOTO 9300:REM**(kz) presence of file 3
     (Also in line 4870)
9285 IF EOF(1) THEN GOTO 11200:REM - file 3 plot completed -
9300 LOCATE 1,1:INPUT  #V,W
9325 B$=INKEY$
```

```
9350 IF B$="*" THEN GOTO 11300 : REM --- To stop from
     further plotting ---
9375 ON ERROR GOTO 10025
9400 IF W=0 OR W=89 OR W=90 OR W=B2 THEN GOTO 9300
9450 IF W<Q THEN GOTO 9300
9500 INPUT  #V,S
9550 W1=((620-25)/(M-Q))*(W-M)+620
9600 Z=(S-K2)*(280)/(K1-K2)
9650 REM PRINT W0,W1,(320-C),(320-Z)
9695 REM ----- 9700 puts square data points on graph ----
9700 LINE (W1,(320-Z))-(W1+2,(320-Z)+2),H,BF
9750 LINE (25,25)-(620,325),4,B
9790 REM - Step 9800, 9900,9225 are for connecting
     data points
9800 IF C=0 AND W0=0 THEN GOTO 9950
9845 REM *---* Set J=1 (same as in 4600) so that the last
     and  first points not be  connected  *-----*
9850 IF 3=Y OR 7=Y OR J= 1 THEN GOTO 9950
9900 LINE (W0,(320-C))-(W1,(320-Z)),H
9950 J=2:REM *-*-*-* This is to prevent it from skipping
     9900 again *-*-*-*
9975 GOTO 9225
10000 END
10010 REM  -- Lines 10050-10800 creates the cursor and
      generates it location (for use with equation only ) --
10025 IF Y=2 OR Y=5 OR Y=6 OR Y=7 OR Y=8 OR Y=9 THEN
      GOTO 11100
10050 B$=INKEY$
10100 LINE (W1,325)-(W1,337),0
10120 LINE (W1,0)-(W1,25),0
10150 W1=((620-25)/(M-Q))*(W-M)+620
10175 N=(M-Q)/100:REM ----- determines rate of cursor ------
10200 IF B$="+" THEN LET W=W+N
10300 IF B$="-" THEN LET W=W-N
10400 LINE (W1,325)-(W1,337),9
10420 LINE (W1,0)-(W1,25),9
10500 IF B$="*" THEN GOTO 11300
10550 IF HI=5 THEN GOTO 10750 :REM To display x-axis
      value only
10600 IF HH=0 THEN GOSUB 24000
10625 IF HH=1 THEN GOSUB 35000
10650 IF HH=2 THEN GOSUB 50000
10700 LOCATE 3,68 : PRINT USING "##.##^^^^";S
10725 LOCATE 3,58 : PRINT W
10750 REM LINE (25,25)-(620,325),4,B
      : REM - refreshes the box -
10800 IF HI<>5 THEN GOTO 10900
      : REM - To display W at another location -
10850 LOCATE 1,1 :PRINT USING "##.###^^^^";W
10900 GOTO 10050
11000 LOCATE 15,27 :PRINT  "------------ DONE ------------"
11100 IF Y=6 OR Y=7 OR Y=8  OR Y=9  THEN  GOTO  4500 : REM
      ********* This begins second plot *********
11200 IF Y<>8 THEN GOTO 11300
```

```
11210 B$=INKEY$
11215 IF B$="/" THEN GOTO 11300
11220 IF B$="+" THEN GOTO 4800
11225 LOCATE 1,1 :PRINT "PRESS / or +"
11230 GOTO 11210
11299 REM Lines 11300-11350  places a name label
      for each plot
11300 LOCATE 3,47 : PRINT Z$
11305 LOCATE 3,47 : PRINT A$
11310 LOCATE 3,58 : PRINT P$
11320 LOCATE 3,68 : PRINT SZ$
11330 LINE(368,25)-(440,25),10,B
11340 LINE(450,25)-(525,25),4,B
11350 LINE(535,25)-(620,25),9,B
11400 IF B$="*" THEN GOTO 11900 :REM -prevents being trapped
      in a loop-
11500 HI=5 : GOTO 10050  : REM ==== see line 10550  ====
11900 LOCATE 1,1 : REM -- This is to place cursor at origin
12000 END



24000 REM --- Enter function in program line 24000-34999 ---
24005 REM ----- Raman Excitation Profile Parameters ----
24010 REM ** t11=> VE1 delta, t22=> VE2, t33=> VE3 delta,
      K= mult  const for Ag
24015 REM ** t1=> V1 delta, t2=> V2 , t3=> V3 delta,
          C= mult const for Bu state

24020 REM ==================== Ag ========================
        T11=.36       :T22=.3      :T33=.37    :T44=.11
        : K=425
24030   VE1=1750      :VE2=1250    :VE3=200    :VE4=1550
       :VG1=1550      :VG2=1200    :VG3=200    :VG4=1550
24035   E1=20175      :E2=E1+(VE3)           :E3=E1+(VE2)
       :E4=E1+(VE1)   :E5=E1+(VE1)+(VE3)    :E6=E1+(VE2)+(VE3)
       :E23†=E1+(VE4)
24040   G1=50         :G2=G1       :G3=G1      :G4=G1
       :G5=G1         :G6=G1       :G23†=G1
24045 REM ================================================
24050 REM ==================== Bu=========================
24060   T1=.17     :T2=.15      :T3=.1      : C=10225
       :V1=1550    :V2=1200     :V3=200
24070  :E7 =23750       :E8 =E7+V1             :E9 =E7+V2
       :E10=E7+V3       :E11=E7+2*(V1)         :E12=E7+2*(V2)
       :E13=E7+(V1+V2)     :E14=E7+(V2+V3)     :E15=E7+(V1+V3)
24075   E16=E7+2*(V1)+V2  :E17=E7+2*(V2)+V1   :E18=E7+3*(V1)
       :E19=E7+(2*(V1)+2*(V2))          :E20=E7+(2*(V1)+V3)
       :E21=E7+(2*(V2)+V3)              :E22=E7+3*(V1)+V2
24090 G7=500    :G8=G7    :G9=G7    :G10=G7   :G11=G7   :G12=G7
     :G13=G7    :G14=G7   :G15=G7   :G16=G7   :G17=G7   :G18=G7
     :G19=G7    :G20=G7   :G21=G7   :G22=G7
24095 REM================================================
```

```
24098 REM ----  Franck-Condon integrals ( Ag state ) ---
24100 F01=2*(.1217)*(((VE1)*(VG1)^.5)/((VE1)+(VG1)))*(T11)
 *(4*((VE1)*(VG1))/(((VE1)+(VG1))^2))*EXP(2*(.0148)
 *((T11)^2)*(((VE1)*(VG1))/((VE1)+(VG1))))
24200 F02=4*(((VE2)*(VG2))/(((VE2)+(VG2))^2))*EXP(2
 *(.0148)*((T22)^2)*(((VE2)*(VG2))/((VE2)+(VG2))))
24300 F03=4*(((VE3)*(VG3))/(((VE3)+(VG3))^2))*EXP(2
 *(.0148)*((T33)^2)*(((VE3)*(VG3))/((VE3)+(VG3))))
24350 F04=4*(((VE4)*(VG4))/(((VE4)+(VG4))^2))*EXP(2
 *(.0148)*((T44)^2)*(((VE4)*(VG4))/((VE4)+(VG4))))
24400 P01=2*(.1217)*(((VG1)*(VE1)^.5)/((VE1)+(VG1)))
 *(T11)*(4*((VE1)*(VG1))/(((VE1)+(VG1))^2))*EXP(2
 *(.0148)*((T11)^2)*(((VE1)*(VG1))/((VE1)+(VG1))))
24450 P02=4*(.0148)*((((VE1)*(VG1))^1.5)/(((VE1)+(VG1))^2))
 *((T11)^2)-2*(((VE1)*(VG1))^.5)/((VE1)+(VG1))
24500 F05=(P01)*(P02)
24600 F06=4*(.0148)*((((VG2)*((VE2)^.5))/((VE2)+(VG2)))^2)
 *((T22)^2)*4*(((VE2)*(VG2))/(((VE2)+(VG2))^2))
 *EXP(-2 *(.0148)
 *((T22)^2)*(((VE2)*(VG2))/((VE2)+(VG2))))
24700 F07=4*(.0148)*((((VG3)*((VE3)^.5))/((VE3)+(VG3)))^2)
 *((T33)^2)*4*(((VE3)*(VG3))/(((VE3)+(VG3))^2))
 *EXP(-2*(.0148)*((T33)^2)*(((VE3)*(VG3))/((VE3)+(VG3))))
24750 F08=4*(.0148)*((((VG4)*((VE4)^.5))/((VE4)+(VG4)))^2)
 *((T44)^2)*4*(((VE4)*(VG4))/(((VE4)+(VG4))^2))
 *EXP(2 *(.0148) *((T44)^2)*(((VE4)*(VG4))/((VE4)+(VG4))))
24895 REM ------------------------------------------------
24900 REM

        (V1)          (V2)          (V3)          (v4)
F01=<1|0><0|0>  F02=<0|0><0|0>  F03 =<0|0><0|0>  F04=<0|0><0|0>
F05=<1|1><1|0>  F06=<0|1><1|0>  F07 =<0|1><1|0>  F08=<0|1><1|0>

24905 REM ------------------------------------------------
24950 A1=K*(F01)*(F02)*(F03)*(F04) :A2=K*(F01)*(F02)*(F07)*(F04)
     :A3=K*(F01)*(F06)*(F03)*(F04)
24960 A4=K*(F05)*(F02)*(F03)*(F04) :A5=K*(F05)*(F02)*(F07)*(F04)
    :A6=K*(F01)*(F06)*(F07)*(F04) :A23=K*(F01)*(F02)*(F03)*(F08)
25000REM================================================

25110 REM ////// Franck-Condon integrals (Bu state) //////
25120 REM F1=EXP(-(.0148*(((T4)^2)*(V4))))
25125 F2=EXP(-(.0148*(((T3)^2)*(V3))))
25130 F3=EXP(-(.0148*(((T2)^2)*(V2))))
25135 F4=.122*((V1)^.5)*(T1)*EXP(-.0148*(V1)*((T1)^2))
25140 F5=.0148*(V2)*((T2)^2)*EXP(-.0148*(V2)*((T2)^2))
25145 F55=.0148*(V3)*((T3)^2)*EXP(-.0148*(V3)*((T3)^2))
25150 REM F01=.0148*(V4)*((T4)^2)*EXP(-.0148*(V4)*((T4)^2))
25155 F6=.122*((V1)^.5)*(T1)*(.0148*(V1)*((T1)^2)-1)
          *EXP(-.0148*(V1)*((T1)^2))
25160 F7=((.0148)^2)*((V2)^2)*((T2)^4)
         *EXP(-(.0148*(V2)*((T2)^2)))
25165 F77=((.0148)^2)*((V3)^2)*((T3)^4)
          *EXP(-(.0148*(V3)*((T3)^2)))
```

```
25170 REM F02=((.0148)^2)*((V4)^2)*((T4)^4)
            *EXP(-(.0148*(V4)*((T4)^2)))
25175 F9=(.00127)*((V1)^1.5)*(.0148*(V1)
       *((T1)^5)-2* ((T1)^3))*EXP(-.0148*(V1)*((T1)^2))
25180 F10=(8.88E-06)*((V1)^2.5)*((.010465)*(V1)
      *((T1)^7)-(2.414) *((T1)^5))*EXP(-.0148*(V1)*((T1)^2))
25210 F11=((.3333)*(.0148)^3)*((V2)^3)*((T2)^6)
         *EXP(-(.0148*(V2)*((T2)^2)))
25242 REM ------------------------------------------------
25244 REM

                 (V1)          |        (V2)          |        (V3)
           F4=<1|0><0|0>       |   F3=<0|0><0|0>      |  F2=<0|0><0|0>
           F6=<1|1><1|0>       |   F5=<0|1><1|0>      |  F55=<0|1><1|0>
25245 REM  F9=<1|2><2|0>       |   F7=<0|2><2|0>      |  F77=<0|2><2|0>
          F10=<1|3><3|0>       |  F11=<0|3><3|0>      |

25248 REM ------------------------------------------------
25250  A7=C*(F4)*(F3)*(F2)        :A8 =C*(F6)*(F3)*(F2)
      :A9=C*(F4)*(F5)*(F2)        :A10=C*(F4)*(F3)*(F55)
      :A11=C*(F9)*(F3)*(F2)       :A12=C*(F4)*(F7)*(F2)
25255 :A13=C*(F6)*(F5)*(F2)       :A14=C*(F4)*(F5)*(F55)
      :A15=C*(F6)*(F3)*(F55       :A16=C*(F9)*(F5)*(F2)
25265  A17=C*(F6)*(F7)*(F2)       :A18=C*(F10)*(F3)*(F2)
25270 :A19=C*(F9)*(F7)*(F2)       :A20=C*(F9)*(F3)*(F55)
      :A21=C*(F4)*(F7)*(F55       :A22=C*(F10)*(F5)*(F2)
25290 REM ------------------------------------------------
```

```
25294 REM ----------------------------
25295 REM  \\\\\\\\ REP EQUATIONS BEGIN HERE \\\\\\\
25300 I1=A1*(((E1-W)*(E3-W)+G1*G3)/(((E1-W)^2)+(G1)^2)) *(A3/(((E3-W)^2)+(G3)^2))
25400 I2=A2*(((E2-W)*(E1-W)+G2*G1)/(((E2-W)^2)+(G2)^2)) *(A1/(((E1-W)^2)+(G1)^2))
25500 I3=A3*(((E3-W)*(E2-W)+G3*G2)/(((E3-W)^2)+(G3)^2)) *(A2/(((E2-W)^2)+(G2)^2))
25600 I4=A4*(((E4-W)*(E6-W)+G4*G6)/(((E4-W)^2)+(G4)^2)) *(A6/(((E6-W)^2)+(G6)^2))
25700 I5=A5*(((E5-W)*(E4-W)+G5*G4)/(((E5-W)^2)+(G5)^2)) *(A4/(((E4-W)^2)+(G4)^2))
25800 I6=A6*(((E6-W)*(E5-W)+G6*G5)/(((E6-W)^2)+(G6)^2)) *(A5/(((E5-W)^2)+(G5)^2))
25900  R1=(A1^2)/(((E1-W)^2)+G1^2)
26000  R2=(A2^2)/(((E2-W)^2)+G2^2)
26100  R3=(A3^2)/(((E3-W)^2)+G3^2)
26200  R4=(A4^2)/(((E4-W)^2)+G4^2)
26300  R5=(A5^2)/(((E5-W)^2)+G5^2)
26400  R6=(A6^2)/(((E6-W)^2)+G6^2)
26500 X1=A1*(((E1-W)*(E4-W)+G1*G4)/(((E1-W)^2)+(G1)^2)) *(A4/(((E4-W)^2)+(G4)^2))
26600 X2=A2*(((E2-W)*(E4-W)+G2*G4)/(((E2-W)^2)+(G2)^2)) *(A4/(((E4-W)^2)+(G4)^2))
26700 X3=A3*(((E3-W)*(E4-W)+G3*G4)/(((E3-W)^2)+(G3)^2)) *(A4/(((E4-W)^2)+(G4)^2))
26800 Y1=A1*(((E1-W)*(E5-W)+G1*G5)/(((E1-W)^2)+(G1)^2)) *(A5/(((E5-W)^2)+(G5)^2))
26900 Y2=A2*(((E2-W)*(E5-W)+G2*G5)/(((E2-W)^2)+(G2)^2)) *(A5/(((E5-W)^2)+(G5)^2))
27000 Y3=A3*(((E3-W)*(E5-W)+G3*G5)/(((E3-W)^2)+(G3)^2)) *(A5/(((E5-W)^2)+(G5)^2))
27100 Z1=A1*(((E1-W)*(E6-W)+G1*G6)/(((E1-W)^2)+(G1)^2)) *(A6/(((E6-W)^2)+(G6)^2))27200 Z2=A2*(((E2-
W)*(E6-W)+G2*G6)/(((E2-W)^2)+(G2)^2)) *(A6/(((E6-W)^2)+(G6)^2))
27300 Z3=A3*(((E3-W)*(E6-W)+G3*G6)/(((E3-W)^2)+(G3)^2)) *(A6/(((E6-W)^2)+(G6)^2))
27400 S1=(R1+R2+R3+R3+R4+R5+R6) +2*(I1+I2+I3+I4+I5+I6+X1+X2+X3+Y1+Y2+Y3+Z1+Z2+Z3)
27410 REM U01-U06 & R7 are an extention for a 7th term
27420 U01=A1*(((E1-W)*(E7-W)+G1*G7)/(((E1-W)^2)+(G1)^2)) *(A7/(((E7-W)^2)+(G7)^2))
```

```
27430 U02=A2*(((E2-W)*(E7-W)+G2*G7)/(((E2-W)^2)+(G2)^2)) *(A7/(((E7-W)^2)+(G7)^2))
27440 U03=A3*(((E3-W)*(E7-W)+G3*G7)/(((E3-W)^2)+(G3)^2)) *(A7/(((E7-W)^2)+(G7)^2))
27450 U04=A4*(((E4-W)*(E7-W)+G4*G7)/(((E4-W)^2)+(G4)^2)) *(A7/(((E7-W)^2)+(G7)^2))
27460 U05=A5*(((E5-W)*(E7-W)+G5*G7)/(((E5-W)^2)+(G5)^2)) *(A7/(((E7-W)^2)+(G7)^2))
27470 U06=A6*(((E6-W)*(E7-W)+G6*G7)/(((E6-W)^2)+(G6)^2)) *(A7/(((E7-W)^2)+(G7)^2))
27480  R7=(A7^2)/(((E7-W)^2)+G7^2)
27490 S2= S1+2*(U01+U02+U03+U04+U05+U06)+R7
27495 REM = = = = = = = = = end of 7th term expressions = = = = = = = = = =
27500 REM  D01-D07 & R8 are an extention for an 8th term
27510 D01=A1*(((E1-W)*(E8-W)+G1*G8)/(((E1-W)^2)+(G1)^2)) *(A8/(((E8-W)^2)+(G8)^2))
27520 D02=A2*(((E2-W)*(E8-W)+G2*G8)/(((E2-W)^2)+(G2)^2)) *(A8/(((E8-W)^2)+(G8)^2))
27530 D03=A3*(((E3-W)*(E8-W)+G3*G8)/(((E3-W)^2)+(G3)^2)) *(A8/(((E8-W)^2)+(G8)^2))
27540 D04=A4*(((E4-W)*(E8-W)+G4*G8)/(((E4-W)^2)+(G4)^2)) *(A8/(((E8-W)^2)+(G8)^2))
27550 D05=A5*(((E5-W)*(E8-W)+G5*G8)/(((E5-W)^2)+(G5)^2)) *(A8/(((E8-W)^2)+(G8)^2))
27560 D06=A6*(((E6-W)*(E8-W)+G6*G8)/(((E6-W)^2)+(G6)^2)) *(A8/(((E8-W)^2)+(G8)^2))
27570 D07=A7*(((E7-W)*(E8-W)+G7*G8)/(((E7-W)^2)+(G7)^2)) *(A8/(((E8-W)^2)+(G8)^2))
27580  R8=(A8^2)/(((E8-W)^2)+G8^2)
27590 S3= S2+2*(D01+D02+D03+D04+D05+D06+D07)+R8
27595 REM ---------- end of 8th term expressions ----------
27600 REM  B01-B08 & R9 are an extention for an 9th term
27610 B01=A1*(((E1-W)*(E9-W)+G1*G9)/(((E1-W)^2)+(G1)^2)) *(A9/(((E9-W)^2)+(G9)^2))
27620 B02=A2*(((E2-W)*(E9-W)+G2*G9)/(((E2-W)^2)+(G2)^2)) *(A9/(((E9-W)^2)+(G9)^2))
27630 B03=A3*(((E3-W)*(E9-W)+G3*G9)/(((E3-W)^2)+(G3)^2)) *(A9/(((E9-W)^2)+(G9)^2))
27640 B04=A4*(((E4-W)*(E9-W)+G4*G9)/(((E4-W)^2)+(G4)^2)) *(A9/(((E9-W)^2)+(G9)^2))
27650 B05=A5*(((E5-W)*(E9-W)+G5*G9)/(((E5-W)^2)+(G5)^2)) *(A9/(((E9-W)^2)+(G9)^2))
27660 B06=A6*(((E6-W)*(E9-W)+G6*G9)/(((E6-W)^2)+(G6)^2)) *(A9/(((E9-W)^2)+(G9)^2))
27670 B07=A7*(((E7-W)*(E9-W)+G7*G9)/(((E7-W)^2)+(G7)^2)) *(A9/(((E9-W)^2)+(G9)^2))
27680 B08=A8*(((E8-W)*(E9-W)+G8*G9)/(((E8-W)^2)+(G8)^2)) *(A9/(((E9-W)^2)+(G9)^2))
27690  R9=(A9^2)/(((E9-W)^2)+G9^2)
27695 S4= S3+2*(B01+B02+B03+B04+B05+B06+B07+B08)+R9
27697 REM = = = = = = end of 9th term expressions = = = = = =
27700 REM  H01-H09 & R10 are an extention for an 10th term
27710 H01=A1*(((E1-W)*(E10-W)+G1*G10)/(((E1-W)^2)+(G1)^2)) *(A10/(((E10-W)^2)+(G10)^2))
27720 H02=A2*(((E2-W)*(E10-W)+G2*G10)/(((E2-W)^2)+(G2)^2)) *(A10/(((E10-W)^2)+(G10)^2))
27730 H03=A3*(((E3-W)*(E10-W)+G3*G10)/(((E3-W)^2)+(G3)^2)) *(A10/(((E10-W)^2)+(G10)^2))
27740 H04=A4*(((E4-W)*(E10-W)+G4*G10)/(((E4-W)^2)+(G4)^2)) *(A10/(((E10-W)^2)+(G10)^2))
27750 H05=A5*(((E5-W)*(E10-W)+G5*G10)/(((E5-W)^2)+(G5)^2)) *(A10/(((E10-W)^2)+(G10)^2))
27760 H06=A6*(((E6-W)*(E10-W)+G6*G10)/(((E6-W)^2)+(G6)^2)) *(A10/(((E10-W)^2)+(G10)^2))
27770 H07=A7*(((E7-W)*(E10-W)+G7*G10)/(((E7-W)^2)+(G7)^2)) *(A10/(((E10-W)^2)+(G10)^2))
27780 H08=A8*(((E8-W)*(E10-W)+G8*G10)/(((E8-W)^2)+(G8)^2)) *(A10/(((E10-W)^2)+(G10)^2))
27790 H09=A9*(((E9-W)*(E10-W)+G9*G10)/(((E9-W)^2)+(G9)^2)) *(A10/(((E10-W)^2)+(G10)^2))
27795  R10=((A10)^2)/(((E10-W)^2)+(G10)^2)
27797 S5= S4+2*(H01+H02+H03+H04+H05+H06+H07+H08+H09)+R10
27799 REM ---------- end of 10th term expressions ----------
27800 REM  L01-L010 & R11 are an extention for an 11th term
27810 L01=A1*(((E1-W)*(E11-W)+G1*G11)/(((E1-W)^2)+(G1)^2)) *(A11/(((E11-W)^2)+(G11)^2))
27820 L02=A2*(((E2-W)*(E11-W)+G2*G11)/(((E2-W)^2)+(G2)^2)) *(A11/(((E11-W)^2)+(G11)^2))
27830 L03=A3*(((E3-W)*(E11-W)+G3*G11)/(((E3-W)^2)+(G3)^2)) *(A11/(((E11-W)^2)+(G11)^2))
27840 L04=A4*(((E4-W)*(E11-W)+G4*G11)/(((E4-W)^2)+(G4)^2)) *(A11/(((E11-W)^2)+(G11)^2))
27850 L05=A5*(((E5-W)*(E11-W)+G5*G11)/(((E5-W)^2)+(G5)^2)) *(A11/(((E11-W)^2)+(G11)^2))
27860 L06=A6*(((E6-W)*(E11-W)+G6*G11)/(((E6-W)^2)+(G6)^2)) *(A11/(((E11-W)^2)+(G11)^2))
27870 L07=A7*(((E7-W)*(E11-W)+G7*G11)/(((E7-W)^2)+(G7)^2)) *(A11/(((E11-W)^2)+(G11)^2))
27880 L08=A8*(((E8-W)*(E11-W)+G8*G11)/(((E8-W)^2)+(G8)^2)) *(A11/(((E11-W)^2)+(G11)^2))
27890 L09=A9*(((E9-W)*(E11-W)+G9*G11)/(((E9-W)^2)+(G9)^2)) *(A11/(((E11-W)^2)+(G11)^2))
```

```
27900 L010=A10*(((E10-W)*(E11-W)+G10*G11)/(((E10 -W)^2) +(G10)^2))*(A11/(((E11-W)^2)+(G11)^2))
27910  R11=((A11)^2)/(((E11-W)^2)+(G11)^2)
27920 S6=S5+2*(L01+L02+L03+L04+L05+L06+L07+L08+L09+L010)+R11
27930 REM = = = = = = = = = end of 11th term expressions = = = = = = = = = = =
28000 REM  J01-J011 & R12 are an extention for an 12th term
28010 J01=A1*(((E1-W)*(E12-W)+G1*G12)/(((E1-W)^2)+(G1)^2)) *(A12/(((E12-W)^2)+(G12)^2))
28020 J02=A2*(((E2-W)*(E12-W)+G2*G12)/(((E2-W)^2)+(G2)^2)) *(A12/(((E12-W)^2)+(G12)^2))
28030 J03=A3*(((E3-W)*(E12-W)+G3*G12)/(((E3-W)^2)+(G3)^2)) *(A12/(((E12-W)^2)+(G12)^2))
28040 J04=A4*(((E4-W)*(E12-W)+G4*G12)/(((E4-W)^2)+(G4)^2)) *(A12/(((E12-W)^2)+(G12)^2))
28050 J05=A5*(((E5-W)*(E12-W)+G5*G12)/(((E5-W)^2)+(G5)^2)) *(A12/(((E12-W)^2)+(G12)^2))
28060 J06=A6*(((E6-W)*(E12-W)+G6*G12)/(((E6-W)^2)+(G6)^2)) *(A12/(((E12-W)^2)+(G12)^2))
28070 J07=A7*(((E7-W)*(E12-W)+G7*G12)/(((E7-W)^2)+(G7)^2)) *(A12/(((E12-W)^2)+(G12)^2))
28080 J08=A8*(((E8-W)*(E12-W)+G8*G12)/(((E8-W)^2)+(G8)^2)) *(A12/(((E12-W)^2)+(G12)^2))
28090 J09=A9*(((E9-W)*(E12-W)+G9*G12)/(((E9-W)^2)+(G9)^2)) *(A12/(((E12-W)^2)+(G12)^2))
28100 J010=A10*(((E10-W)*(E12-W)+G10*G12)/(((E10-W)^2) +(G10)^2))*(A12/(((E12-W)^2)+(G12)^2))
28110 J011=A11*(((E11-W)*(E12-W)+G11*G12)/(((E11-W)^2) +(G11)^2))*(A12/(((E12-W)^2)+(G12)^2))
28120  R12=((A12)^2)/(((E12-W)^2)+(G12)^2)
28130 S7=  S6+2*(J01+J02+J03+J04+J05+J06+J07+J08 +J09+J010+J011)+R12
28140 REM ------ end of 12th term expressions -------
28200 REM  O01-O011 & R13 are an extention for an 13th term
28210 O01=A1*(((E1-W)*(E13-W)+G1*G13)/(((E1-W)^2)+(G1)^2)) *(A13/(((E13-W)^2)+(G13)^2))
28220 O02=A2*(((E2-W)*(E13-W)+G2*G13)/(((E2-W)^2)+(G2)^2)) *(A13/(((E13-W)^2)+(G13)^2))
28230 O03=A3*(((E3-W)*(E13-W)+G3*G13)/(((E3-W)^2)+(G3)^2)) *(A13/(((E13-W)^2)+(G13)^2))
28240 O04=A4*(((E4-W)*(E13-W)+G4*G13)/(((E4-W)^2)+(G4)^2)) *(A13/(((E13-W)^2)+(G13)^2))
28250 O05=A5*(((E5-W)*(E13-W)+G5*G13)/(((E5-W)^2)+(G5)^2)) *(A13/(((E13-W)^2)+(G13)^2))
28260 O06=A6*(((E6-W)*(E13-W)+G6*G13)/(((E6-W)^2)+(G6)^2)) *(A13/(((E13-W)^2)+(G13)^2))
28270 O07=A7*(((E7-W)*(E13-W)+G7*G13)/(((E7-W)^2)+(G7)^2)) *(A13/(((E13-W)^2)+(G13)^2))
28280 O08=A8*(((E8-W)*(E13-W)+G8*G13)/(((E8-W)^2)+(G8)^2)) *(A13/(((E13-W)^2)+(G13)^2))
28290 O09=A9*(((E9-W)*(E13-W)+G9*G13)/(((E9-W)^2)+(G9)^2)) *(A13/(((E13-W)^2)+(G13)^2))
28300 O010=A10*(((E10-W)*(E13-W)+G10*G13)/(((E10-W)^2) +(G10)^2))*(A13/(((E13-W)^2)+(G13)^2))
28310 O011=A11*(((E11-W)*(E13-W)+G11*G13)/(((E11-W)^2) +(G11)^2))*(A13/(((E13-W)^2)+(G13)^2))
28320 O012=A12*(((E12-W)*(E13-W)+G12*G13)/(((E12-W)^2) +(G12)^2))*(A13/(((E13-W)^2)+(G13)^2))
28330 R13=((A13)^2)/(((E13-W)^2)+(G13)^2)
28340 S8 = S7+2*(O01+O02+O03+O04+O05+O06+O07+O08+O09 +O010+O011+O012)+R13
28350 REM = = = = = = = = end of 13th term expressions = = = = = = = =
28400 REM  Q1-Q13 & R14 are an extention for an 14th term
28410 Q1=A1*(((E1-W)*(E14-W)+G1*G14)/(((E1-W)^2)+(G1)^2)) *(A14/(((E14-W)^2)+(G14)^2))
28420 Q2=A2*(((E2-W)*(E14-W)+G2*G14)/(((E2-W)^2)+(G2)^2)) *(A14/(((E14-W)^2)+(G14)^2))
28430 Q3=A3*(((E3-W)*(E14-W)+G3*G14)/(((E3-W)^2)+(G3)^2)) *(A14/(((E14-W)^2)+(G14)^2))
28440 Q4=A4*(((E4-W)*(E14-W)+G4*G14)/(((E4-W)^2)+(G4)^2)) *(A14/(((E14-W)^2)+(G14)^2))
28450 Q5=A5*(((E5-W)*(E14-W)+G5*G14)/(((E5-W)^2)+(G5)^2)) *(A14/(((E14-W)^2)+(G14)^2))
28460 Q6=A6*(((E6-W)*(E14-W)+G6*G14)/(((E6-W)^2)+(G6)^2)) *(A14/(((E14-W)^2)+(G14)^2))
28470 Q7=A7*(((E7-W)*(E14-W)+G7*G14)/(((E7-W)^2)+(G7)^2)) *(A14/(((E14-W)^2)+(G14)^2))
28480 Q8=A8*(((E8-W)*(E14-W)+G8*G14)/(((E8-W)^2)+(G8)^2)) *(A14/(((E14-W)^2)+(G14)^2))
28490 Q9=A9*(((E9-W)*(E14-W)+G9*G14)/(((E9-W)^2)+(G9)^2)) *(A14/(((E14-W)^2)+(G14)^2))
28500 Q10=A10*(((E10-W)*(E14-W)+G10*G14)/(((E10-W)^2)+(G10)^2)) *(A14/(((E14-W)^2)+(G14)^2))
28510 Q11=A11*(((E11-W)*(E14-W)+G11*G14)/(((E11-W)^2) +(G11)^2))*(A14/(((E14-W)^2)+(G14)^2))
28520 Q12=A12*(((E12-W)*(E14-W)+G12*G14)/(((E12-W)^2) +(G12)^2))*(A14/(((E14-W)^2)+(G14)^2))
28530 Q13=A13*(((E13-W)*(E14-W)+G13*G14)/(((E13-W)^2) +(G13)^2))*(A14/(((E14-W)^2)+(G14)^2))
28540  R14=((A14)^2)/(((E14-W)^2)+(G14)^2)
28550 S9=S8+2*(Q1+Q2+Q3+Q4+Q5+Q6+Q7+Q8+Q9+Q10+Q11+Q12+Q13)+R14
28560 REM ***** end of 14th term expressions *******
28700 REM  N1-N14 & R15 are an extention for an 15th term
28710 N1=A1*(((E1-W)*(E15-W)+G1*G15)/(((E1-W)^2)+(G1)^2)) *(A15/(((E15-W)^2)+(G15)^2))
```

```
28720 N2=A2*(((E2-W)*(E15-W)+G2*G15)/(((E2-W)^2)+(G2)^2)) *(A15/(((E15-W)^2)+(G15)^2))
28730 N3=A3*(((E3-W)*(E15-W)+G3*G15)/(((E3-W)^2)+(G3)^2)) *(A15/(((E15-W)^2)+(G15)^2))
28740 N4=A4*(((E4-W)*(E15-W)+G4*G15)/(((E4-W)^2)+(G4)^2)) *(A15/(((E15-W)^2)+(G15)^2))
28750 N5=A5*(((E5-W)*(E15-W)+G5*G15)/(((E5-W)^2)+(G5)^2)) *(A15/(((E15-W)^2)+(G15)^2))
28760 N6=A6*(((E6-W)*(E15-W)+G6*G15)/(((E6-W)^2)+(G6)^2)) *(A15/(((E15-W)^2)+(G15)^2))
28770 N7=A7*(((E7-W)*(E15-W)+G7*G15)/(((E7-W)^2)+(G7)^2)) *(A15/(((E15-W)^2)+(G15)^2))
28780 N8=A8*(((E8-W)*(E15-W)+G8*G15)/(((E8-W)^2)+(G8)^2)) *(A15/(((E15-W)^2)+(G15)^2))
28790 N9=A9*(((E9-W)*(E15-W)+G9*G15)/(((E9-W)^2)+(G9)^2)) *(A15/(((E15-W)^2)+(G15)^2))
28800 N10=A10*(((E10-W)*(E15-W)+G10*G15)/(((E10-W)^2) +(G10)^2)) *(A15/(((E15-W)^2)+(G15)^2))
28810 N11=A11*(((E11-W)*(E15-W)+G11*G15)/(((E11-W)^2) +(G11)^2))*(A15/(((E15-W)^2)+(G15)^2))
28820 N12=A12*(((E12-W)*(E15-W)+G12*G15)/(((E12-W)^2) +(G12)^2)) *(A15/(((E15-W)^2)+(G15)^2))
28830 N13=A13*(((E13-W)*(E15-W)+G13*G15)/(((E13-W)^2) +(G13)^2)) *(A15/(((E15-W)^2)+(G15)^2))
28840 N14=A14*(((E14-W)*(E15-W)+G14*G15)/(((E14-W)^2) +(G14)^2)) *(A15/(((E15-W)^2)+(G15)^2))
28850  R15=((A15)^2)/(((E15-W)^2)+(G15)^2)
28860 S10=S9+2*(N1+N2+N3+N4+N5+N6+N7+N8+N9+N10+N11 +N12+N13+N14)+R15
28870 REM *-*-*-*-*- end of 15th term expressions -*-*-*-*-
29000 REM  M1-M15 & R16 are an extention for an 16th term
29010 M1=A1*(((E1-W)*(E16-W)+G1*G16)/(((E1-W)^2)+(G1)^2)) *(A16/(((E16-W)^2)+(G16)^2))
29020 M2=A2*(((E2-W)*(E16-W)+G2*G16)/(((E2-W)^2)+(G2)^2)) *(A16/(((E16-W)^2)+(G16)^2))
29030 M3=A3*(((E3-W)*(E16-W)+G3*G16)/(((E3-W)^2)+(G3)^2)) *(A16/(((E16-W)^2)+(G16)^2))
29040 M4=A4*(((E4-W)*(E16-W)+G4*G16)/(((E4-W)^2)+(G4)^2)) *(A16/(((E16-W)^2)+(G16)^2))
29050 M5=A5*(((E5-W)*(E16-W)+G5*G16)/(((E5-W)^2)+(G5)^2)) *(A16/(((E16-W)^2)+(G16)^2))
29060 M6=A6*(((E6-W)*(E16-W)+G6*G16)/(((E6-W)^2)+(G6)^2)) *(A16/(((E16-W)^2)+(G16)^2))
29070 M7=A7*(((E7-W)*(E16-W)+G7*G16)/(((E7-W)^2)+(G7)^2)) *(A16/(((E16-W)^2)+(G16)^2))
29080 M8=A8*(((E8-W)*(E16-W)+G8*G16)/(((E8-W)^2)+(G8)^2)) *(A16/(((E16-W)^2)+(G16)^2))
29090 M9=A9*(((E9-W)*(E16-W)+G9*G16)/(((E9-W)^2)+(G9)^2)) *(A16/(((E16-W)^2)+(G16)^2))
29100 M10=A10*(((E10-W)*(E16-W)+G10*G16)/(((E10-W)^2) +(G10)^2))*(A16/(((E16-W)^2)+(G16)^2))
29110 M11=A11*(((E11-W)*(E16-W)+G11*G16)/(((E11-W)^2) +(G11)^2))*(A16/(((E16-W)^2)+(G16)^2))
29120 M12=A12*(((E12-W)*(E16-W)+G12*G16)/(((E12-W)^2) +(G12)^2))*(A16/(((E16-W)^2)+(G16)^2))
29130 M13=A13*(((E13-W)*(E16-W)+G13*G16)/(((E13-W)^2) +(G13)^2)) *(A16/(((E16-W)^2)+(G16)^2))
29140 M14=A14*(((E14-W)*(E16-W)+G14*G16)/(((E14-W)^2) +(G14)^2))*(A16/(((E16-W)^2)+(G16)^2))
29150 M15=A15*(((E15-W)*(E16-W)+G15*G16)/(((E15-W)^2) +(G15)^2))*(A16/(((E16-W)^2)+(G16)^2))
29160 R16=((A16)^2)/(((E16-W)^2)+(G16)^2)
29170 S11= S10+2*(M1+M2+M3+M4+M5+M6+M7+M8+M9+M10+M11 +M12+M13+M14+M15)+R16
29180 REM -*-*-*-*- end of 16th term expressions -*-*-*-*-
29200 REM  P1-P16 & R17 are an extention for an 17th term
29210 P1=A1*(((E1-W)*(E17-W)+G1*G17)/(((E1-W)^2)+(G1)^2)) *(A17/(((E17-W)^2)+(G17)^2))
29220 P2=A2*(((E2-W)*(E17-W)+G2*G17)/(((E2-W)^2)+(G2)^2)) *(A17/(((E17-W)^2)+(G17)^2))29230 P3=A3 *(((E3-
W)*(E17-W)+G3*G17)/(((E3-W)^2)+(G3)^2)) *(A17/(((E17-W)^2)+(G17)^2))
29240 P4=A4*(((E4-W)*(E17-W)+G4*G17)/(((E4-W)^2)+(G4)^2)) *(A17/(((E17-W)^2)+(G17)^2))
29250 P5=A5*(((E5-W)*(E17-W)+G5*G17)/(((E5-W)^2)+(G5)^2)) *(A17/(((E17-W)^2)+(G17)^2))
29260 P6=A6*(((E6-W)*(E17-W)+G6*G17)/(((E6-W)^2)+(G6)^2)) *(A17/(((E17-W)^2)+(G17)^2))
29270 P7=A7*(((E7-W)*(E17-W)+G7*G17)/(((E7-W)^2)+(G7)^2)) *(A17/(((E17-W)^2)+(G17)^2))
29280 P8=A8*(((E8-W)*(E17-W)+G8*G17)/(((E8-W)^2)+(G8)^2)) *(A17/(((E17-W)^2)+(G17)^2))
29290 P9=A9*(((E9-W)*(E17-W)+G9*G17)/(((E9-W)^2)+(G9)^2)) *(A17/(((E17-W)^2)+(G17)^2))
29300 P10=A10*(((E10-W)*(E17-W)+G10*G17)/(((E10-W)^2) +(G10)^2)) *(A17/(((E17-W)^2)+(G17)^2))
29310 P11=A11*(((E11-W)*(E17-W)+G11*G17)/(((E11-W)^2) +(G11)^2))*(A17/(((E17-W)^2)+(G17)^2))
29320 P12=A12*(((E12-W)*(E17-W)+G12*G17)/(((E12-W)^2) +(G12)^2))*(A17/(((E17-W)^2)+(G17)^2))
29330 P13=A13*(((E13-W)*(E17-W)+G13*G17)/(((E13-W)^2) +(G13)^2))*(A17/(((E17-W)^2)+(G17)^2))
29340 P14=A14*(((E14-W)*(E17-W)+G14*G17)/(((E14-W)^2) +(G14)^2))*(A17/(((E17-W)^2)+(G17)^2))
29350 P15=A15*(((E15-W)*(E17-W)+G15*G17)/(((E15-W)^2) +(G15)^2))*(A17/(((E17-W)^2)+(G17)^2))
29360 P16=A16*(((E16-W)*(E17-W)+G16*G17)/(((E16-W)^2) +(G16)^2))*(A17/(((E17-W)^2)+(G17)^2))
29370  R17=((A17)^2)/(((E17-W)^2)+(G17)^2)
29380 S12= S11+2*(P1+P2+P3+P4+P5+P6+P7+P8+P9+P10+P11 +P12+P13+P14+P15+P16)+R17
```

```
29390 REM -*-*-*- end of 17th term expressions -*-*-*-*-
29400 REM k01-k017 & R18 are an extention for an 18th term
29410 K01=A1*(((E1-W)*(E18-W)+G1*G18)/(((E1-W)^2)+(G1)^2)) *(A18/(((E18-W)^2)+(G18)^2))
29420 K02=A2*(((E2-W)*(E18-W)+G2*G18)/(((E2-W)^2)+(G2)^2)) *(A18/(((E18-W)^2)+(G18)^2))
29430 K03=A3*(((E3-W)*(E18-W)+G3*G18)/(((E3-W)^2)+(G3)^2)) *(A18/(((E18-W)^2)+(G18)^2))
29440 K04=A4*(((E4-W)*(E18-W)+G4*G18)/(((E4-W)^2)+(G4)^2)) *(A18/(((E18-W)^2)+(G18)^2))
29450 K05=A5*(((E5-W)*(E18-W)+G5*G18)/(((E5-W)^2)+(G5)^2)) *(A18/(((E18-W)^2)+(G18)^2))
29460 K06=A6*(((E6-W)*(E18-W)+G6*G18)/(((E6-W)^2)+(G6)^2)) *(A18/(((E18-W)^2)+(G18)^2))
29470 K07=A7*(((E7-W)*(E18-W)+G7*G18)/(((E7-W)^2)+(G7)^2)) *(A18/(((E18-W)^2)+(G18)^2))
29480 K08=A8*(((E8-W)*(E18-W)+G8*G18)/(((E8-W)^2)+(G8)^2)) *(A18/(((E18-W)^2)+(G18)^2))
29490 K09=A9*(((E9-W)*(E18-W)+G9*G18)/(((E9-W)^2)+(G9)^2)) *(A18/(((E18-W)^2)+(G18)^2))
29500 K010=A10*(((E10-W)*(E18-W)+G10*G18)/(((E10-W)^2) +(G10)^2))*(A18/(((E18-W)^2)+(G18)^2))
29510 K011=A11*(((E11-W)*(E18-W)+G11*G18)/(((E11-W)^2) +(G11)^2))*(A18/(((E18-W)^2)+(G18)^2))
29520 K012=A12*(((E12-W)*(E18-W)+G12*G18)/(((E12-W)^2) +(G12)^2))*(A18/(((E18-W)^2)+(G18)^2))
29530 K013=A13*(((E13-W)*(E18-W)+G13*G18)/(((E13-W)^2) +(G13)^2))*(A18/(((E18-W)^2)+(G18)^2))
29540 K014=A14*(((E14-W)*(E18-W)+G14*G18)/(((E14-W)^2) +(G14)^2))*(A18/(((E18-W)^2)+(G18)^2))
29550 K015=A15*(((E15-W)*(E18-W)+G15*G18)/(((E15-W)^2) +(G15)^2))*(A18/(((E18-W)^2)+(G18)^2))
29560 K016=A16*(((E16-W)*(E18-W)+G16*G18)/(((E16-W)^2) +(G16)^2))*(A18/(((E18-W)^2)+(G18)^2))
29570 K017=A17*(((E17-W)*(E18-W)+G17*G18)/(((E17-W)^2) +(G17)^2))*(A18/(((E18-W)^2)+(G18)^2))
29580  R18=((A18)^2)/(((E18-W)^2)+(G18)^2)
29590  S13= S12+2*(K01+K02+K03+K04+K05+K06+K07+K08+K09+K010
+K011+K012+K013+K014+K015+K016+K017)+R18
29595 REM -*-*-*-*- end of 18th term expressions -*-*-*-*-*
30000 REM  U1-U18 & R19 are an extention for an 19th term
30010 U1=A1*(((E1-W)*(E19-W)+G1*G19)/(((E1-W)^2)+(G1)^2)) *(A19/(((E19-W)^2)+(G19)^2))
30020 U2=A2*(((E2-W)*(E19-W)+G2*G19)/(((E2-W)^2)+(G2)^2)) *(A19/(((E19-W)^2)+(G19)^2))
30030 U3=A3*(((E3-W)*(E19-W)+G3*G19)/(((E3-W)^2)+(G3)^2)) *(A19/(((E19-W)^2)+(G19)^2))
30040 U4=A4*(((E4-W)*(E19-W)+G4*G19)/(((E4-W)^2)+(G4)^2)) *(A19/(((E19-W)^2)+(G19)^2))
30050 U5=A5*(((E5-W)*(E19-W)+G5*G19)/(((E5-W)^2)+(G5)^2)) *(A19/(((E19-W)^2)+(G19)^2))
30060 U6=A6*(((E6-W)*(E19-W)+G6*G19)/(((E6-W)^2)+(G6)^2)) *(A19/(((E19-W)^2)+(G19)^2))
30070 U7=A7*(((E7-W)*(E19-W)+G7*G19)/(((E7-W)^2)+(G7)^2)) *(A19/(((E19-W)^2)+(G19)^2))
30080 U8=A8*(((E8-W)*(E19-W)+G8*G19)/(((E8-W)^2)+(G8)^2)) *(A19/(((E19-W)^2)+(G19)^2))
30090 U9=A9*(((E9-W)*(E19-W)+G9*G19)/(((E9-W)^2)+(G9)^2)) *(A19/(((E19-W)^2)+(G19)^2))
30100 U10=A10*(((E10-W)*(E19-W)+G10*G19)/(((E10-W)^2) +(G10)^2))*(A19/(((E19-W)^2)+(G19)^2))
30110 U11=A11*(((E11-W)*(E19-W)+G11*G19)/(((E11-W)^2) +(G11)^2))*(A19/(((E19-W)^2)+(G19)^2))
30120 U12=A12*(((E12-W)*(E19-W)+G12*G19)/(((E12-W)^2) +(G12)^2))*(A19/(((E19-W)^2)+(G19)^2))
30130 U13=A13*(((E13-W)*(E19-W)+G13*G19)/(((E13-W)^2) +(G13)^2))*(A19/(((E19-W)^2)+(G19)^2))
30140 U14=A14*(((E14-W)*(E19-W)+G14*G19)/(((E14-W)^2) +(G14)^2))*(A19/(((E19-W)^2)+(G19)^2))
30150 U15=A15*(((E15-W)*(E19-W)+G15*G19)/(((E15-W)^2) +(G15)^2))*(A19/(((E19-W)^2)+(G19)^2))
30160 U16=A16*(((E16-W)*(E19-W)+G16*G19)/(((E16-W)^2) +(G16)^2))*(A19/(((E19-W)^2)+(G19)^2))
30170 U17=A17*(((E17-W)*(E19-W)+G17*G19)/(((E17-W)^2) +(G17)^2))*(A19/(((E19-W)^2)+(G19)^2))
30180 U18=A18*(((E18-W)*(E19-W)+G18*G19)/(((E18-W)^2) +(G18)^2))*(A19/(((E19-W)^2)+(G19)^2))
30190  R19=((A19)^2)/(((E19-W)^2)+(G19)^2)
30195 S14=S13+2*(U1+U2+U3+U4+U5+U6+U7+U8+U9+U10+U11+U12 +U13+U14+U15+U16+U17+U18)+R19
30197 REM *-*-*-*-*- end of 19th term expressions -*-*-*-*-*
30200 REM  D1-D19 & R20 are an extention for an 20th term
30210 D1=A1*(((E1-W)*(E20-W)+G1*G20)/(((E1-W)^2)+(G1)^2)) *(A20/(((E20-W)^2)+(G20)^2))
30220 D2=A2*(((E2-W)*(E20-W)+G2*G20)/(((E2-W)^2)+(G2)^2)) *(A20/(((E20-W)^2)+(G20)^2))
30230 D3=A3*(((E3-W)*(E20-W)+G3*G20)/(((E3-W)^2)+(G3)^2)) *(A20/(((E20-W)^2)+(G20)^2))
30240 D4=A4*(((E4-W)*(E20-W)+G4*G20)/(((E4-W)^2)+(G4)^2)) *(A20/(((E20-W)^2)+(G20)^2))
30250 D5=A5*(((E5-W)*(E20-W)+G5*G20)/(((E5-W)^2)+(G5)^2)) *(A20/(((E20-W)^2)+(G20)^2))
30260 D6=A6*(((E6-W)*(E20-W)+G6*G20)/(((E6-W)^2)+(G6)^2)) *(A20/(((E20-W)^2)+(G20)^2))
30270 D7=A7*(((E7-W)*(E20-W)+G7*G20)/(((E7-W)^2)+(G7)^2)) *(A20/(((E20-W)^2)+(G20)^2))
30280 D8=A8*(((E8-W)*(E20-W)+G8*G20)/(((E8-W)^2)+(G8)^2)) *(A20/(((E20-W)^2)+(G20)^2))
```

```
30290 D9=A9*(((E9-W)*(E20-W)+G9*G20)/(((E9-W)^2)+(G9)^2)) *(A20/(((E20-W)^2)+(G20)^2))
30300 D10=A10*(((E10-W)*(E20-W)+G10*G20)/(((E10-W)^2) +(G10)^2))*(A20/(((E20-W)^2)+(G20)^2))
30310 D11=A11*(((E11-W)*(E20-W)+G11*G20)/(((E11-W)^2) +(G11)^2))*(A20/(((E20-W)^2)+(G20)^2))
30320 D12=A12*(((E12-W)*(E20-W)+G12*G20)/(((E12-W)^2) +(G12)^2))*(A20/(((E20-W)^2)+(G20)^2))
30330 D13=A13*(((E13-W)*(E20-W)+G13*G20)/(((E13-W)^2) +(G13)^2))*(A20/(((E20-W)^2)+(G20)^2))
30340 D14=A14*(((E14-W)*(E20-W)+G14*G20)/(((E14-W)^2) +(G14)^2))*(A20/(((E20-W)^2)+(G20)^2))
30350 D15=A15*(((E15-W)*(E20-W)+G15*G20)/(((E15-W)^2) +(G15)^2))*(A20/(((E20-W)^2)+(G20)^2))
30360 D16=A16*(((E16-W)*(E20-W)+G16*G20)/(((E16-W)^2) +(G16)^2))*(A20/(((E20-W)^2)+(G20)^2))
30370 D17=A17*(((E17-W)*(E20-W)+G17*G20)/(((E17-W)^2) +(G17)^2))*(A20/(((E20-W)^2)+(G20)^2))
30380 D18=A18*(((E18-W)*(E20-W)+G18*G20)/(((E18-W)^2) +(G18)^2))*(A20/(((E20-W)^2)+(G20)^2))
30390 D19=A19*(((E19-W)*(E20-W)+G19*G20)/(((E19-W)^2) +(G19)^2))*(A20/(((E20-W)^2)+(G20)^2))
30400  R20=((A20)^2)/(((E20-W)^2)+(G20)^2)
30410 S15= S14+2*(D1+D2+D3+D4+D5+D6+D7+D8+D9+D10+D11+D12
+D13+D14+D15+D16+D17+D18+D19)+R20
30420 REM -*-*-*-*-*- end of 20th term expressions -*-*-*-*-*-*
30500  REM B1-B20 & R21 are an extention for an 21th term
30510 B1=A1*(((E1-W)*(E21-W)+G1*G21)/(((E1-W)^2)+(G1)^2)) *(A21/(((E21-W)^2)+(G21)^2))
30520 B2=A2*(((E2-W)*(E21-W)+G2*G21)/(((E2-W)^2)+(G2)^2)) *(A21/(((E21-W)^2)+(G21)^2))
30530 B3=A3*(((E3-W)*(E21-W)+G3*G21)/(((E3-W)^2)+(G3)^2)) *(A21/(((E21-W)^2)+(G21)^2))
30540 B4=A4*(((E4-W)*(E21-W)+G4*G21)/(((E4-W)^2)+(G4)^2)) *(A21/(((E21-W)^2)+(G21)^2))
30550 B5=A5*(((E5-W)*(E21-W)+G5*G21)/(((E5-W)^2)+(G5)^2)) *(A21/(((E21-W)^2)+(G21)^2))
30560 B6=A6*(((E6-W)*(E21-W)+G6*G21)/(((E6-W)^2)+(G6)^2)) *(A21/(((E21-W)^2)+(G21)^2))
30570 B7=A7*(((E7-W)*(E21-W)+G7*G21)/(((E7-W)^2)+(G7)^2)) *(A21/(((E21-W)^2)+(G21)^2))
30580 B8=A8*(((E8-W)*(E21-W)+G8*G21)/(((E8-W)^2)+(G8)^2)) *(A21/(((E21-W)^2)+(G21)^2))
30590 B9=A9*(((E9-W)*(E21-W)+G9*G21)/(((E9-W)^2)+(G9)^2)) *(A21/(((E21-W)^2)+(G21)^2))
30600 B10=A10*(((E10-W)*(E21-W)+G10*G21)/(((E10-W)^2) +(G10)^2))*(A21/(((E21-W)^2)+(G21)^2))
30610 B11=A11*(((E11-W)*(E21-W)+G11*G21)/(((E11-W)^2) +(G11)^2))*(A21/(((E21-W)^2)+(G21)^2))
30620 B12=A12*(((E12-W)*(E21-W)+G12*G21)/(((E12-W)^2) +(G12)^2))*(A21/(((E21-W)^2)+(G21)^2))
30630 B13=A13*(((E13-W)*(E21-W)+G13*G21)/(((E13-W)^2) +(G13)^2))*(A21/(((E21-W)^2)+(G21)^2))
30640 B14=A14*(((E14-W)*(E21-W)+G14*G21)/(((E14-W)^2) +(G14)^2))*(A21/(((E21-W)^2)+(G21)^2))
30650 B15=A15*(((E15-W)*(E21-W)+G15*G21)/(((E15-W)^2) +(G15)^2))*(A21/(((E21-W)^2)+(G21)^2))
30660 B16=A16*(((E16-W)*(E21-W)+G16*G21)/(((E16-W)^2) +(G16)^2))*(A21/(((E21-W)^2)+(G21)^2))
30670 B17=A17*(((E17-W)*(E21-W)+G17*G21)/(((E17-W)^2) +(G17)^2))*(A21/(((E21-W)^2)+(G21)^2))
30680 B18=A18*(((E18-W)*(E21-W)+G18*G21)/(((E18-W)^2) +(G18)^2))*(A21/(((E21-W)^2)+(G21)^2))
30690 B19=A19*(((E19-W)*(E21-W)+G19*G21)/(((E19-W)^2) +(G19)^2))*(A21/(((E21-W)^2)+(G21)^2))
30700 B20=A20*(((E20-W)*(E21-W)+G20*G21)/(((E20-W)^2) +(G20)^2))*(A21/(((E21-W)^2)+(G21)^2))
30710  R21=((A21)^2)/(((E21-W)^2)+(G21)^2)
30720 S16= S15+2*(B1+B2+B3+B4+B5+B6+B7+B8+B9+B10+B11
+B12+B13+B14+B15+B16+B17+B18+B19+B20)+R21
30730 REM -*-*-*-*-*- end of 21th term expressions -*-*-*-*-*-*
31000 REM  H1-H21 & R22 are an extention for an 22th term
31010 H1=A1*(((E1-W)*(E22-W)+G1*G22)/(((E1-W)^2)+(G1)^2)) *(A22/(((E22-W)^2)+(G22)^2))
31020 H2=A2*(((E2-W)*(E22-W)+G2*G22)/(((E2-W)^2)+(G2)^2)) *(A22/(((E22-W)^2)+(G22)^2))
31030 H3=A3*(((E3-W)*(E22-W)+G3*G22)/(((E3-W)^2)+(G3)^2)) *(A22/(((E22-W)^2)+(G22)^2))
31040 H4=A4*(((E4-W)*(E22-W)+G4*G22)/(((E4-W)^2)+(G4)^2)) *(A22/(((E22-W)^2)+(G22)^2))
31050 H5=A5*(((E5-W)*(E22-W)+G5*G22)/(((E5-W)^2)+(G5)^2)) *(A22/(((E22-W)^2)+(G22)^2))
31060 H6=A6*(((E6-W)*(E22-W)+G6*G22)/(((E6-W)^2)+(G6)^2)) *(A22/(((E22-W)^2)+(G22)^2))
31070 H7=A7*(((E7-W)*(E22-W)+G7*G22)/(((E7-W)^2)+(G7)^2)) *(A22/(((E22-W)^2)+(G22)^2))
31080 H8=A8*(((E8-W)*(E22-W)+G8*G22)/(((E8-W)^2)+(G8)^2)) *(A22/(((E22-W)^2)+(G22)^2))
31090 H9=A9*(((E9-W)*(E22-W)+G9*G22)/(((E9-W)^2)+(G9)^2)) *(A22/(((E22-W)^2)+(G22)^2))
31100 H10=A10*(((E10-W)*(E22-W)+G10*G22)/(((E10-W)^2) +(G10)^2))*(A22/(((E22-W)^2)+(G22)^2))
31110 H11=A11*(((E11-W)*(E22-W)+G11*G22)/(((E11-W)^2) +(G11)^2))*(A22/(((E22-W)^2)+(G22)^2))
31120 H12=A12*(((E12-W)*(E22-W)+G12*G22)/(((E12-W)^2) +(G12)^2))*(A22/(((E22-W)^2)+(G22)^2))
31130 H13=A13*(((E13-W)*(E22-W)+G13*G22)/(((E13-W)^2) +(G13)^2))*(A22/(((E22-W)^2)+(G22)^2))
```

```
31140 H14=A14*(((E14-W)*(E22-W)+G14*G22)/(((E14-W)^2) +(G14)^2))*(A22/(((E22-W)^2)+(G22)^2))
31150 H15=A15*(((E15-W)*(E22-W)+G15*G22)/(((E15-W)^2) +(G15)^2))*(A22/(((E22-W)^2)+(G22)^2))
31160 H16=A16*(((E16-W)*(E22-W)+G16*G22)/(((E16-W)^2) +(G16)^2))*(A22/(((E22-W)^2)+(G22)^2))
31170 H17=A17*(((E17-W)*(E22-W)+G17*G22)/(((E17-W)^2) +(G17)^2))*(A22/(((E22-W)^2)+(G22)^2))
31180 H18=A18*(((E18-W)*(E22-W)+G18*G22)/(((E18-W)^2) +(G18)^2))*(A22/(((E22-W)^2)+(G22)^2))
31190 H19=A19*(((E19-W)*(E22-W)+G19*G22)/(((E19-W)^2) +(G19)^2))*(A22/(((E22-W)^2)+(G22)^2))
31200 H20=A20*(((E20-W)*(E22-W)+G20*G22)/(((E20-W)^2) +(G20)^2))*(A22/(((E22-W)^2)+(G22)^2))
31210 H21=A21*(((E21-W)*(E22-W)+G21*G22)/(((E21-W)^2) +(G21)^2))*(A22/(((E22-W)^2)+(G22)^2))
31220  R22=((A22)^2)/(((E22-W)^2)+(G22)^2)
31230 S17= S16+2*(H1+H2+H3+H4+H5+H6+H7+H8+H9+H10+H11+H12+H13
+H14+H15+H16+H17+H18+H19+H20+H21)+R22
31240 REM *-*-*-*-*- end of 22th term expressions -*-*-*-*-*
31300 REM  L1-L22 & R23 are an extention for an 23th term
31310 L1=A1*(((E1-W)*(E23-W)+G1*G23)/(((E1-W)^2)+(G1)^2)) *(A23/(((E23-W)^2)+(G23)^2))
31320 L2=A2*(((E2-W)*(E23-W)+G2*G23)/(((E2-W)^2)+(G2)^2)) *(A23/(((E23-W)^2)+(G23)^2))
31330 L3=A3*(((E3-W)*(E23-W)+G3*G23)/(((E3-W)^2)+(G3)^2)) *(A23/(((E23-W)^2)+(G23)^2))
31340 L4=A4*(((E4-W)*(E23-W)+G4*G23)/(((E4-W)^2)+(G4)^2)) *(A23/(((E23-W)^2)+(G23)^2))
31350 L5=A5*(((E5-W)*(E23-W)+G5*G23)/(((E5-W)^2)+(G5)^2)) *(A23/(((E23-W)^2)+(G23)^2))
31360 L6=A6*(((E6-W)*(E23-W)+G6*G23)/(((E6-W)^2)+(G6)^2)) *(A23/(((E23-W)^2)+(G23)^2))
31370 L7=A7*(((E7-W)*(E23-W)+G7*G23)/(((E7-W)^2)+(G7)^2)) *(A23/(((E23-W)^2)+(G23)^2))
31380 L8=A8*(((E8-W)*(E23-W)+G8*G23)/(((E8-W)^2)+(G8)^2)) *(A23/(((E23-W)^2)+(G23)^2))
31390 L9=A9*(((E9-W)*(E23-W)+G9*G23)/(((E9-W)^2)+(G9)^2)) *(A23/(((E23-W)^2)+(G23)^2))
31400 L10=A10*(((E10-W)*(E23-W)+G10*G23)/(((E10-W)^2) +(G10)^2))*(A23/(((E23-W)^2)+(G23)^2))
31410 L11=A11*(((E11-W)*(E23-W)+G11*G23)/(((E11-W)^2) +(G11)^2))*(A23/(((E23-W)^2)+(G23)^2))
31420 L12=A12*(((E12-W)*(E23-W)+G12*G23)/(((E12-W)^2) +(G12)^2))*(A23/(((E23-W)^2)+(G23)^2))
31430 L13=A13*(((E13-W)*(E23-W)+G13*G23)/(((E13-W)^2) +(G13)^2))*(A23/(((E23-W)^2)+(G23)^2))
31440 L14=A14*(((E14-W)*(E23-W)+G14*G23)/(((E14-W)^2) +(G14)^2))*(A23/(((E23-W)^2)+(G23)^2))
31450 L15=A15*(((E15-W)*(E23-W)+G15*G23)/(((E15-W)^2) +(G15)^2))*(A23/(((E23-W)^2)+(G23)^2))
31460 L16=A16*(((E16-W)*(E23-W)+G16*G23)/(((E16-W)^2) +(G16)^2))*(A23/(((E23-W)^2)+(G23)^2))
31470 L17=A17*(((E17-W)*(E23-W)+G17*G23)/(((E17-W)^2) +(G17)^2))*(A23/(((E23-W)^2)+(G23)^2))
31480 L18=A18*(((E18-W)*(E23-W)+G18*G23)/(((E18-W)^2) +(G18)^2))*(A23/(((E23-W)^2)+(G23)^2))
31490 L19=A19*(((E19-W)*(E23-W)+G19*G23)/(((E19-W)^2) +(G19)^2))*(A23/(((E23-W)^2)+(G23)^2))
31500 L20=A20*(((E20-W)*(E23-W)+G20*G23)/(((E20-W)^2) +(G20)^2))*(A23/(((E23-W)^2)+(G23)^2))
31510 L21=A21*(((E21-W)*(E23-W)+G21*G23)/(((E21-W)^2) +(G21)^2))*(A23/(((E23-W)^2)+(G23)^2))
31520 L22=A22*(((E22-W)*(E23-W)+G22*G23)/(((E22-W)^2) +(G22)^2))*(A23/(((E23-W)^2)+(G23)^2))
31530  R23=((A23)^2)/(((E23-W)^2)+(G23)^2)
31540 S18= S17+2*(L1+L2+L3+L4+L5+L6+L7+L8+L9+L10+L11+L12
+L13+L14+L15+L16+L17+L18+L19+L20+L21+L22)+R23
31545 GOTO 34850
31550 REM *-*-*-*-*- end of 23th term expressions -*-*-*-*-*
31600 REM  J1-J23 & R24 are an extention for an 24th term
31610 J1=A1*(((E1-W)*(E24-W)+G1*G24)/(((E1-W)^2)+(G1)^2)) *(A24/(((E24-W)^2)+(G24)^2))
31620 J2=A2*(((E2-W)*(E24-W)+G2*G24)/(((E2-W)^2)+(G2)^2)) *(A24/(((E24-W)^2)+(G24)^2))
31630 J3=A3*(((E3-W)*(E24-W)+G3*G24)/(((E3-W)^2)+(G3)^2)) *(A24/(((E24-W)^2)+(G24)^2))
31640 J4=A4*(((E4-W)*(E24-W)+G4*G24)/(((E4-W)^2)+(G4)^2)) *(A24/(((E24-W)^2)+(G24)^2))
31650 J5=A5*(((E5-W)*(E24-W)+G5*G24)/(((E5-W)^2)+(G5)^2)) *(A24/(((E24-W)^2)+(G24)^2))
31660 J6=A6*(((E6-W)*(E24-W)+G6*G24)/(((E6-W)^2)+(G6)^2)) *(A24/(((E24-W)^2)+(G24)^2))
31670 J7=A7*(((E7-W)*(E24-W)+G7*G24)/(((E7-W)^2)+(G7)^2)) *(A24/(((E24-W)^2)+(G24)^2))
31680 J8=A8*(((E8-W)*(E24-W)+G8*G24)/(((E8-W)^2)+(G8)^2)) *(A24/(((E24-W)^2)+(G24)^2))
31690 J9=A9*(((E9-W)*(E24-W)+G9*G24)/(((E9-W)^2)+(G9)^2)) *(A24/(((E24-W)^2)+(G24)^2))
31700 J10=A10*(((E10-W)*(E24-W)+G10*G24)/(((E10-W)^2) +(G10)^2))*(A24/(((E24-W)^2)+(G24)^2))
31710 J11=A11*(((E11-W)*(E24-W)+G11*G24)/(((E11-W)^2) +(G11)^2))*(A24/(((E24-W)^2)+(G24)^2))
31720 J12=A12*(((E12-W)*(E24-W)+G12*G24)/(((E12-W)^2) +(G12)^2))*(A24/(((E24-W)^2)+(G24)^2))
31730 J13=A13*(((E13-W)*(E24-W)+G13*G24)/(((E13-W)^2) +(G13)^2))*(A24/(((E24-W)^2)+(G24)^2))
```

```
31740 J14=A14*(((E14-W)*(E24-W)+G14*G24)/(((E14-W)^2) +(G14)^2))*(A24/(((E24-W)^2)+(G24)^2))
31750 J15=A15*(((E15-W)*(E24-W)+G15*G24)/(((E15-W)^2) +(G15)^2))*(A24/(((E24-W)^2)+(G24)^2))
31760 J16=A16*(((E16-W)*(E24-W)+G16*G24)/(((E16-W)^2) +(G16)^2))*(A24/(((E24-W)^2)+(G24)^2))
31770 J17=A17*(((E17-W)*(E24-W)+G17*G24)/(((E17-W)^2) +(G17)^2))*(A24/(((E24-W)^2)+(G24)^2))
31780 J18=A18*(((E18-W)*(E24-W)+G18*G24)/(((E18-W)^2) +(G18)^2))*(A24/(((E24-W)^2)+(G24)^2))
31790 J19=A19*(((E19-W)*(E24-W)+G19*G24)/(((E19-W)^2) +(G19)^2))*(A24/(((E24-W)^2)+(G24)^2))
31800 J20=A20*(((E20-W)*(E24-W)+G20*G24)/(((E20-W)^2) +(G20)^2))*(A24/(((E24-W)^2)+(G24)^2))
31810 J21=A21*(((E21-W)*(E24-W)+G21*G24)/(((E21-W)^2) +(G21)^2))*(A24/(((E24-W)^2)+(G24)^2))
31820 J22=A22*(((E22-W)*(E24-W)+G22*G24)/(((E22-W)^2) +(G22)^2))*(A24/(((E24-W)^2)+(G24)^2))
31830 J23=A23*(((E23-W)*(E24-W)+G23*G24)/(((E23-W)^2) +(G23)^2))*(A24/(((E24-W)^2)+(G24)^2))
31840  R24=((A24)^2)/(((E24-W)^2)+(G24)^2)
31850 S19= S18+2*(J1+J2+J3+J4+J5+J6+J7+J8+J9+J10+J11
+J12+J13+J14+J15+J16+J17+J18+J19+J20+J21+J22+J23)+R24
31860 REM *-*-*-*- end of 24th term expressions -*-*-*-*
32000 REM O1-O24 & R25 are an extention for an 25th term
32010 O1=A1*(((E1-W)*(E25-W)+G1*G25)/(((E1-W)^2)+(G1)^2)) *(A25/(((E25-W)^2)+(G25)^2))
32020 O2=A2*(((E2-W)*(E25-W)+G2*G25)/(((E2-W)^2)+(G2)^2)) *(A25/(((E25-W)^2)+(G25)^2))
32030 O3=A3*(((E3-W)*(E25-W)+G3*G25)/(((E3-W)^2)+(G3)^2)) *(A25/(((E25-W)^2)+(G25)^2))
32040 O4=A4*(((E4-W)*(E25-W)+G4*G25)/(((E4-W)^2)+(G4)^2)) *(A25/(((E25-W)^2)+(G25)^2))
32050 O5=A5*(((E5-W)*(E25-W)+G5*G25)/(((E5-W)^2)+(G5)^2)) *(A25/(((E25-W)^2)+(G25)^2))
32060 O6=A6*(((E6-W)*(E25-W)+G6*G25)/(((E6-W)^2)+(G6)^2)) *(A25/(((E25-W)^2)+(G25)^2))
32070 O7=A7*(((E7-W)*(E25-W)+G7*G25)/(((E7-W)^2)+(G7)^2)) *(A25/(((E25-W)^2)+(G25)^2))
32080 O8=A8*(((E8-W)*(E25-W)+G8*G25)/(((E8-W)^2)+(G8)^2)) *(A25/(((E25-W)^2)+(G25)^2))
32090 O9=A9*(((E9-W)*(E25-W)+G9*G25)/(((E9-W)^2)+(G9)^2)) *(A25/(((E25-W)^2)+(G25)^2))
32100 O10=A10*(((E10-W)*(E25-W)+G10*G25)/(((E10-W)^2) +(G10)^2))*(A25/(((E25-W)^2)+(G25)^2))
32110 O11=A11*(((E11-W)*(E25-W)+G11*G25)/(((E11-W)^2) +(G11)^2))*(A25/(((E25-W)^2)+(G25)^2))
32120 O12=A12*(((E12-W)*(E25-W)+G12*G25)/(((E12-W)^2) +(G12)^2))*(A25/(((E25-W)^2)+(G25)^2))
32130 O13=A13*(((E13-W)*(E25-W)+G13*G25)/(((E13-W)^2) +(G13)^2))*(A25/(((E25-W)^2)+(G25)^2))
32140 O14=A14*(((E14-W)*(E25-W)+G14*G25)/(((E14-W)^2) +(G14)^2))*(A25/(((E25-W)^2)+(G25)^2))
32150 O15=A15*(((E15-W)*(E25-W)+G15*G25)/(((E15-W)^2) +(G15)^2))*(A25/(((E25-W)^2)+(G25)^2))
32160 O16=A16*(((E16-W)*(E25-W)+G16*G25)/(((E16-W)^2) +(G16)^2))*(A25/(((E25-W)^2)+(G25)^2))
32170 O17=A17*(((E17-W)*(E25-W)+G17*G25)/(((E17-W)^2) +(G17)^2))*(A25/(((E25-W)^2)+(G25)^2))
32180 O18=A18*(((E18-W)*(E25-W)+G18*G25)/(((E18-W)^2) +(G18)^2))*(A25/(((E25-W)^2)+(G25)^2))
32190 O19=A19*(((E19-W)*(E25-W)+G19*G25)/(((E19-W)^2) +(G19)^2))*(A25/(((E25-W)^2)+(G25)^2))
32200 O20=A20*(((E20-W)*(E25-W)+G20*G25)/(((E20-W)^2) +(G20)^2))*(A25/(((E25-W)^2)+(G25)^2))
32210 O21=A21*(((E21-W)*(E25-W)+G21*G25)/(((E21-W)^2) +(G21)^2))*(A25/(((E25-W)^2)+(G25)^2))
32220 O22=A22*(((E22-W)*(E25-W)+G22*G25)/(((E22-W)^2) +(G22)^2))*(A25/(((E25-W)^2)+(G25)^2))
32230 O23=A23*(((E23-W)*(E25-W)+G23*G25)/(((E23-W)^2) +(G23)^2))*(A25/(((E25-W)^2)+(G25)^2))
32240 O24=A24*(((E24-W)*(E25-W)+G24*G25)/(((E24-W)^2) +(G24)^2))*(A25/(((E25-W)^2)+(G25)^2))
32250  R25=((A25)^2)/(((E25-W)^2)+(G25)^2)
32260 S20= S19+2*(O1+O2+O3+O4+O5+O6+O7+O8+O9+O10+O11
+O12+O13+O14+O15+O16+O17+O18+O19+O20+O21+O22+O23+O24)+R25
32270 REM *-*-*-*- end of 25th term expressions -*-*-*-*
34850  S=S18 : REM  USING ONLY 23 TERMS (see line 31545)
34900 RETURN
```

```
34998 REM=================================================
34999 REM   Lines 35000- represent  the second Equation
35000 REM --- Enter function in program line 35000-38900 ---
35050 REM *** These equations represent Absorption as a
            function of cm-1 *****
35090  REM ** t11=> VE1 delta, t22=> VE2, t33=> VE3 delta,
       K= mult const for Ag
35095  REM ** t1=> V1 delta, t2=> V2 , t3=> V3 delta,
       C= mult const for Bu state

35100 REM ====================== Ag ========================
35125  T11=.36     :T22=.3     :T33=.37     :T44=.11     :K=.65
35150  VE1=1750    :VE2=1250   :VE3=200     :VE4=1550
      :VG1=1550    :VG2=1200   :VG3=200     :VG4=1550
35175   E1=20175   :E2=E1+(VE3)             :E3=E1+(VE2)
       :E4=E1+(VE1)           :E5=E1+(VE1)+(VE3)
       :E6=E1+(VE2)+(VE3)     :E23'=E1+(VE4)
35180     G1=75          :G2=G1        :G3=G1        :G4=G1
         :G5=G1          :G6=G1        :G23'=G1
35195 REM =================================================

35295 REM ====================== Bu ========================
35300     T1=.17     :T2=.15     :T3=.1     : C=.4895
         :V1=1550    :V2=1200    :V3=200
35350     G7=170     :G8=G7      :G9=G7     :G10=G7   :G11=G7
         :G12=G7     :G13=G7     :G14=G7    :G15=G7   :G16=G7
         :G17=G7     :G18=G7     :G19=G7    :G20=G7   :G21=G7
         :G22=G7
35400 :E7 =23060     :E8 =E7+V1        :E9=E7+V2
      :E10=E7+V3     :E11=E7+2*(V1)    :E12=E7+2*(V2)
      :E13=E7+(V1+V2)                  :E14=E7+(V2+V3)
      :E15=E7+(V1+V3)
35405  E16=E7+2*(V1)+V2       :E17=E7+2*(V2)+V1
      :E18=E7+3*(V1)          :E19=E7+(2*(V1)+2*(V2))
      :E20=E7+(2*(V1)+V3)     :E21=E7+(2*(V2)+V3)
      :E22=E7+3*(V1)+V2



35990 REM === 31000-31800 are the Frank-Condon integrals ===
35998 REM \-\-\-  Frank-Condon integrals ( Ag state ) \-\-\-
.....................................................................
36000 F01=2*((((VE1)*(VG1))^.5)/((VE1)+(VG1)))*EXP(-(.0148)
 *((T11)^2)*(((VE1)*(VG1))/((VE1)+(VG1))))
36025 F02=2*((((VE2)*(VG2))^.5)/((VE2)+(VG2)))*EXP(-(.0148)
 *((T22)^2)*(((VE2)*(VG2))/((VE2)+(VG2))))
36050 F03=2*((((VE3)*(VG3))^.5)/((VE3)+(VG3)))*EXP(-(.0148)
 *((T33)^2)*(((VE3)*(VG3))/((VE3)+(VG3))))
36060 F04=2*((((VE4)*(VG4))^.5)/((VE4)+(VG4)))*EXP(-(.0148)
 *((T44)^2)*(((VE4)*(VG4))/((VE4)+(VG4))))
36061 REM ---------------------------------------------------
36075 F05=2*((.0148)^.5)*(((VG1)*((VE1)^.5))/((VE1)+(VG1)))
 *(T11)*2*((((VE1)*(VG1))^.5)/((VE1)+(VG1)))*EXP(-(.0148)
 *((T11)^2)*(((VE1)*(VG1))/((VE1)+(VG1))))
```

```
36100 F06=2*((.0148)^.5)*(((VG2)*((VE2)^.5))/((VE2)+(VG2)))
 *(T22)*2*((((VE2)*(VG2))^.5)/((VE2)+(VG2)))*EXP((.0148)
 *((T22)^2) *(((VE2)*(VG2))/((VE2)+(VG2))))
36125 F07=2*((.0148)^.5)*(((VG3)*((VE3)^.5))/((VE3)+(VG3)))
 *(T33)*2*((((VE3)*(VG3))^.5)/((VE3)+(VG3)))*EXP(-(.0148)
 *((T33)^2)*(((VE3)*(VG3))/((VE3)+(VG3))))
36150 F08=2*((.0148)^.5)*(((VG4)*((VE4)^.5))/((VE4)+(VG4)))
 *(T44)*2*((((VE4)*(VG4))^.5)/((VE4)+(VG4)))*EXP(-(.0148)
 *((T44)^2)*(((VE4)*(VG4))/((VE4)+(VG4))))
36200 REM ------------------------------------------------
36250 A1=K*(F01)*(F02)*(F03)*(F04)
:A2=K*(F01)*(F02)*(F07)*(F04)
     :A3=K*(F01)*(F06)*(F03)*(F04)
36300 A4=K*(F05)*(F02)*(F03)*(F04)
:A5=K*(F05)*(F02)*(F07)*(F04)
     :A6=K*(F01)*(F06)*(F07)*(F04)
:A23=K*(F01)*(F02)*(F03)*(F08)

36495 REM ------------------------------------------------
36500 REM
            (V1)   |    (V2)    |     (V3)     |     (V4)
      F01=<0|0>    | F02=<0|0>  | F03=<0|0>    | F04=<0|0>
      F05=<0|1>    | F06=<0|1>  | F07=<0|1>    | F08=<0|1>
36505 REM ------------------------------------------------

36525 F1=EXP(-.0148*(((T1)^2)*(V1/2)))
36550 F2=EXP(-.0148*(((T2)^2)*(V2/2)))
36575 F3=EXP(-.0148*(((T3)^2)*(V3/2)))
36585 REM F33=EXP(-.0148*(((T4)^2)*(V4/2)))
36600 F4=((.0148)^.5)*((V1)^.5)*(T1)*EXP(-.0148
 *(V1/2)*((T1)^2))
36625 F5=((.0148)^.5)*((V2)^.5)*(T2)*EXP(-.0148
 *(V2/2)*((T2)^2))
36650 F6=((.0148)^.5)*((V3)^.5)*(T3)*EXP(-.0148
 *(V3/2)*((T3)^2))
36660 REM F66=((.0148)^.5)*((V4)^.5)*(T4)*EXP(-.0148
 *(V4/2)*((T4)^2))
36675 F7=.0148*(V1)*((T1)^2)*EXP(-.0148*(V1/2)*((T1)^2))
36700 F8=.0148*(V2)*((T2)^2)*EXP(-.0148*(V2/2)*((T2)^2))
36725 F9=.0148*(V3)*((T3)^2)*EXP(-.0148*(V3/2)*((T3)^2))
36735 REM F99=.0148*(V4)*((T4)^2)*EXP(-.0148
 *(V4/2)*((T4)^2))
36750 F10=((.5774)*(.0148)^1.5)*((V1)^1.5)*((T1)^3)*EXP(-
.0148 *(V1/2)*((T1)^2))

36890  REM ------------------------------------------------
36900  A7 =C*(F1)*(F2)*(F3)       :A8 =C*(F4)*(F2)*(F3)
      :A9 =C*(F1)*(F5)*(F3)       :A10=C*(F1)*(F2)*(F6)
      :A11=C*(F7)*(F2)*(F3)       :A12=C*(F1)*(F8)*(F3)
36905 :A13=C*(F4)*(F5)*(F3)       :A14=C*(F1)*(F5)*(F6)
      :A15=C*(F4)*(F2)*(F6)       :A16=C*(F7)*(F5)*(F3)
36915 :A17=C*(F4)*(F8)*(F3)       :A18=C*(F10)*(F2)*(F3)
      :A19=C*(F7)*(F8)*(F3)       :A20=C*(F7)*(F2)*(F6)
      :A21=C*(F1)*(F8)*(F6)       :A22=C*(F10)*(F5)*(F3)
```

```
36920  REM ------------------------------------------------
36925  REM
          __|__V1,V2,V3____||  ___________|___V1,V2,V3___
   F1,F2,F3  |    <0|0>     ||  F4,F5,F6    |    <0|1>
   F7,F8,F9  |    <0|2>     ||  F10         |    <0|3>

36998  REM ------------------------------------------------

37000  R1=(W)*(G1)*((A1^2)/(((E1-W)^2)+G1^2))
37010  R2=(W)*(G2)*((A2^2)/(((E2-W)^2)+G2^2))
37020  R3=(W)*(G3)*((A3^2)/(((E3-W)^2)+G3^2))
37030  R4=(W)*(G4)*((A4^2)/(((E4-W)^2)+G4^2))
37040  R5=(W)*(G5)*((A5^2)/(((E5-W)^2)+G5^2))
37050  R6=(W)*(G6)*((A6^2)/(((E6-W)^2)+G6^2))
37060  R7=(W)*(G7)*((A7^2)/(((E7-W)^2)+G7^2))
37070  R8=(W)*(G8)*((A8^2)/(((E8-W)^2)+G8^2))
37080  R9=(W)*(G9)*((A9^2)/(((E9-W)^2)+G9^2))
37090  R10=(W)*(G10)*((A10^2)/(((E10-W)^2)+G10^2))
37100  R11=(W)*(G11)*((A11^2)/(((E11-W)^2)+G11^2))
37110  R12=(W)*(G12)*((A12^2)/(((E12-W)^2)+G12^2))
37120  R13=(W)*(G13)*((A13^2)/(((E13-W)^2)+G13^2))
37130  R14=(W)*(G14)*((A14^2)/(((E14-W)^2)+G14^2))
37140  R15=(W)*(G15)*((A15^2)/(((E15-W)^2)+G15^2))
37150  R16=(W)*(G16)*((A16^2)/(((E16-W)^2)+G16^2))
37160  R17=(W)*(G17)*((A17^2)/(((E17-W)^2)+G17^2))
37170  R18=(W)*(G18)*((A18^2)/(((E18-W)^2)+G18^2))
37180  R19=(W)*(G19)*((A19^2)/(((E19-W)^2)+G19^2))
37190  R20=(W)*(G20)*((A20^2)/(((E20-W)^2)+G20^2))
37200  R21=(W)*(G21)*((A21^2)/(((E21-W)^2)+G21^2))
37210  R22=(W)*(G22)*((A22^2)/(((E22-W)^2)+G22^2))
37220  R23=(W)*(G23)*((A23^2)/(((E23-W)^2)+G23^2))
39000   S=R1+R2+R3+R4+R5+R6+R7+R8+R9+R10+R11+R12+R13
 +R14+R15+R16+R17+R18+R19+R20+R21+R22+R23
39500 RETURN
39995 REM
=========================================================


40000 CHAIN "cal",40000!:REM-*- Call on a program (otherwise
out of memory) -*-
50000 REM ================================================
50001 REM -*- Lines 50000- represent  the Third Equation -*-
50002 REM *-*-* Enter function in program line 50000-51900 -
*-*-*
50025 REM *-*-*-*- Equations for calculation of the
                   Franck-Condon integrals -*-*-*-
50050 REM t1=> V1 delta, t2=> V2 , t3=> V3 delta,
          C= mult const for Bu state
50100     T1=W      :T2=.15    :T3=.1    : C=1000
         :V1=1550   :V2=1200   :V3=200
50195 REM ------------------------------------------------
50200 F2=EXP(-(.0148*(((T3)^2)*(V3))))
50250 F3=EXP(-(.0148*(((T2)^2)*(V2))))
50300 F4=.122*((V1)^.5)*(T1)*EXP(-.0148*(V1)*((T1)^2))
```

```
50350 F5=.0148*(V2)*((T2)^2)*EXP(-.0148*(V2)*((T2)^2))
50400 F55=.0148*(V3)*((T3)^2)*EXP(-.0148*(V3)*((T3)^2))
50450 F6=.122*((V1)^.5)*(T1)*(.0148*(V1)*((T1)^2)-1)
     *EXP(-.0148*(V1)*((T1)^2))
50500 F7=((.0148)^2)*((V2)^2)*((T2)^4)
     *EXP(-(.0148*(V2)*((T2)^2)))
50550 F77=((.0148)^2)*((V3)^2)*((T3)^4)
     *EXP(-(.0148*(V3)*((T3)^2)))
50600 F9=(.00127)*((V1)^1.5)*(.0148*(V1)*((T1)^5)-2
     * ((T1)^3))*EXP(-.0148*(V1)*((T1)^2))
50625 F10=(8.88E-06)*((V1)^2.5)*((.010465)*(V1)
     *((T1)^7)-(2.414)*((T1)^5))*EXP(-.0148*(V1)*((T1)^2))
50650 F11=((.3333)*(.0148)^3)*((V2)^3)*((T2)^6)
     *EXP(-(.0148*(V2)*((T2)^2)))
50655 FF11=((.3333)*(.0148)^3)*((V1)^3)*((T1)^6)
     *EXP(-(.0148*(V1)*((T1)^2)))
50675 F12=(.0148)*(V1)*((T1)^2)*(((FF11)/8)+((F10)/4))
50695 REM ------------------------------------------------
50700  A7=C*(F4)*(F3)*(F2)            :A8 =C*(F6)*(F3)*(F2)
      :A9=C*(F4)*(F5)*(F2)            :A10=C*(F4)*(F3)*(F55)
      :A11=C*(F9)*(F3)*(F2)           :A12=C*(F4)*(F7)*(F2)
50710 :A13=C*(F6)*(F5)*(F2)           :A14=C*(F4)*(F5)*(F55)
      :A15=C*(F6)*(F3)*(F55)          :A16=C*(F9)*(F5)*(F2)
50720  A17=C*(F6)*(F7)*(F2)           :A18=C*(F10)*(F3)*(F2)
50725 :A19=C*(F9)*(F7)*(F2)           :A20=C*(F9)*(F3)*(F77)
      :A21=C*(F10)*(F7)*(F2)          :A22=C*(F10)*(F5)*(F2)
50730  A23=C*(F9)*(F3)*(F55)          :A24=C*(F4)*(F7)*(F55)
      :A25=C*(F12)*(F3)*(F2)
50750 REM   --------- See 25244-5 for F# definition --------
50900 S= A13
51000 RETURN
59999 REM ----------------
60000 CHAIN "cal",60000!
```

"cal"

```
40000  REM -*-*-* 40000- is for Performing Calculation on
    Equations Below -*-*-*-  ENTER Parameters in  40100 -*-*-*-
40050 REM *-*-* Equations for calculation of the Franck-Condon
               factors -*-*-*-
40095 REM   t1=> V1 delta,  t2=> V2,  t3=> V3 delta,
            C= mult const for Bu state
40100    T1=.17    :T2=.15    :T3=.1    : C=1000
        :V1=1550   :V2=1200   :V3=200
40195 REM ------------------------------------------------
40200 F2=EXP(-(.0148*(((T3)^2)*(V3))))
40250 F3=EXP(-(.0148*(((T2)^2)*(V2))))
40300 F4=.122*((V1)^.5)*(T1)*EXP(-.0148*(V1)*((T1)^2))
40350 F5=.0148*(V2)*((T2)^2)*EXP(-.0148*(V2)*((T2)^2))
40400 F55=.0148*(V3)*((T3)^2)*EXP(-.0148*(V3)*((T3)^2))
```

```
40450 F6=.122*((V1)^.5)*(T1)*(.0148*(V1)*((T1)^2)-1)
 *EXP(-.0148*(V1)*((T1)^2))
40500 F7=((.0148)^2)*((V2)^2)*((T2)^4)*EXP(-(.0148
 *(V2)*((T2)^2)))
40550 F77=((.0148)^2)*((V3)^2)*((T3)^4)*EXP(-(.0148
 *(V3)*((T3)^2)))
40600 F9=(.00127)*((V1)^1.5)*(.0148*(V1)*((T1)^5)-2*((T1)^3))
 *EXP(-.0148*(V1)*((T1)^2))
40625 F10=(8.88E-06)*((V1)^2.5)*((.010465)*(V1)*((T1)^7)-(2.414)
 *((T1)^5))*EXP(-.0148*(V1)*((T1)^2))
40650 F11=((.3333)*(.0148)^3)*((V2)^3)*((T2)^6)*EXP(-(.0148
 *(V2)*((T2)^2)))
40655 FF11=((.3333)*(.0148)^3)*((V1)^3)*((T1)^6)*EXP(-(.0148
 *(V1)*((T1)^2)))
40675 F12=(.0148)*(V1)*((T1)^2)*(((FF11)/8)+((F10)/4))
40695 REM ------------------------------------------------
40700   A7=C*(F4)*(F3)*(F2)       :A8 =C*(F6)*(F3)*(F2)
       :A9=C*(F4)*(F5)*(F2)       :A10=C*(F4)*(F3)*(F55)
      :A11=C*(F9)*(F3)*(F2)       :A12=C*(F4)*(F7)*(F2)
40710 :A13=C*(F6)*(F5)*(F2)       :A14=C*(F4)*(F5)*(F55)
      :A15=C*(F6)*(F3)*(F55)      :A16=C*(F9)*(F5)*(F2)
40720  A17=C*(F6)*(F7)*(F2)       :A18=C*(F10)*(F3)*(F2)
40725 :A19=C*(F9)*(F7)*(F2)       :A20=C*(F9)*(F3)*(F77)
      :A21=C*(F10)*(F7)*(F2)      :A22=C*(F10)*(F5)*(F2)
40730  A23=C*(F9)*(F3)*(F55)      :A24=C*(F4)*(F7)*(F55)
      :A25=C*(F12)*(F3)*(F2)
40750 REM ------------------------------------------------
40755 REM       (V1)          |       (V2)          |     (V3)
           F4=<1|0><0|0>      |  F3=<0|0><0|0>      |  F2=<0|0><0|0>
           F6=<1|1><1|0>      |  F5=<0|1><1|0>      |  F55=<0|1><1|0>
40760 REM  F9=<1|2><2|0>      |  F7=<0|2><2|0>      |  F77=<0|2><2|0>
           F10=<1|3><3|0>     | F11=<0|3><3|0>      |  F12=<1|4><4|0>
40765 REM ------------------------------------------------
40800  CLS
40900 LOCATE 2,25 :PRINT "Franck-Condon factors "
41450 LOCATE 6,6 :PRINT A7,A8,A9,A10
41500 LOCATE 9,6 :PRINT A11,A12,A13,A14,A15,A16,A17,
                  A18,A19,A20,A21,A22,A23,A24,A25
42000 LOCATE 24,1
42050 REM -*-*- Lines 42100-42200 prevents 42500 from
              responding instantly -*-*-
42100 B$=INKEY$
42150 IF B$="*" THEN GOTO 42500
42200 GOTO 42100
42500 CHAIN "ve4"
43000 END
49990 REM
================================================================
49995 REM *-*- Lines 50000- represent  the Third Equation -*-*
60000 REM
================================================================
60010  REM -*- 60000- is for Performing Calculation on Equations
       Below -*-*-*-*  ENTER Parameters in  60025-60030  *-*-*-*
60020 REM ========================= Ag ======================
```

```
60025  T11=.36   :T22=.3         :T33=.37   :T44=.11    : K=1000
60030     VE1=1750   :VE2=1250   :VE3=200    :VE4=1550
        :VG1=1550   :VG2=1200   :VG3=200    :VG4=1550
60045 REM ==========================================================
60098 REM \-\-\-\-  Franck-Condon factors ( Ag state ) -\-\-\-\
..........................................................................
60100 F01=2*(.1217)*(((VE1)*(VG1)^.5)/((VE1)+(VG1)))*(T11)
 *(4*((VE1)*(VG1))/(((VE1)+(VG1))^2))*EXP(-2*(.0148)
 *((T11)^2)*(((VE1)*(VG1))/((VE1)+(VG1))))
60200 F02=4*(((VE2)*(VG2))/(((VE2)+(VG2))^2))*EXP(-2*(.0148)
 *((T22)^2)*(((VE2)*(VG2))/((VE2)+(VG2))))
60300 F03=4*(((VE3)*(VG3))/(((VE3)+(VG3))^2))*EXP(-2*(.0148)
 *((T33)^2)*(((VE3)*(VG3))/((VE3)+(VG3))))
60350 F04=4*(((VE4)*(VG4))/(((VE4)+(VG4))^2))*EXP(-2*(.0148)
 *((T44)^2)*(((VE4)*(VG4))/((VE4)+(VG4))))
60400 P01=2*(.1217)*(((VG1)*(VE1)^.5)/((VE1)+(VG1)))
 *(T11)*(4*((VE1)*(VG1))/(((VE1)+(VG1))^2))*EXP(-2*(.0148)
 *((T11)^2)*(((VE1)*(VG1))/((VE1)+(VG1))))
60450 P02=4*(.0148)*((((VE1)*(VG1))^1.5)/(((VE1)+(VG1))^2))
 *((T11)^2)-2*(((VE1)*(VG1))^.5)/((VE1)+(VG1))
60500 F05=(P01)*(P02)
60600 F06=4*(.0148)*((((VG2)*((VE2)^.5))/((VE2)+(VG2)))^2)
 *((T22)^2)*4*(((VE2)*(VG2))/(((VE2)+(VG2))^2))*EXP(-2*(.0148)
 *((T22)^2)*(((VE2)*(VG2))/((VE2)+(VG2))))
60700 F07=4*(.0148)*((((VG3)*((VE3)^.5))/((VE3)+(VG3)))^2)
 *((T33)^2)*4*(((VE3)*(VG3))/(((VE3)+(VG3))^2))*EXP(-2*(.0148)
 *((T33)^2)*(((VE3)*(VG3))/((VE3)+(VG3))))
60750 F08=4*(.0148)*((((VG4)*((VE4)^.5))/((VE4)+(VG4)))^2)
 *((T44)^2)*4*(((VE4)*(VG4))/(((VE4)+(VG4))^2))*EXP(-2*(.0148)
 *((T44)^2)*(((VE4)*(VG4))/((VE4)+(VG4))))
60895 REM ----------------------------------------------------
60900 REM (V1)     |    (V2)          |    (V3)          |      (v4)
   F01=<1|0><0|0>|F02=<0|0><0|0>|F03 =<0|0><0|0>|  F04=<0|0><0|0>
   F05=<1|1><1|0>|F06=<0|1><1|0>|F07 =<0|1><1|0>|  F08=<0|1><1|0>
60905 REM ----------------------------------------------------
60950 A1=K*(F01)*(F02)*(F03)*(F04) :A2=K*(F01)*(F02)*(F07)*(F04)
     :A3=K*(F01)*(F06)*(F03)*(F04)
60960 A4=K*(F05)*(F02)*(F03)*(F04) :A5=K*(F05)*(F02)*(F07)*(F04)
     :A6=K*(F01)*(F06)*(F07)*(F04) :A23=K*(F01)*(F02)*(F03)*(F08)
60970 REM ==========================================================
61000  CLS
61010 LOCATE 2,25 :PRINT "Franck-Condon factors "
61025 LOCATE 6,6 :PRINT "origin "
61050 LOCATE 6,26 :PRINT A1
61100 LOCATE 10,6 :PRINT "fundamentals"
61125 LOCATE 11,6 :PRINT "(v3,v2,v1)"
61150 LOCATE 10,26 :PRINT A2,A3,A4
61160 LOCATE 14,6 :PRINT "v8 & combination"
61165 LOCATE 15,6 :PRINT "(v8,v1+v3, v2+v3)"
61170 LOCATE 14,26 :PRINT A23,A5,A6
62000 LOCATE 23,1
62050 REM -*-*- Lines 62100-62200 prevents 62500 from
               responding instantly -*-*-
62100 B$=INKEY$
```

```
62150 IF B$="*" THEN GOTO 42500
62200 GOTO 42100
62500 CHAIN "ve4"
63000 END
```

† For the REP and absorption model an additional term, namely E_{23}, was added to the 2^1A_g state after the model was completed. For this reason the number is out of sequence.

† † This program written in GW-Basic is easily converted to Quick-BASIC. This can be done by breaking down the REP equations into two expressions; and for earlier version of Quick-BASIC it is necessary to replace the "on error ..." command with another appropriate command. Thereafter the program will run faster.

APPENDIX II

Table A. Franck-Condon Integrals used for the Raman Excitation Profile model. (1-16 utilized for the 1^1B_u state; and 1-6 for the 2^1A_g state only.)

1.	ν_{00}	$[\langle 1_g \mid 0_e\rangle\langle 0_e \mid 0_g\rangle]_{\nu_1}[\langle 0_g \mid 0_e\rangle\langle 0_e \mid 0_g\rangle]_{\nu_2}[\langle 0_g \mid 0_e\rangle\langle 0_e \mid 0_g\rangle]_{\nu_3}$
2.	ν_3	$[\langle 1_g \mid 0_e\rangle\langle 0_e \mid 0_g\rangle]_{\nu_1}[\langle 0_g \mid 1_e\rangle\langle 1_e \mid 0_g\rangle]_{\nu_2}[\langle 0_g \mid 1_e\rangle\langle 1_e \mid 0_g\rangle]_{\nu_3}$
3.	ν_2	$[\langle 1_g \mid 0_e\rangle\langle 0_e \mid 0_g\rangle]_{\nu_1}[\langle 0_g \mid 1_e\rangle\langle 1_e \mid 0_g\rangle]_{\nu_2}[\langle 0_g \mid 0_e\rangle\langle 0_e \mid 0_g\rangle]_{\nu_3}$
4.	$\nu_2+\nu_3$	$[\langle 1_g \mid 0_e\rangle\langle 0_e \mid 0_g\rangle]_{\nu_1}[\langle 0_g \mid 1_e\rangle\langle 1_e \mid 0_g\rangle]_{\nu_2}[\langle 0_g \mid 1_e\rangle\langle 1_e \mid 0_g\rangle]_{\nu_3}$
5.	ν_1	$[\langle 1_g \mid 1_e\rangle\langle 1_e \mid 0_g\rangle]_{\nu_1}[\langle 0_g \mid 1_e\rangle\langle 1_e \mid 0_g\rangle]_{\nu_2}[\langle 0_g \mid 0_e\rangle\langle 0_e \mid 0_g\rangle]_{\nu_3}$
6.	$\nu_1+\nu_3$	$[\langle 1_g \mid 1_e\rangle\langle 1_e \mid 0_g\rangle]_{\nu_1}[\langle 0_g \mid 0_e\rangle\langle 0_e \mid 0_g\rangle]_{\nu_2}[\langle 0_g \mid 1_e\rangle\langle 1_e \mid 0_g\rangle]_{\nu_3}$
7.	$2\nu_2$	$[\langle 1_g \mid 0_e\rangle\langle 0_e \mid 0_g\rangle]_{\nu_1}[\langle 0_g \mid 2_e\rangle\langle 2_e \mid 0_g\rangle]_{\nu_2}[\langle 0_g \mid 0_e\rangle\langle 0_e \mid 0_g\rangle]_{\nu_3}$
8.	$2\nu_2+\nu_3$	$[\langle 1_g \mid 0_e\rangle\langle 0_e \mid 0_g\rangle]_{\nu_1}[\langle 0_g \mid 2_e\rangle\langle 2_e \mid 0_g\rangle]_{\nu_2}[\langle 0_g \mid 1_e\rangle\langle 1_e \mid 0_g\rangle]_{\nu_3}$
9.	$\nu_1+\nu_2$	$[\langle 1_g \mid 1_e\rangle\langle 1_e \mid 0_g\rangle]_{\nu_1}[\langle 0_g \mid 1_e\rangle\langle 1_e \mid 0_g\rangle]_{\nu_2}[\langle 0_g \mid 0_e\rangle\langle 0_e \mid 0_g\rangle]_{\nu_3}$
10.	$2\nu_1$	$[\langle 1_g \mid 2_e\rangle\langle 2_e \mid 0_g\rangle]_{\nu_1}[\langle 0_g \mid 0_e\rangle\langle 0_e \mid 0_g\rangle]_{\nu_2}[\langle 0_g \mid 0_e\rangle\langle 0_e \mid 0_g\rangle]_{\nu_3}$
11.	$2\nu_1+\nu_3$	$[\langle 1_g \mid 2_e\rangle\langle 2_e \mid 0_g\rangle]_{\nu_1}[\langle 0_g \mid 0_e\rangle\langle 0_e \mid 0_g\rangle]_{\nu_2}[\langle 0_g \mid 1_e\rangle\langle 1_e \mid 0_g\rangle]_{\nu_3}$
12.	$2\nu_2+\nu_1$	$[\langle 1_g \mid 1_e\rangle\langle 1_e \mid 0_g\rangle]_{\nu_1}[\langle 0_g \mid 2_e\rangle\langle 2_e \mid 0_g\rangle]_{\nu_2}[\langle 0_g \mid 0_e\rangle\langle 0_e \mid 0_g\rangle]_{\nu_3}$
13.	$2\nu_1+\nu_2$	$[\langle 1_g \mid 2_e\rangle\langle 2_e \mid 0_g\rangle]_{\nu_1}[\langle 0_g \mid 1_e\rangle\langle 1_e \mid 0_g\rangle]_{\nu_2}[\langle 0_g \mid 0_e\rangle\langle 0_e \mid 0_g\rangle]_{\nu_3}$
14.	$3\nu_1$	$[\langle 1_g \mid 3_e\rangle\langle 3_e \mid 0_g\rangle]_{\nu_1}[\langle 0_g \mid 0_e\rangle\langle 0_e \mid 0_g\rangle]_{\nu_2}[\langle 0_g \mid 0_e\rangle\langle 0_e \mid 0_g\rangle]_{\nu_3}$
15.	$2\nu_1+2\nu_2$	$[\langle 1_g \mid 2_e\rangle\langle 2_e \mid 0_g\rangle]_{\nu_1}[\langle 0_g \mid 2_e\rangle\langle 2_e \mid 0_g\rangle]_{\nu_2}[\langle 0_g \mid 0_e\rangle\langle 0_e \mid 0_g\rangle]_{\nu_3}$
16.	$3\nu_1+\nu_2$	$[\langle 1_g \mid 3_e\rangle\langle 3_e \mid 0_g\rangle]_{\nu_1}[\langle 0_g \mid 1_e\rangle\langle 1_e \mid 0_g\rangle]_{\nu_2}[\langle 0_g \mid 0_e\rangle\langle 0_e \mid 0_g\rangle]_{\nu_3}$

Table A.

Table B. Franck-Condon Integrals used for the absorption spectrum model. (1-16 utilized for the 1^1B_u state; and 1-6 for the 2^1A_g state only.)

1.	ν_{00}	$[\langle 0_g \mid 0_e \rangle]_{\nu_1} [\langle 0_g \mid 0_e \rangle]_{\nu_2} [\langle 0_g \mid 0_e \rangle]_{\nu_3}$
2.	ν_3	$[\langle 0_g \mid 0_e \rangle]_{\nu_1} [\langle 0_g \mid 0_e \rangle]_{\nu_2} [\langle 0_g \mid 1_e \rangle]_{\nu_3}$
3.	ν_2	$[\langle 0_g \mid 0_e \rangle]_{\nu_1} [\langle 0_g \mid 1_e \rangle]_{\nu_2} [\langle 0_g \mid 0_e \rangle]_{\nu_3}$
4.	$\nu_2+\nu_3$	$[\langle 0_g \mid 0_e \rangle]_{\nu_1} [\langle 0_g \mid 1_e \rangle]_{\nu_2} [\langle 0_g \mid 1_e \rangle]_{\nu_3}$
5.	ν_1	$[\langle 0_g \mid 1_e \rangle]_{\nu_1} [\langle 0_g \mid 0_e \rangle]_{\nu_2} [\langle 0_g \mid 0_e \rangle]_{\nu_3}$
6.	$\nu_1+\nu_3$	$[\langle 0_g \mid 1_e \rangle]_{\nu_1} [\langle 0_g \mid 0_e \rangle]_{\nu_2} [\langle 0_g \mid 1_e \rangle]_{\nu_3}$
7.	$2\nu_2$	$[\langle 0_g \mid 0_e \rangle]_{\nu_1} [\langle 0_g \mid 2_e \rangle]_{\nu_2} [\langle 0_g \mid 0_e \rangle]_{\nu_3}$
8.	$2\nu_2+\nu_3$	$[\langle 0_g \mid 0_e \rangle]_{\nu_1} [\langle 0_g \mid 2_e \rangle]_{\nu_2} [\langle 0_g \mid 1_e \rangle]_{\nu_3}$
9.	$\nu_1+\nu_2$	$[\langle 0_g \mid 1_e \rangle]_{\nu_1} [\langle 0_g \mid 1_e \rangle]_{\nu_2} [\langle 0_g \mid 0_e \rangle]_{\nu_3}$
10.	$2\nu_1$	$[\langle 0_g \mid 2_e \rangle]_{\nu_1} [\langle 0_g \mid 0_e \rangle]_{\nu_2} [\langle 0_g \mid 0_e \rangle]_{\nu_3}$
11.	$2\nu_1+\nu_3$	$[\langle 0_g \mid 2_e \rangle]_{\nu_1} [\langle 0_g \mid 0_e \rangle]_{\nu_2} [\langle 0_g \mid 1_e \rangle]_{\nu_3}$
12.	$2\nu_2+\nu_1$	$[\langle 0_g \mid 1_e \rangle]_{\nu_1} [\langle 0_g \mid 2_e \rangle]_{\nu_2} [\langle 0_g \mid 0_e \rangle]_{\nu_3}$
13.	$2\nu_1+\nu_2$	$[\langle 0_g \mid 2_e \rangle]_{\nu_1} [\langle 0_g \mid 1_e \rangle]_{\nu_2} [\langle 0_g \mid 0_e \rangle]_{\nu_3}$
14.	$3\nu_1$	$[\langle 0_g \mid 3_e \rangle]_{\nu_1} [\langle 0_g \mid 0_e \rangle]_{\nu_2} [\langle 0_g \mid 0_e \rangle]_{\nu_3}$
15.	$2\nu_1+2\nu_2$	$[\langle 0_g \mid 2_e \rangle]_{\nu_1} [\langle 0_g \mid 2_e \rangle]_{\nu_2} [\langle 0_g \mid 0_e \rangle]_{\nu_3}$
16.	$3\nu_1+\nu_2$	$[\langle 0_g \mid 3_e \rangle]_{\nu_1} [\langle 0_g \mid 1_e \rangle]_{\nu_2} [\langle 0_g \mid 0_e \rangle]_{\nu_3}$

Table B.

REFERENCES

REFERENCES

1 G. Herzberg, Electronic Spectra of Polyatomic Molecules (Van Nostrand Reinhold, New York, 1966), p.132.

2 K. Schulten and M. Karplus, Chem. Phys. Lett. **14**, 305 (1972).

3. B. S. Hudson and B. E. Kohler, Ann. Rev. Phys. **25**, 437 (1974).

4. H. L. B. Fang, R. J. Thrash, and G. E. Leroi, J. Chem. Phys. **67**, 3389 (1977).

5. H. L. B. Fang, R. J. Thrash, and G. E. Leroi, Chem. Phys. Lett. **57**, 59 (1978).

6. B. E. Kohler, C. Spangler, and C. Westerfield, J. Chem. Phys. **89**, 5422 (1988).

7. J. H. Simpson, L. McLaughlin, D. S. Smith, and R. L. Christensen, J. Chem. Phys. **87**, 3360 (1987).

8. B. E. Kohler and J. B. Snow, J. Chem. Phys. **79**, 2134 (1983).

9. J. S. Horwitz, T.Itoh, B. E. Kohler, and C. W. Spangler, J. Chem. Phys. **87**, 2433 (1987).

10. B. S. Hudson and B. E. Kohler, J. Chem. Phys. **59**, 4984 (1973).

11. B. S. Hudson, B. E. Kohler, and K. Schulten in: Excited States, Vol.6 edited by E. C. Lim (Academic, New York, 1982) p. 1.

12. B. S. Hudson and B. E. Kohler, Chem. Phys. Lett. **14**, 299 (1972).

13. K. L. D'Amico, C. Manos, and R. L. Christensen, J. Am. Chem. Soc. **102**, 1777 (1980).

14. R. M. Gavin Jr., S. Risemberg and S. A. Rice, J. Chem. Phys. **58**, 3160 (1973).

15. C. Tric and V. Lejeune, Photochem. Photobiol. **12**, 339 (1970).

16. R. J. Thrash, H. L. B. Fang, and G. E. Leroi, Photochem. Photobiol. **29**, 1049 (1979).

17. L. Rimai, M. E. Heyde, H. C. Heller, and D. Gill, Chem. Phys. Lett. **10**, 207 (1971).

18. H. Hashimoto and Y. Koyama, Chem. Phys. Lett. **154**, 321 (1989).

19. G. M. Korenowski, L. D. Ziegler, and A. C. Albrecht, J. Chem. Phys. **68**, 1248 (1978).

20 R. J. Thrash, H. L. B. Fang, and G. E. Leroi, J. Chem. Phys. **67**, 5930 (1977).

21. M. Z. Zgierski, J. Raman Spectrosc. **6**, 53 (1977).

22 C. M. Phillips, W. Brown, and G. E. Leroi in: Raman Spectroscopy, Linear and Nonlinear, eds. J. Lascombe and P. V. Huong (Wiley Heyden, Chichester,1982) p.135

23. J. Friedman and R. M. Hochstrasser, Chem. Phys. Lett. **32**, 414 (1975).

24 I. W. Sztainbuch and G.E. Leroi (Manuscript in preparation).

25. N. Ohta and M. Ito, Chem. Phys. **20**, 71 (1977).

26. R. J. H. Clark and T. J. Dines in: Adv. in IR and Raman Spectrosc. Vol. 9, eds. R. J. H. Clark and R. E. Hester (Heyden, London, 1982) p. 282.

27. S. Hassing and E. N. Svendson, Chem. Phys. Lett. **86**, 343 (1982).

28. R. J. H. Clark and T. J. Dines, Chem. Phys. Lett. **79**, 321 (1981).

29. M. Masthay, Ph.D. Dissertation, Carnegie-Mellon Univ., Pittsburgh, PA. (1988).

30. C. W. Spangler, R. K. McCoy, A. A. Dembek, L. S. Sapochak, and B.D. Gates, J. Chem. Soc. Perkin Trans. 1, 151 (1989).

31. C. W. Spangler, E. Nickel, and T. Hall, Polymer Preprints **28(1)**, 219 (1987).

32. Exciton Laser Dye Catalog (1989) pp. 8,12.

33. G. Placzek in: Handbuch der Radiologie, edited by E. Marx (Akademische Vertag, Leipzig, 1934) Vol. 6, Part 2, p. 209.

34. H. A. Kramers and W. Heisenberg, Z. Phys. **31**, 681 (1925).

35. A. C. Albrecht, J. Chem. Phys. **34**, 1476 (1961).

36. O. S. Mortensen and S. Hassing in: Adv. in IR and Raman Spectrosc. Vol. 6, edited by R. J. H. Clark and R. E. Hester (Heyden, London, 1980) p. 1.

37. A. Warshel and P. Dauber, J. Chem. Phys. **66**, 5477 (1977).

38. A. B. Myers and R. R. Birge, J. Chem. Phys. **73**, 5314 (1980).

39. S. Sufra, G. Dellepiane, G. Masetti, and G. Zerbi, J. Raman Spectrosc. **6**, 267 (1977).

40. A. B. Myers, R. A. Mathies, D. J. Tannor, and E. J. Heller, J. Chem. Phys. **77**, 3857 (1982).

41. R. J. H. Clark and T. J. Dines, Mol. Phys. **45**, 1153 (1982).

42. G. Smulevich and M. P. Marzocchi, Chem. Phys. Lett. **105**, 159 (1986).

43. W. Siebrand and M. Z. Zgierski, J. Chem. Phys. 71, 3561 (1979).

44. C. Manneback, Physica, 17, 1001 (1951).

45. R. J. H. Clark and T. J. Dines, Mol. Phys. 42, 193 (1981).

46. J. E. Cotting, L. C. Hoskins, and M. E. Levan, J. Chem. Phys. 77, 1081 (1982).

47. A. R. Mantini, M. P. Marzocchi and G. Smulevich, J. Chem. Phys. 91, 85 (1989).

48. J. T. Lurito, I. R. Dunkin, and L. Andrews, J. Mol. Spectrosc. 114, 54 (1985).

49. H. Yoshida and M. Tasumi, J. Chem. Phys. 89, 2803 (1988).

50. S. Saito and M. Tasumi, J. Raman Spectrosc. 14, 310 (1984).

51. R. L. Christensen and B. E. Kohler, J. Chem. Phys. 63, 1837 (1975).

52. J. A. Pople and J. W. Sidman, J. Chem. Phys. 27, 1270 (1957).

53. D. N. Batchelder and D. Bloor in: Adv. in IR and Raman Spectrosc. Vol. 11, edited by R. J. H. Clark and R. E. Hester (Heyden, London, 1982) p. 133.

54. T. Itoh and B. E. Kohler, J. Phys. Chem. 91, 1760 (1987).

55. B. E. Kohler and T. Itoh, J. Phys. Chem. 92, 5120 (1988).

56. B. E. Kohler, T. A. Spiglanin, R. J. Hemley, and M. Karplus, J. Chem. Phys. 80, 23 (1984).

57. M. F. Granville, B. E. Kohler, and J. B. Snow, J. Chem. Phys. 75, 3765 (1981).

58. M. F. Granville, G. H. Holtom, and B. E. Kohler, J. Chem. Phys. 72, 4671 (1980).

59. A. C. Lasaga, R. J. Aerni, and M. Karplus, J. Chem. Phys. **73**, 5230 (1980).

60. F. Zerbetto and M. Z. Zgierski, Chem. Phys. Lett. **141**, 138 (1987).

61. M. Aoyagi, I.Ohmine, and B. E. Kohler, J. Phys. Chem. **94**, 3922 (1990).

62. L. C. Hoskins, J. Chem. Phys. **72**, 4487 (1980).

63. L. C. Hoskins, J. Chem. Phys. **74**, 882 (1981).

64. Z. Z. Ho, R. C. Hanson, and S. H. Lin, J. Chem. Phys. **77**, 3414 (1982).

65. H. Okamoto, S. Saito, H. O. Hamaguchi, M. Tasumi, and C. H. Eugster, J. Raman Spectrosc. **15**, 331 (1984).

66. J. A. Bennett and R. R. Birge, J. Chem. Phys. **73**, 4234 (1980).

67. R. R. Chadwick, D. P. Gerrity, and B. S. Hudson, Chem. Phys. Lett. **115**, 24 (1985).

68. W. J. Buma, B. E. Kohler, and K. Song, J. Chem. Phys. **92**, 4622 (1990).

69. T. Noguchi, S. Kolaczkowski, C. Arbour, S. Aramaki, G. H. Atkinson, H. Hayashi, and M. Tasumi, Photochem. Photobiol. **50**, 603 (1989).